AL-MUSTANSIRIYAH JOURNAL OF SCIENCE

Volume 4, No. 1, June 1979

College of SCIENCE, AL-MUSTANSIRIYAH UNIVERSITY BAGHDAD-IRAQ

CONTENT

Title — Page

* The distribution of blood groups in Al-Yazidiyah .
A.L.F. Al-Baldawi and H.J. Al-Ani 5

* The drugs which inhibit the short-circuit current of everted small intestine of the rat .
I.W. Muflih and W.F. Widdas 11

* Spectroscopic studies of the -radiolysis of potassium iodide in 7M KOH glasses at 77° K .
Saad K. Ismail and G. Scholes 27

* -irradiation of benzophenone in organic glasses at 77° K .
Saad K. Ismail and G. Scholes 45

* Amino pyridine and related compounds part-I preparation and condensation of ethyl N-2-pyridyl formimidates with some aliphatic and aromatic amines .
K.S. Al-Dulaimi , A.S. Abdul-Razzak and Abdul-Jabbar A.Mukhles .73

* Application of the electrical prospecting method to evaluate the shallow formation in " ABU MINA BASIN " .
T. A. Abdel-Latif ,M. A. Sayed and S. E. Khalil 83

* Application of X-ray diffraction to study the interdiffusion in the RBI-KI solid solution .
Y. N. Obaid 97

* A dual-model of hadrons beyond the narrow width approximation .
A. K. Bassiouny 109

* Dielectric properties of some oils at low frequency region .
S.H.M. El-Sabeh, K.N. Abd-El-Nour, A.S.J. Al-Ani and T.A. AL-Dhahir.115

AL-MUSTANSIRIYAH JOURNAL OF SCIENCE

Volume 4, No. 1, June 1979

College of science, Al-Mustansiriyah University Baghdad-Iraq

Instructions for Authors:

1. Manuscripts should be Submitted in triplicate, they should be typewritten with double spacings. A margin of about 2.5 cm should be left onthe left hand side.
2. Both Arabic and English abstracts should be submitted, typed on separate sheets of paper.
3. The title of the Paper together with the name and address of the author (s) should be typed on a separate sheet. Name of author shouldbe written in full e.g Ahmed M. Ali.
4. Figures and illustrations should be drawn in black china ink on tracing Papers. Three photocopies of each diagram should also be submitted. Captions to figures should be written on the trace paper.
5. Tables should be arranged in such away so as to make them legible .
6. The same facts should not be given in tables and figures except when it is absoutely necessary to do so.
7. Reference numbers should be written between square brackets []. A list of referances should be given on a separate sheet of paper.
8. Where possible, Papers should follow the Pattern: Introduction, Experimental, Results and Discussion.

AL-MUSTANSIRIYAH JOURNAL OF SCIENCE

Volume 4, No. 1, June 1979

THE DISTRIBUTION OF BLOOD GROUPS IN AL-YAZIDIYAH

A.L.F. Al-Baldawi* and H.J. Al-Ani*

A B S T R A C T

The ABO Rh blood groups were determined in Al-Yazidiyah. One thousand and ninety six students of different boys and girls primary school in Singar and Saykan were tested. The gene frequency for A, B and O was 15-36%, 20-02 and 65-62% respectively. The Rh-negative individuals are absent in the population.

The results are discussed in relation to the blood group distribution in Iraq and other world populations.

INTRODUCTION

No aspect of haematology has wider ramifications among the medical and other biological sciences than has the study of the blood groups. Discovered by immunological techniques became an essential part of the background of clinical medicine, on the clinical conexion was enhanced when the Rh groups were

* Animal Production Department, College of Agriculture Baghdad University, Baghdad, Iraq.

discovered and then shown to play the main apart not only in the aetiology of haemolytic disease of the new-born but also in making possible a rational and effective treatment of this disease.

The great advance in our knowledge of the blood groups have arisen, from the discovery that they are inherited as Mendelian characters. This has not only contributed very greatly to the management of haemolytic disease of the new-born as a family problem, but has made the study of blood groups an essential part both of human genetics and of anthropology.

One of the most important aims of human genetic study is is the complete mapping of the gern plasm whereas in certain animals this can be achieved by deliverate breading scale, using congentital abnormalities as indicators, in man we have to rely on observation of unplanned breeding, and our chief marker genes are those of the blood groups. Investigations let to the discovery of linkage between certain blood-group genes on the one hand and the genes for certain congenital abnormalities, and for ABO secretion, on the other.

It is inevitable, that more and more linkage will be found between the genes of the blood groups and other genes. While the blood groups are likely to continue for many years to be the most important markers genes in such investigations, numerous other

biochemical polymorphisms are being discovered and linkages of the genes for these with one another, with those for the blood groups and with those for other conditions, are to be expected.

In the human biology field, we are likely to learn more of the blood groups function in natural selection and this will, make a valuable contribution to the growing study of human population genetics and anthropology.

The published data about the major blood groups distribution in Iraq is very little. This makes a gap in our knowledge especially for the medical works and other fields. We thought it is very important to investigate the blood distribution according to different places and religions in this country. Al-Yazidiyah is one of the religion who lived in northern of Iraq as small comunity [1] without any miscegenation with other religions.

MATERIALS AND METHODS

The ABO and Rh blood groups were determined by the slide agglutionation method at room temperature with fresh samples of high titre anti-A, anti-B, and anti-D sera (antisera used were prepared for the method by the manufacturers, Ortho Diagnostics, Raritan, New Jersey).

Students of different boys & girls primary schools in Singar and Saykan are tested. Origin of the student (from which tribe) is not taken as a basis in distribution of individuals in schools, so the sample taken could be considered random and representative of the Al-Yazidiyah population.

RESULTS AND DISCUSSION

Table 1. shows the distribution of ABO blood groups in Al-Yazidiyah. The higher value for gene frequency O than for group O is of course due to the fact that many of the individuals who are of group A and B are heterozygous and carry one O gene together with an A or a B gene. The gene frequencies for the Arab, Kurd, and total population of the world are shown in Table 2). The differences between Al-Yazidiyah and Arab;is less than between Al-Yazidiyah and Kurds. This could be due to historical admixture of Arabic blood with that of Asiatic groups like Persians (whole Al-Yazidiyah originated from [1]. Throughout the past millennium or so [2].

Table 1. - Distribution of ABO blood groups in Al-Yazidiyah

Item	A	B	C	AB
No.	313	229	472	82
%	28.558	20.894	43.066	7.482
gene freq.	15.36%	20.02%	65.62%	-

Table 2 - Gene frequencies (%) of ABO blood groups in Arabs, Kurds, and World populations.

Nationality	A	B	C
Arab	20.160	20.295	59.000
Kurd	24.900	17.290	57.567
World	21.500	16.200	62.300

It is interesting to know that Rh-negative individuals are nearly absent in Al-Yazidiyah compare with 4.86% Arab and 4.85% in Kurds [2]. This is similar to Chinese, Japanese, Burmese, Indonesian and Eskimo populations [3].

It is interesting to note that blood group B is very uncommon in such dissimilar groups as American Indians, Australian aborigines and the English [4]. Group B is commonest in Asiatic indians, Chinese, Arabs, Kurds and Al-Yazidiyah.

Differences is ABO and Rh blood groups between Iraqi and European polulations should be stressed from clinical point of view because most of the Iraqicclinicians their figures depend on American and British references which are quoted from their communities. The incidence of some diseases like doudenal ulceration, stomach carcinoman and permicions anaemia are expected to be different according to their incidences in groups O and A respectively [5,6].

Haemolytic disease of the newborn due to Rh group incompatbility is expected to be much lower in Arab & Kurd and nothing in Al-Yazidiyah compar with Eurpean countries due to lower incidence of Rh negativity in Iraq.

REFERENCES

(1) A.R. Al-Hasani. Al-Yazidiyah in their present and past. House of the New Books, Baghdad (1974).

(2) A.M. Al-Hilali. ABO & Rh(D) Blood group in Arabs and Kurds of Iraq. Journal of the Faculty of Medicine 16, 49-55 (1974).

(3) A.E. Mourant. The Distribution of Human Blood Groups. Blackwell Scientific Publications, Oxford & Edinburgh (1954).

(4) R.R. Race and Sanger, Blood Groups in Man Springfield, III Ed. 3 Charles, C. Thomas (1958).

(5) I. Aird and H.H. Bentall, A relationship between cancer of the stomach and the ABO blood groups: Brit-Med. J-i, 799 (1953).

(6) J.A. Fraser, Some Associations between Blood Group and Diseas. Brit. Med. Bull., 15, 129 (1959).

THE DRUGS WHICH INHIBIT THE SHORT-CIRCUIT CURRENT OF THE EVERTED SMALL INTESTINE OF THE RAT

I.W. Muflih* and W.F. Widdas

A B S T R A C T

1. Cytochalasin B, the hexose transport inhibitor, of the human erythrocyte inhibited the short-circuit current induced by the actively transported sugars-glucose and galactose-acrose the intestinal segment of the rat.

2. The inhibitory characteristics of cytochalasin B is found to be different from the inhibitory mode of phloridzin.

3. The results of the inhibitory effects of DNP obtained in the present work seems to confirm the findings of Schultz and Zalusky [1] in the rabbit's small intestine.

INTRODUCTION

Muflih & Widdas [2] observed the inhibitory effects of a number of non-transportable sugars and sugar derivatives on the short circuit current of the everted small intestine of the rat. The technique used was to obtain an increase in short circuit current by adding a fixed concentration of a transported sugar such as galactose and then observe the depression of the short circuit current when the inhibitor and transported sugar were both present.

---

* Now at the Physiology department, college of Medicine, Al-Mustansiriyah University.

Al-Mustansiriyah Journal of Science vol. 4 No. 1 (1979).

The inhibition could be due to competition between the inhibitor and transported sugar for the current generating transport process but the method does not depend on competition. In the present work the same technique was used to study the effects of three inhibitors. These were cytochalasin B, a fungal metabolite which is a very potent inhibitor of hexose transfers in red cells, 2,4-dintrophenol (DNP), an energy decoupling agent, and phloridian, a specific inhibitor of the intestinal hexose absorption mechanism.

Taverns & Langdon [3] and Bloch [4] showed that cytochalasin B was a potent inhibitor of glucose exit in human erythrocytes and appeared to be non-competitive; however, Lin & Spudich [5] and Jung & Rampal [6] reported experiments which suggested that it was a competitive inhibitor. Basketter & Widdas [7 , 8] have confirmed that Cytochalasin B competitively inhibits glucose exchange but appears to be non-competitive in exit experiements. This can be explained on the basis of the inhibitor reacting with the internal site of the hexose transfer system in the human red cell and not the external site. Such chemical asymmetry in the red cell hexose system suggested that it would be interesting to see if Cytochalasin B had a high affinity for the intestinal sugar absorption system.

EXPERIMENTAL

The animals used, Albino rats of Wistar strain, were prepared as described [2] . The everted gut was mounted on a perforated cannula in the apparatus previously described with the exception that potential measurement and short circulating was provided by an electronic circuit as described by de Jesus & Smith [9] . This allowed part of the basal short circuit current to be backed off before starting an experiment.

TABLE 1

Inhibition of the increment in short circuit current due to glycine in the mucosel solution in the presence of Cytochalasin B in the mucosal bathing medium.

(Glycine) mM	(Cytochalasin B) uM	$I_{S.C.}$ uA
23.7	0	19.0
23.7	25	15.0
23.7	50	6.0
23.7	75	-4.0*
After 10 mins. in new medium		
23.7	0	-7.5
44.5	0	25.0
44.5	46	14.0
After 10 mins. in new medium		
44.5	0	8.0

* The negative sign indicates inhibition beyond the baseline value obtained prior to adding glycine.

Note absence of any recovery when bathed in a Cytochalasin free solution.

2,4-dinitrophenol

With short circuit currents induced by 6.6 mM glucose 2,4-dinitrophenol up to 180 uM was needed to completely inhibit the increment in short circuit current due to the sugar.

The effect was partly reversible since on bathing the preparation in fresh Krebs' containing the same concentration of glucose (6.6 mM) but free of 2,4-dinitrophenol the short circuit current recovered to more than one third of its initial value within 15 minutes.

Smaller concentrations of DNP were able to inhibit the increment of short circuit current induced by 6.6 mM galactose. Fig. 4 shows the partial inhibition of the galactose short circuit current with up to 8 uM of DNP.

In this result DNP appeared to be approaching a saturation effect and if one assumes the reagent to be occupying sites which in some way reduces the energy or sites available for generating the sugar short circuit current one could write

$$\triangle I_{sc} = k \frac{C}{C + K_I} \quad \ldots\ldots\ldots (1)$$

where $\triangle I_{sc}$ is the change in short circuit current, C is the concentration of DNP, K_I its affinity constant and k a constant.

This can be Linearised as

$C/\triangle I_{sc} = \frac{1}{K} (C + K_i)$ to give a Hanes plot and such a plot is shown in Fig. 5.

The K_I for the inhibition of galactose short circuit current was ca. 4 uM whereas that for the glucose short circuit current was over 200 uM. What this implies is that in the presence of glucose a saturable inhibition is not seen and DNP is having its effect in another manner.

Phloridzin

Fig. 6 shows the inhibition of the short circuit current produced by 6.6 uM galactose in the presence of phloridzin up to 1.2 uM.

The Hanes plot of these results is curved and can only give an approximate K_I which is of the order of 0.6-1.0 uM.

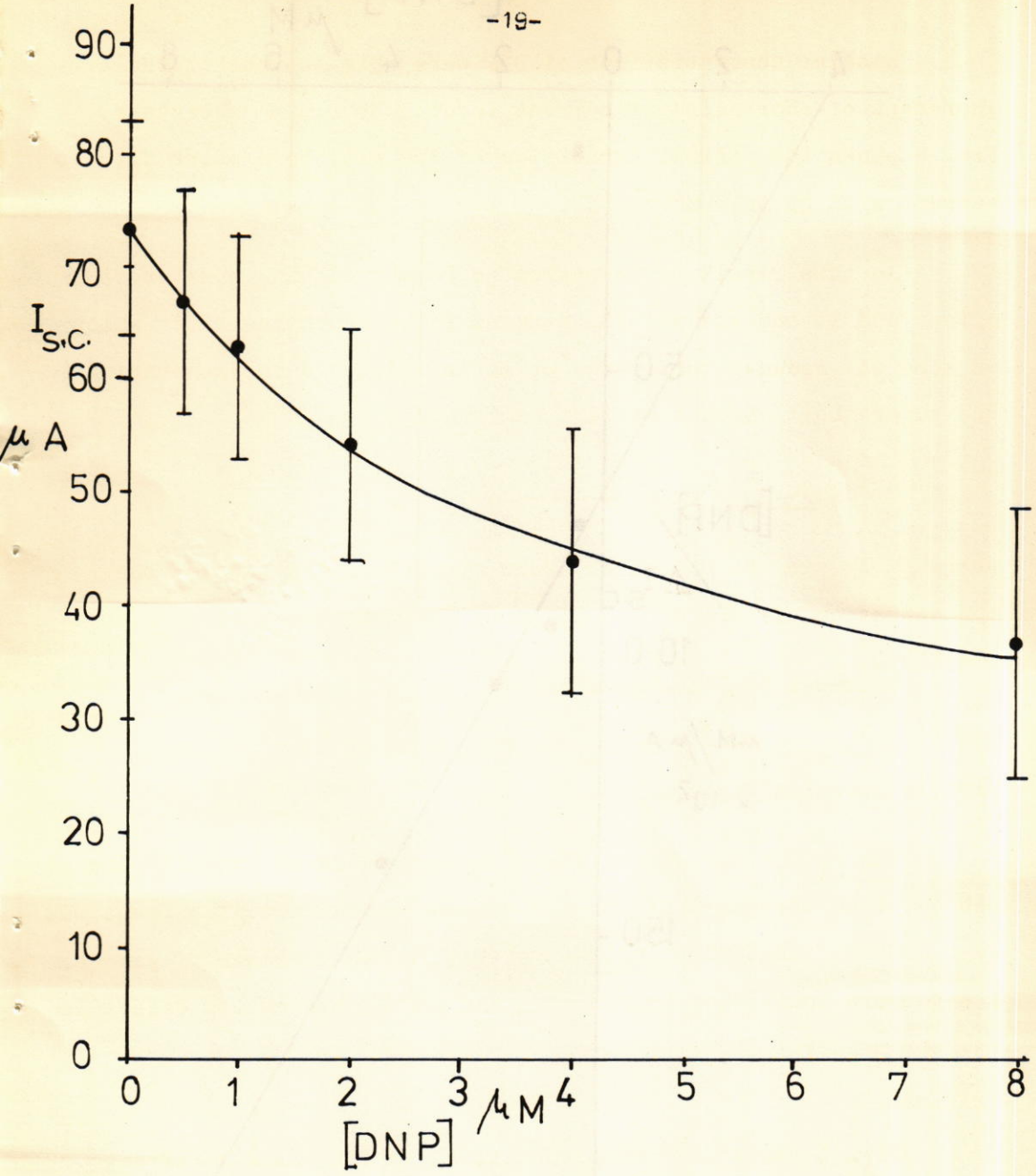

Fig. 4. Inhibition of short circuit current induced by 6.6 mM Galactose in the presence of low concentrations of DNP. Points are the means and S.E. of two experimental results. The continuous Line corresponds to the straight line in the Hanes plot in Fig. 5.

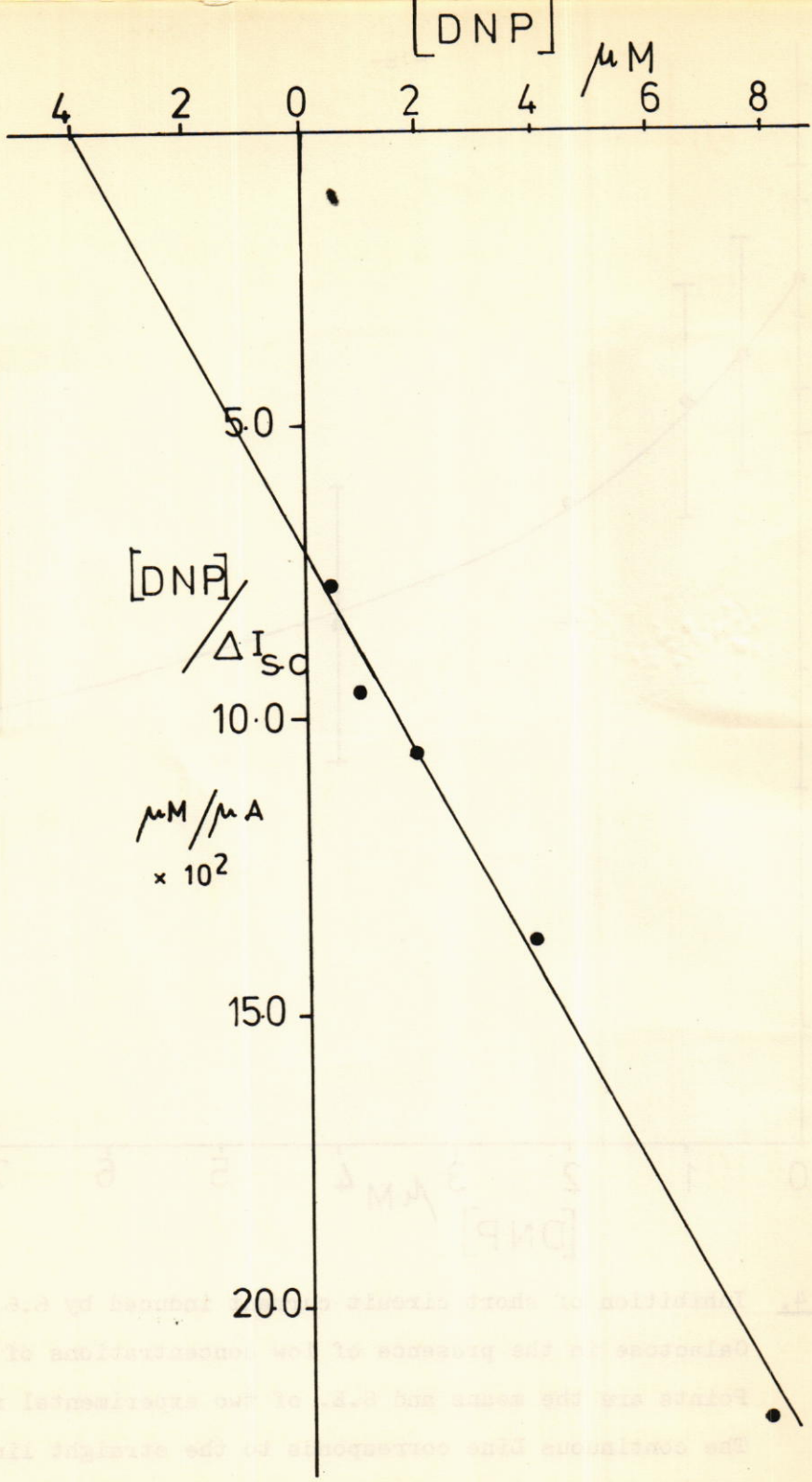

Fig. 5. Hanes plot of the results from Fig. 4. The K_I is given by the intercept on the abscissa and is about 4 uM.

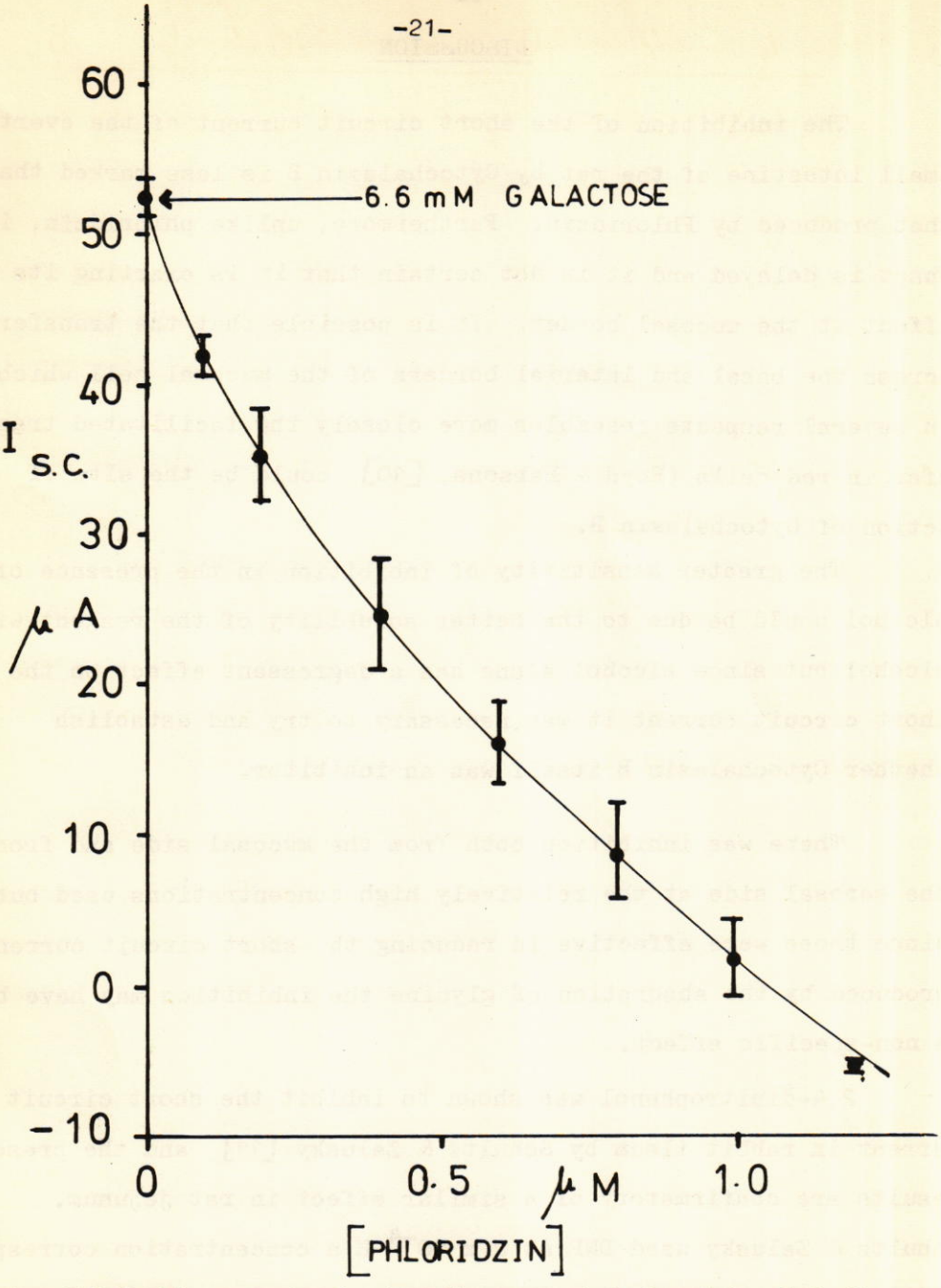

Fig. 6. Inhibition of short circuit current induced by 6.6 mM Galactose in the presence of phloridzin. Points are the means and S.E. of two results. Negative values of current represent inhibition beyond the baseline obtained prior to adding galactose.

DISCUSSION

The inhibition of the short circuit current of the everted small intestine of the rat by Cytochalasin B is less marked than that produced by Phloridzin. Furthermore, unlike phloridzin, its onset is delayed and it is not certain that it is exerting its effect at the mucosal border. It is possible that the transfer across the basal and laterial borders of the mucosal cell which in several respects resembles more closely the facilitated transfer in red cells (Boyd & Parsons, [10] could be the site of action of Cytochalasin B.

The greater sensitivity of inhibition in the presence of alcohol could be due to the better solubility of the reagent with alcohol but since alcohol alone has a degressant effect on the short circuit current it was necessary to try and establish whether Cytochalasin B itself was an inhibitor.

There was inhibition both from the mucosal side and from the serosal side at the relatively high concentrations used but since those were effective in reducing th short circuit current produced by the absorption of glycine the inhibitica may have been a non-specific effect.

2,4-dinitrophenol was shown to inhibit the short circuit current in rabbit ileum by Schultz & Zalusky [11] and the present results are confirmatory of a similar effect in rat jejunum. Schultz & Zalusky used DNP at 2×10^{-4} M a concentration corresponding to the maximum used in inhibiting the glucose short circuit current in the present experiments. The inhibition of the galactose short circuit current was effected at much lower concentration than that of glucose. This may indicate that glucose, which usually induces a higher increment in the short circuit current than

galactose, supplies an energy need as well as being actively transferred and that this energy provision reduces the effectiveness of DNP in blocking the overall energy supply. The saturation effect shown in the inhibition of the galactose short circuit current may simply reflect the way in which the energy for which the galactose transfer is competing is being progressively reduced or it may indicate a fall in the electrical potential gradient which could contribute to the driving force (Schultz & Zalusky, [1]).

Phloridzin still appears to be the most effective and specific inhibitor of the short circuit current increment induced by a transportable sugar. Most workers have used phloridzin at one inhibitory concentration. Thus Schultz & Zalusky [1] used 5×10^{-4} M as did Barry, Smyth & Wright [12]. The concentration which half-inhibited the short circuit current due to galactose transfer was smaller by two orders of magnitude than these and also that found by Muflih & Widdas [2] to inhibit the basal short circuit current. This suggests the latter action was probably at a different site and perhaps at the basal or lateral surfaces of the mucosal cells but this possibility would require further study.

This work was carried out while on Study Leave in the Department of Physiology, Bedford College, University of London 1977.

REFERENCES

1. S.G. Schultz, & R. Zalusky, Ion transport in isolated rabbit ileum. II. The interaction between active sodium and active sugar transport, J. Gen. Physiol 47, 1043-1059 (1964b).

2. I.W. Muflih, & W.F. Widdas, Sugars and sugar derivatives which inhibit the short-circuit current of the everted small intestine of the rat, J. Physiol. 263, 101-114 (1976).

3. R.D. Taverna, & R.G. Langdon, Reversible association of Cytochalasin B with the human erythrocyte membrane. Inhibition of glucose transport and the stoichiometry of Cytochalasin binding, Biochim, biophys Acta 323, 207-219 (1973).

4. R. Bloch, Inhibition of glucose transport in the human erythrocyte by Cytochalasin B., Biochemistry 12, 4799-4801 (1973).

5. S. Lin, & J.A. Spudich, Biochemical studies on the mode of action of Cytochalasin B. Cytochalasin B binding to red cell membrane in relation to glucose transport, J. Biol. Chem. 249, 5778-5783 (1974).

6. C.Y. Jung, & A.L. Rampal, Effects of Cythochalasin B on Equilibrium exchange flux of D-glucose across human erythrocyte membranes, Fed. Proc. 34, 238 (1975).

7. D.A. Basketter, & W.F. Widdas, Competitive inhibition of hexose transfer in human erythrocytes by Cytochalasin B., J. Physiol. 265, 39-40p. (1977)

8. D.A. Basketter, & W.F. Widdas, Asymmetry of the hexose transfer system in human erythrocytes. Comparison of the effects of Cytochalasin B, Phloretin and Maltose as competitive inhibitors., J. Physiol. (1978).

9. C.H. De Jesus, & M.W. Smith, Protein and glucose-induced changes in sodium transport across the pig small intestine, J. Physiol. 243, 225-242 (1974).

10. C.A.R. Boyd, & D.S. Parsons, Movement of sugars between compartments of vascularly perfused intestine, J. Physiol. 258, 12-13p. (1976).

11. S.G. Schultz, & R. Zalusky, Ion transport in isolated rabbit ileum. I. Short-circuit current and Na fluxes, J. Gen. Physiol. 47, 567-584 (1964a).

12. R.J.C. Barry, & D.H. Smyth, & E.M. Wright, Short circuit current and solute transfer by rat jejunum, J. Physiol. 181. 410-431 (1965).

oooooooooo
oooooooooo

SPECTROSCOPIC STUDIES OF THE γ-RADIOLYSIS OF POTASSIUM IODIDE IN 7M KOH GLASSES AT 77°K

Saad K. Ismail* and G. Scholes

A B S T R A C T

A spectroscopic technique has been used to study the oxidation of I^- ion by either OH radicals or O^- in γ-irradiated 7M alkaline glasses. Absorption bands at 340 nm, 350 nm and 381 nm and 450 nm are assigned to an intermediate (IO^{2-} or IOH^-), I_3^-, I_2^- and I_2 respectively. The effect of electron scavengers and of ethanol on the transient yields have been studied.

I N T R O D U C T I O N

It has been found that [1] X_2^- radical anions (where X represents a halide ion) are formed by flash photolysis of the halide ions in water. These transients have main absorption band peaks at 385 nm, 360 nm and 350 nm for I_2^-, Br_2^- and Cl_2^- respectively, and a common smaller band near 300 nm. It was suggested that these species were in equilibrium with the atom and the monoatomic ion. It has been also indicated 2 that an equilibrium may be occurring between I, I^-, and I_2^-, as indicated in the flash photolysis work.

---

* Chemistry Department, College of Science, Al-Mustansiriyah University, Baghdad, IRAQ.

Al-Mustansiriyah Journal of Science, Vol.4, No.1. (1979)

A number of papers [3, 4] have been publisned concerning the pulse radiolysis of aqueous solutions of alkali halides at various PH values. The transient species absorbing light in the U.V. region were identified as Ci_2^- , Br_2^- and I_2^- in these works. The following formation of Br_2^- and I_2^- at neutral pH was given :

$$X^- + OH \longrightarrow X + \dot{O}H \quad \ldots\ldots\ldots (1)$$

then

$$X + X^- \longrightarrow X_2^- \quad \ldots\ldots\ldots (2)$$

Dainton et.al. [5] have provided evidence for the production of an oxidizing radical and I_2^- formation on pulse radiolysis of iodide ions in methanol. Theard and Burton [6] investigated ^{60}Co γ-irradiation of methanol solutions of KI and several other salts and suggested tnat the methoxy radical oxidized the iodide ion in a manner similar to reaction (1) as,

$$X^- + RO \longrightarrow X + RO^- \quad \ldots\ldots\ldots (3)$$

Hamill [7] proposed that X could be formed at high concentration or halide ions by the reaction

$$H_2O^+ + X^- \longrightarrow H_2O + X \quad \ldots\ldots\ldots (4)$$

other authors [8 - 10] have supported the idea of I_2^- formation from both pulse radiolysis and γ -radiolysis experiments.

We have now extended this work by studying (a) the absorption spectra at longer wavelengths where the trapped electrons absorbs (up to 800 nm), using strong alkaline medium (glassy systems at 77^oK) ; (b) the efrects or some other solutes, e.g. nitrous oxide and ethanol.

EXPERIMENTAL

1.) Materials :-

Potassium hydroxide and Potassium iodide are both B.D.H. Analar grade, used without any further purifications. Ethanol (Hopkin and Williams) spectrosol grade bottled under nitrogen gas was used without any further purification. Acetone (Hopkin and Williams) Analar grade was used without any further purification. Nitrous oxide (British oxygen Co. Ltd.) gas was collected into evacuated pyrex glass storage vessel surrounded by liquid nitrogen and attached to the vacuum line. Gaseous impurities not condensable at $77^{o}K$ were removed by thaw-freeze-pump cycles. Further purification was obtained by several distillations to and from a second storage vessel cooled in liquid nitrogen. Only the middle fractions of the distillates were retained. All aqueous solutions were made using triple distilled water.

2.) Thermal annealing :-

Thermal annealing of the samples was carried out in order to observe subsequent chemical reactions which occurred upon warming in the system investigated. Using the temperature control which was available and fitted with the RIIC unit (sample heaters), one could raise the temperature of the system very slowly by switching the sample heaters on and evaporating the liquid nitrogen [11] By doing this, and cooling down after switching the sample heaters off, the spectra of the trapped intermediates were recorded at different temperatures.

Resolution of the absorption bands :-

The Du Pont curve resolver was used to resolve all the absorption bands obtained in this work. The instrument utilizes a series of function generating channels (upto 10), each capable of generating a single distribution function on a cathode ray tube. Any given number of these functions can be positioned, shaped and summed until a trace is obtained that will match the experimental curve envelope. The instrument is capable of generating peaks corresponding to Gaussian, Lorentizian or other common distribution or modification thereof. Assymetrical shapes caused by skewing or base line distortion can easily be accomodated. In this manner, the instrument enables the experimenter to rapidly resolve a curve envelope containing a variety of widely differing, overlapping peaks with a minimal instruction period. Since the Gaussian, or normal distribution function is common to all types of U.V.-visible spectroscopy, the above distribution was used to resolve all the curves obtained in this work.

4.) Irradiation and dosimetry, optical absorption measurements at 77°K, variable temperature unit, sample preparation and photobleaching processes are all given in a previous paper[11].

RESULTS AND DISCUSSION

1.) Radiolysis of potassium iodide in 7M KOH glass at 77°K

In this work, oxygen free (deaerated) potassium iodide

solutions of different concentrations (0.1 M - 2 M) were γ-irradiated in 7M KOH glass at 77°K and studied spectroscopically. An absorption at 383 nm is attributed to the I_2^- radical anion obtained by thermally annealing the samples. The I_2^- radical anion can be formed, either initially via OH radical reaction or via O^- reaction, since in 7M KOH glass the OH radical reacts with $\bar{O}H$ ions to form O^- ;

$$OH + \bar{O}H \longrightarrow O^- + H_2O \quad \ldots\ldots\ldots (5)$$

The following reactions are proposed for the formation of both the intermediates and the I_2^- radical anions in such a medium.

either $I^- + O^- \longrightarrow IO^{2-}$ ..... (6)

then $IO^{2-} + I^- \longrightarrow I_2^- + O^{2-}$ ..... (7)

or $I^- + OH \longrightarrow IOH^-$ ..... (8)

then $IOH^- + I^- \longrightarrow I_2^- + OH^-$ ..... (9)

High concentrations (2M) of Potassium iodide in 7M KOH glass are γ-irradiated at 77°K and their spectra shows before annealing a sharp absorption at 370 nm with a broad overlapping absorption located between 300 nm and 350 nm. After annealing the above absorption, two absorption bands were obtained peaking at 341 nm and 380 nm as shown in Fig.(1). The first absorption is attributed to an intermediate formed by either reactions (6) and (8), while the second absorption is attributed to the I_2^- radical anion.

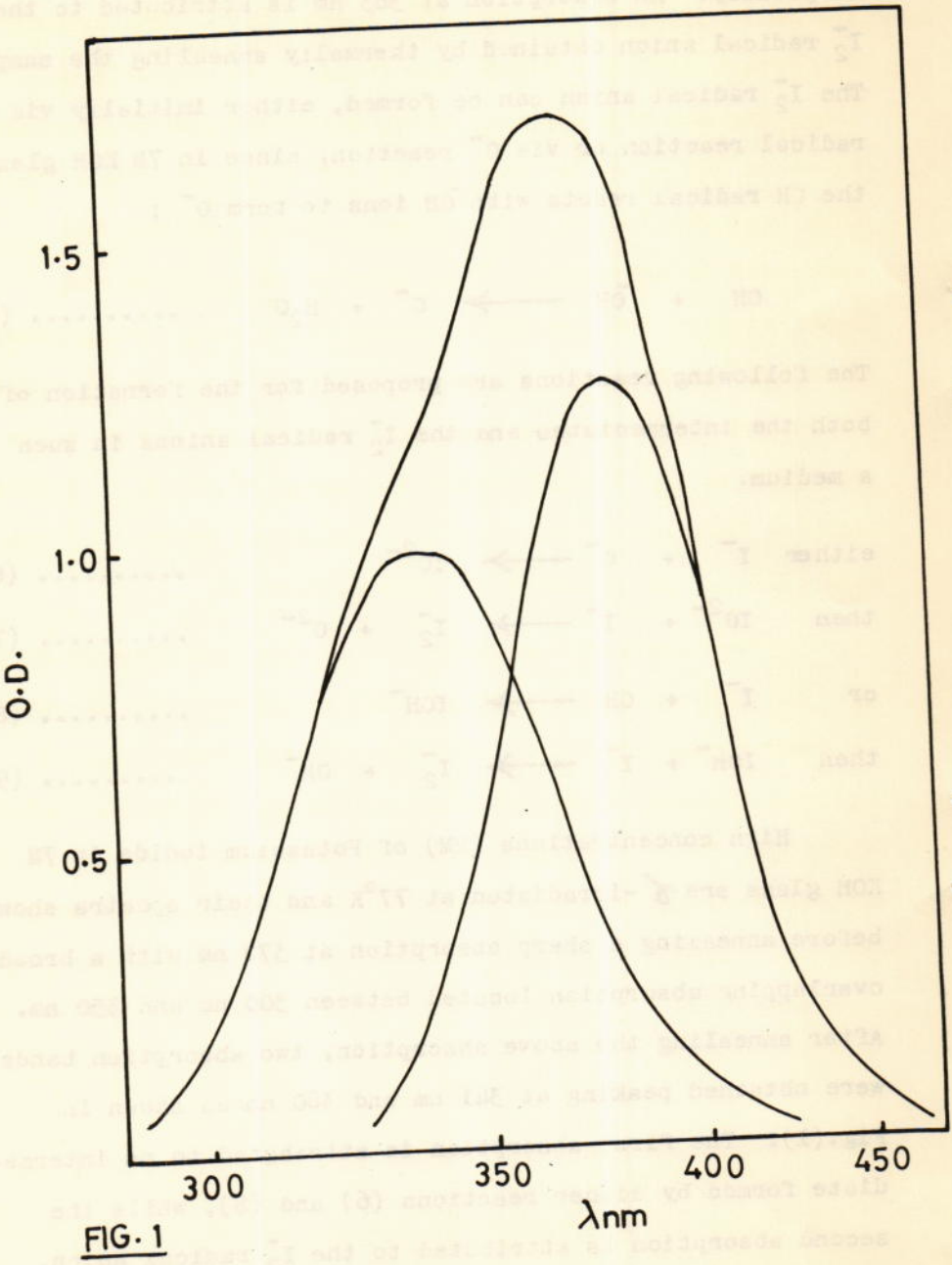

FIG. 1

After excluding both iodine atom formation [12] and IO_2^- formation [13] it seems reasonable to conclude that the 341 nm is probably due to IO^{2-} and/or IOH^-. The broad absorption at 300 - 350 nm was found to be unstable on annealing and disappeared, after elevating the temperature to about 160 - 165°K leaving the 370 nm absorption which by this time shifted to a longer wavelength (380 nm) and increased in intensity. This absorption spectrum was resolved into two absorption bands (i) a very strong absorption band peaking at 380 nm and attributed to the I_2^- radical anion and (ii) a broad, weak band located at 446 nm which is assigned to I_2 formed during the decay of the I_2^-. Iodine absorbs in aqueous and alcoholic solutions between 430 nm and 470 nm, inagreement to this assignment.

After further annealing the sample, the absorption at 380 nm decayed slowly giving rise to a very broad absorption of reasonable intensity. This on analysis was found to consist or three bands peaking at 352 nm, 383 nm and 446 nm (Fig.2). The 383 nm absorption is presumed to be due to the I_2^- radical anion. The 352 nm absorption, which is broad and of reasonable intensity is assigned to I_3^- formed during the decay of I_2^-. Thus both I_2 and I_3^- exist in equilibrium with each other at low temperature.

$$I_2 + I^- \rightleftharpoons I_3^- \qquad \ldots\ldots\ldots\ldots (10)$$

The above explanation is supported by some experiments [14,15]. Assuming that I_3^- and I_2 at room temperature are the same as in glassy systems at liquid nitrogen temperature, a

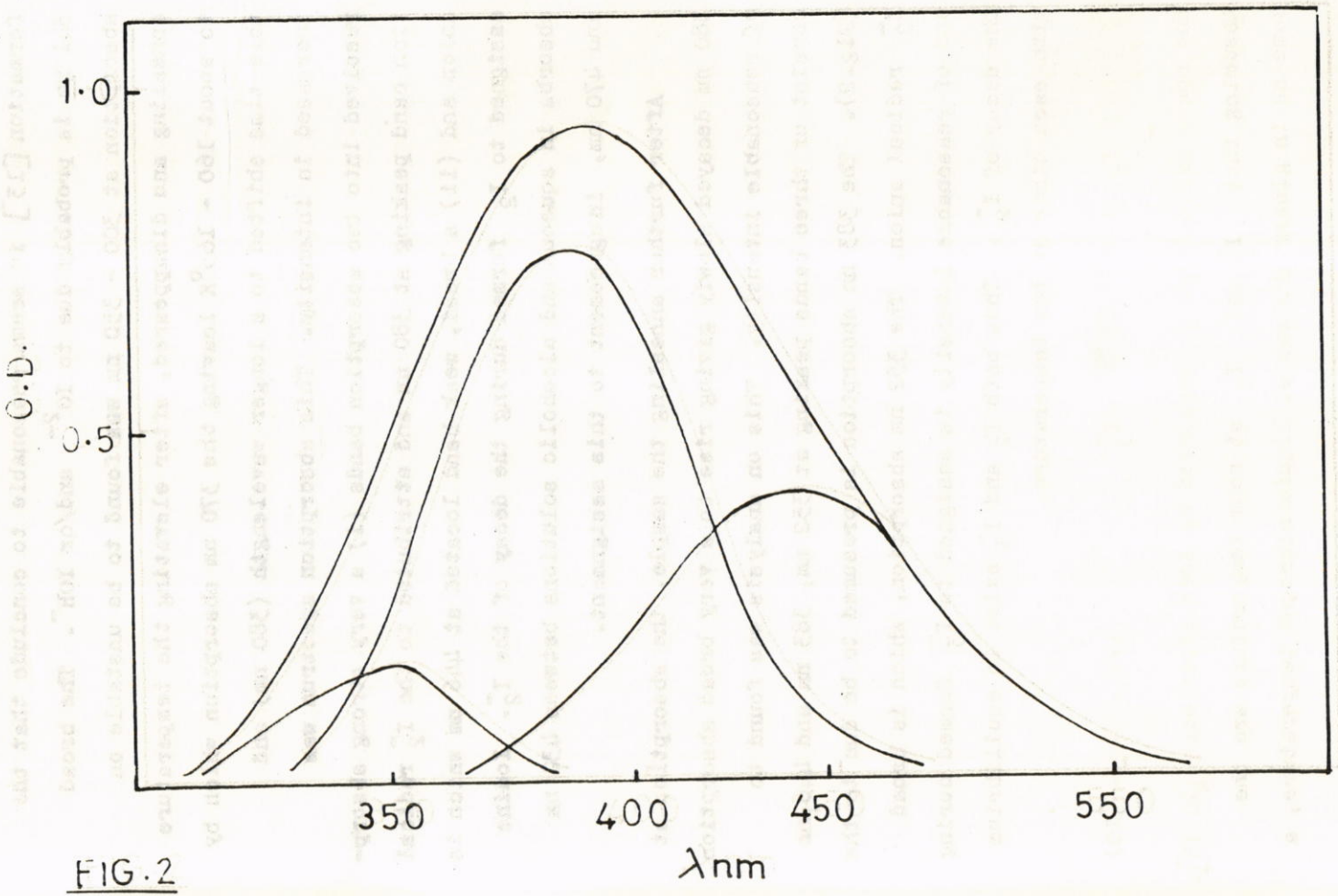

FIG·2

value or 0.798×10^{-3} M^{-1} for K_{10} is obtained. This value agrees well with that obtained by Awtrer and Connick [16], e.g. 0.654×20^{-3} M^{-1} at 1°C.

It is well known that both I_2 and I_3^- are very unstable in 7M KOH at room temperature, but it may be possible for the above entities to exist at low temperatures. It is well known [17] that the yield of O^- increases with increasing ^-OH concentration, also the yield - dose plots[18] for O^- formation in irradiated alkaline glasses are approximate linearity to at least 13 M rads. The two above statements give support to the explanation of I_2^- formation via O^-. However, when 2 M potassium iodide was given different doses in 7 M KOH glass, the I_2^- yield product was increased linearly with increasing dose. This linearity is shown in (Fig. 3). The evaluation of the data leads us to G (I_2^-) at 383 nm = 0.8 ± 0.05. Comparing the above value of $G(I_2^-)$ with the reported $G(O^-) = 1.7$ [17], gives further support for the I_2^- formation through O^- reaction. The small difference between the two values is attributed to the possibility of some I_2^- decay during the annealing process.

It was found that increasing the iodide concentration led to a decrease in the absorption at 580 nm attributed to e_{tr}^-. The decrease was linear with iodide concentration as shown in the plot of the optical density at 580 nm against iodide concentration (Fig. 4). The above phenomena was noticed in the high concentration of iodide and attributed

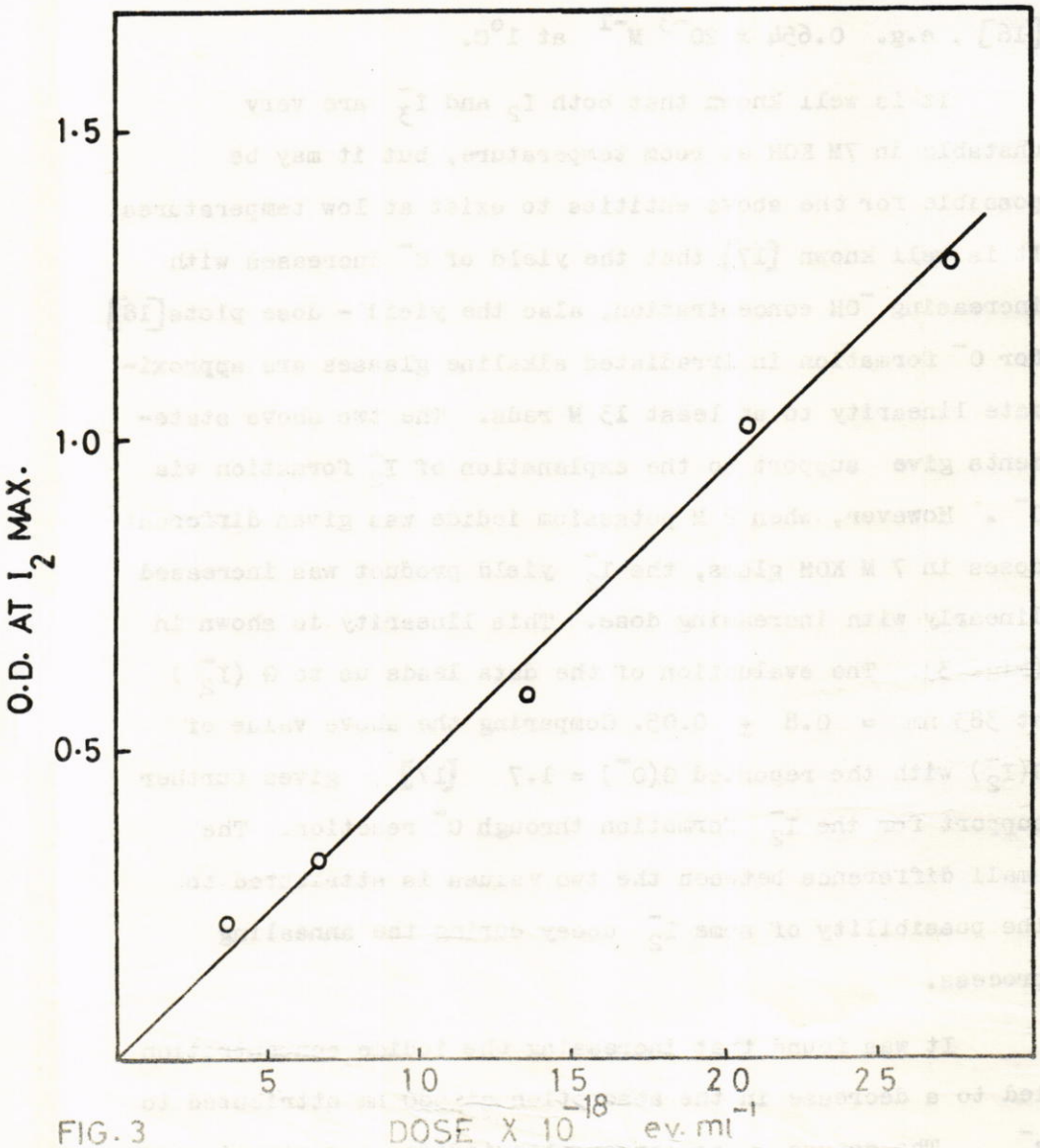

FIG. 3

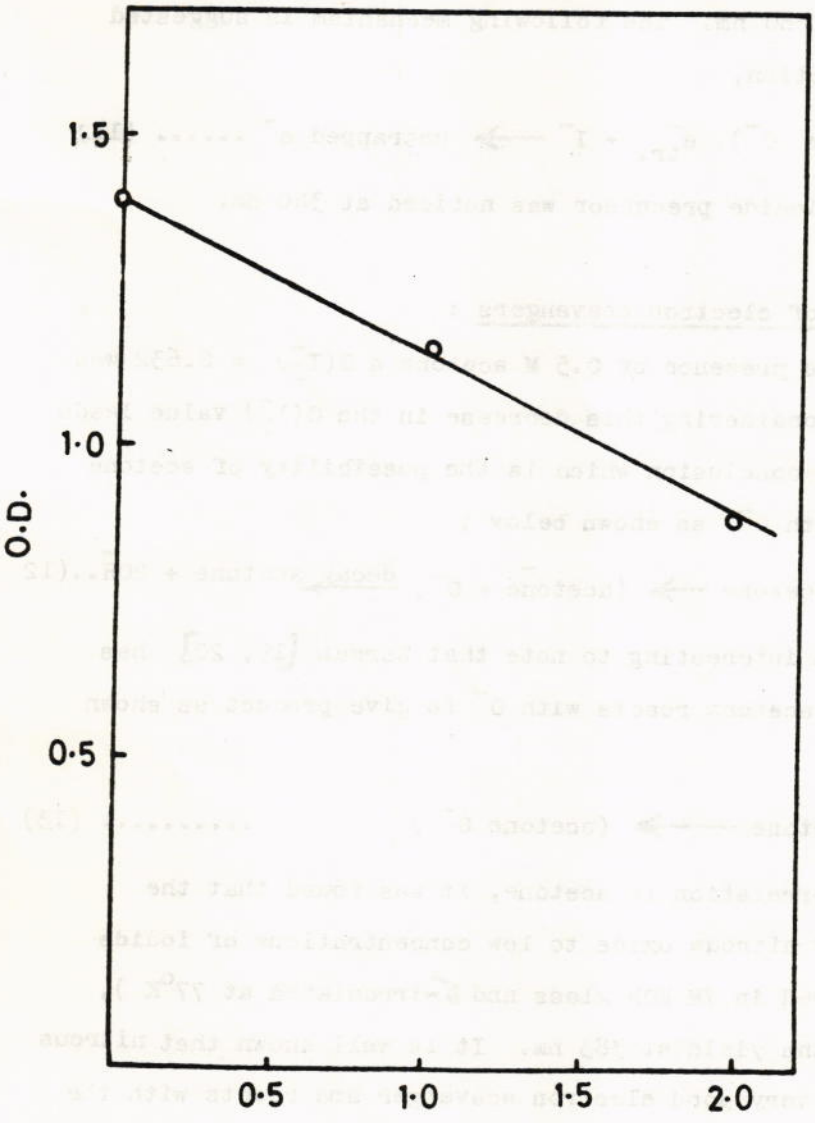

FIG. 4

to a correlation between the hole (H_2O^+ or O^-), the electron e^-_{tr} and the iodide ion. In this correlation it is suggested that some iodide ions oxidized by the hole leaving the trapped electrons untrapped and causing the decrease at 580 nm. The following mechanism is suggested for the reaction,

$$(H_2O^+ \text{ or } O^-), e^-_{tr.} + I^- \longrightarrow \text{untrapped } e^- \quad \ldots\ldots (11)$$

since some iodide precursor was noticed at 340 nm.

2.) <u>The effect of electron scavengers</u> :

In the presence of 0.5 M acetone a $G(I_2^-)$ = 0.632 was obtained. Considering this decrease in the $G(I_2^-)$ value leads us to a new conclusion which is the possibility of acetone reacting with O^- as shown below ;

$$(e^- + O^-) + \text{acetone} \longrightarrow (\text{acetone} + O^-) \xrightarrow{\text{decay}} \text{acetone} + 2OH^- \ldots (12)$$

It is interesting to note that Warman [19, 20] has found that acetone reacts with O^- to give product as shown below ;

$$O^- + \text{acetone} \longrightarrow (\text{acetone } O^-) \quad \ldots\ldots\ldots (13)$$

In correlation to acetone, it was found that the addition of nitrous oxide to low concentrations of iodide (all prepared in 7M KOH glass and γ-irradiated at 77°K), increases the yield at 383 nm. It is well known that nitrous oxide is a very good electron scavenger and reacts with the electron (in solution) to form O^- according to the following reaction;

$$e^- + N_2O \longrightarrow N_2O^- \longrightarrow N_2 + O^- \quad \ldots\ldots\ldots (14)$$

In the presence of 3 atmospheres of nitrous oxide a $G(I_2^-)$ = 1.62 ± 0.1 was obtained which is almost double the value obtained in the absence of nitrous oxide. From the above increase in the $G(I_2^-)$ value it is concluded that one of two things occurred, (1) either an oxidation of I^- by the formed N_2O^- from reaction above, or (2) reaction (14) is true in glassy medium at low temperature from which N_2O act as a good supplier of O^-, which causes the oxidation of the iodide ion. However in both cases (1) and (2) more I_2^- is expected. In the presence of nitrous oxide a more distinct absorption at 340 nm attributed to the suggested intermediate $(IO)^{2-}$ was obtained.

Competition study with ethanol ;

It was found that the presence of ethanol in γ-irradiated 0.2M potassium iodide in 7M KOH at 77°K decreases the absorption at 383 nm in the competition study. A linear relation (Fig.5) was obtained by plotting the optical density at 383 nm after annealing versus ethanol concentration. A similar relationship was obtained by plotting 1/O.D. versus ethanol concentration. It has been reported that O^- react with ethanol, methanol, and isopropanol [19, 20] in the gas phase and with ethanol and methanol [21] in the liquid phase. The decrease in the 383 nm absorption is attributed to a competition between I^- and ethanol towards O^-. The following reactions are suggested ;

$I^- + O^- \longrightarrow$ Product ..... (15)

E $+ O^- \longrightarrow$ Product ..... (16)

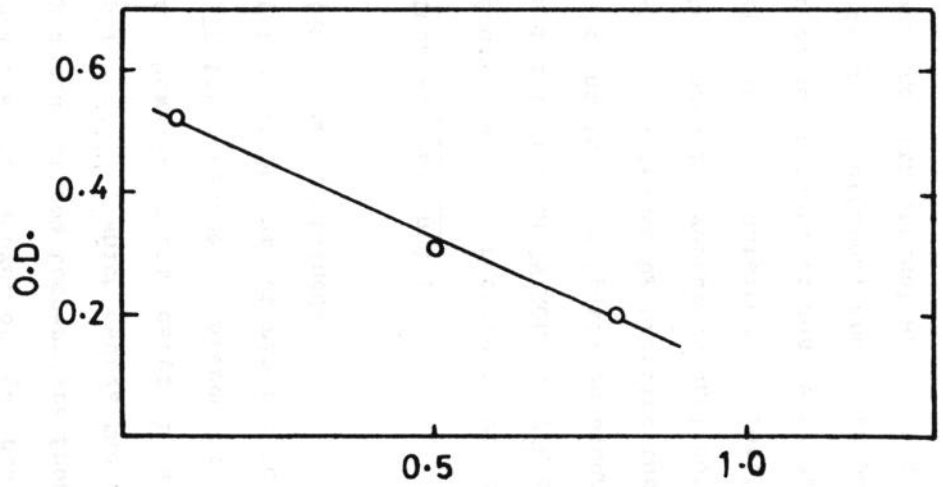

FIG. 5

From the above reactions it follows that :

$$\frac{1}{(O.D)_{obs.}} = \frac{1}{(O.D)_{max.}} + \frac{1}{(O.D)_{max}} \cdot \frac{K_{16}}{K_{15}} \cdot \frac{[E]}{[I^-]} \quad \ldots\ldots\ldots (17)$$

where $(O.D)_{max.}$ and $(O.D)_{obs.}$ represent the optical density in the absence and the presence of ethanol respectively. From the slope it can be deduced that $K_{16} = 6.1\ K_{15}$. It is of interest to note that Buxton has reported a K_{16} value of $(8.4 \pm 1.7) \times 10^8\ M^{-1}\ s^{-1}$ and $K_{15} = 9.4 \times 10^{18}\ M^{-1}\ s^{-1}$ [22] .

REFERENCES

1.) L.I. Grossweiner and M.S. Matheson, J. Phys. Chem.,61, 1089 (1957).

2.) J.K. Thomas, Private Communication.

3.) M.Anbar and J.K. Thomas, J. Phys. Chem., 68, 2829 (1964).

4.) J.H. Baxendale, P.L.T. Bevan and D.A. Scott, Trans. Farad. Soc., 64, 2398 (1968).

5.) F.S. Dainton et.al., J. Chem., Soc., D(7), 335-6 (1969).

6.) L.M. Theard and M. Burton, J. Phys. Chem., 67, 59 (1963).

7.) W.H. Hamill, J. Phys. Chem., 73, 1341 (1969).

8.) F.S. Dainton, I.V. Janovsky and G.A. Salmon, Chem. Commun., 335 (1969).

9.) A. Zalionk - Gitter and A. Treinin, J.Chem. Phys., 42 (6), 2019 - 28 (1965).

10.) C.J. Delbecq, W. Hayes and P.H. Yuster, Phys. Rev., 121, 1043 (1961).

11.) S.K. Ismail, Al-Mustansiriyah J. of Science, Vol.3 (1978).

12.) M.E. Langmuir and E. Hayon, J. Phys. Chem., 71, 3808 - 14 (1967).

13.) O. Amichai and A. Treinin, J. Phys. Chem, 74 (4), 830 (1970).

14.) D. Meyerstein and A. Treinin, Trans. Farad. Soc., 59, 1114 (1963).

15.) E.N. Borisova and L.T. Bugaenko, M.U. Lomonosov, Moscow State University, Translated from Khimiya Vysokikh Energii, Vol. 3, No.3, p.p. 279 (1969).

16.) A.D. Awtrer and R.G. Connick, J.Am. Chem. Soc., 73, 1842 (1951).

17.) P.N. Morthy and J.J. Weiss, Phil. Mag., 10, 659 (1964).

18.) J. Zimbrick and L. Kevan, J.Am. Chem. Soc, 89, 2483 (1967)

19.) J.M. Warman, Nature, 213, 5074, 381 - 2 (1967).

20.) J.M. Warman, J. Phys. Chem., 72, 52 - 56 (1968).

21.) G.V. Buxton, Trans. Farad. Soc., 66 (7), 1656 - 60 (1970)

22.) G.V. Buxton, Trans. Farad. Soc., 65, 2150 (1969)

γ - IRRADIATION OF BENZOPHENONE IN ORGANIC GLASSES AT 77° K

Saad K. Ismail* and G. Scholes

A B S T R A C T

A spectroscopic technique has been used to study the transients formed in the γ-irradiation of benzophenone in basic isopropanol and in some other organic glasses at 77°K. Absorption bands at 610 nm is assigned to the benzophenone radical anion and the mechanism for its formation is discussed. Electron transfer from acetone negative ion to benzophenone has been studied. The effects of added electron scavengers (nitrous oxide SF_6, and oxygen) have been investigated.

I N T R O D U C T I O N

The formation of trapped electrons in the γ-radiolysis of glassy matrices has been demonstrated by Hamill [1]. The effect of added solute illumination with visible light or U.V. light and thermal annealing of the visible and the U.V. spectra of γ-irradiated glassy methanol were investigated [2 - 4]. Shuttle worth [5] proposed the possibility that

* Chemistry Department, College of Science, Al-Mustansiriyah University, Baghdad, IRAQ.

Al-Mustansiriyah Journal of Science, Vol.4 No.1 (1979).

the absorption spectrum of the trapped electron in 2-propanol glass is a reflection of the concentration of alkoxonium ions and is depended on the relative rates of protonation equilibria.

The formation of benzophenone radical anion and Ketyl radical have been studied by many authors in both organic and aqueous media [6 - 28] . Most of the studies are carried out in solution at room temperature. Under these conditions the radicals decayed very rapidly. In all cases the authors observed the transient of benzophenone radical anion at 610 - 650 nm, while they found the Ketyl radical absorbing at 545 - 550 nm. The above two species are formed either photochemically or by pulse radiolysis. Some authors [15, 16] have suggested that the Ketyl radical anion formed in the solution is associated with an alkali metal positive ion and the following structures were suggested ;

and

in the case of a divalent positive ion [17] .

On the basis of the above mentioned observations in the present work, the γ-irradiation of benzophenone in both aqueous and organic basic glasses were suggested.

EXPERIMENTAL

1.) Materials :

Sodium hydroxide is B.D.H. and of AnalaR grade used without any further purification.

2- Propanol (Hopkin and Williams) spectrosol grade bottled under nitrogen gas, used without further purification. Acetone, ethanol, methanol, isobutanol and n- propanol (Hopkin and Williams) of AnalaR grade used without further purifications. t-butanol was purified by two successive vacuum - distillations in an atmosphere of dry nitrogen into a storage bulb attached to the vacuum line and only the middle fractions of the distillates were retained for use. nitrous oxide, oxygen, and SF_6 were from British oxygen Co.Ltd. Purified before use as in the procedure mentioned before [29] . Hexene was purified by triple fractionation under vacuum and only the middle fractions were used.

2.) All other experimental details are given in a previous paper [29, 30] .

RESULTS AND DISCUSSION

1.) -radiolysis of benzophenone in 7M NaoH glass at $77^{o}K$

A broad absorption located at 600 nm was obtained by γ -irradiation of benzophenone in 7M NaOH glass. This absorption was found to be unstable at high temperatures

($160^{o}k$). It decreases in intensity to give another broad absorption at 620 nm. This new absorption is similar to the one obtained by Adams et.al [18] . The first absorption (600 nm) is assigned to an overlapping between two absorptions, (1) the trapped electron and (2) a transient for the benzophenone. The absorption at 620 nm is attributed to the negative ion formed from direct electron attachment to benzophenone ;

$$\Phi_2 CO + e^- \longrightarrow (\Phi_2 CO)^- \quad \ldots\ldots\ldots (1)$$

The yield of this negative ion may be found to be very small, due to the low concentration used (low solubility of the compound in 7M NaOH). The calculated $G(\Phi_2 CO)^-$ is found to be 0.5, by assuming that the benzophenone radical anion and its neutralized form are the same as in solution at room temperature. This G value may be too high, since some of the trapped electron may well be present. Fig.(1) shows all details.

2.) <u>-irradiation of benzophenone in basic isopropanol glass (0.1 - 0.4 M NaoH) at $77^{o}K$</u> ;

In this system the samples are either (a) thermally annealed or (b) photobleached, then thermally annealed.

(a) An initial broad absorption located at 640 nm was obtained by γ-irradiating 10^{-3} M benzophenone in basic isopropanol glass Fig.(2). This disappeared after annealing to about $160^{o}K$ and instead a new absorption at

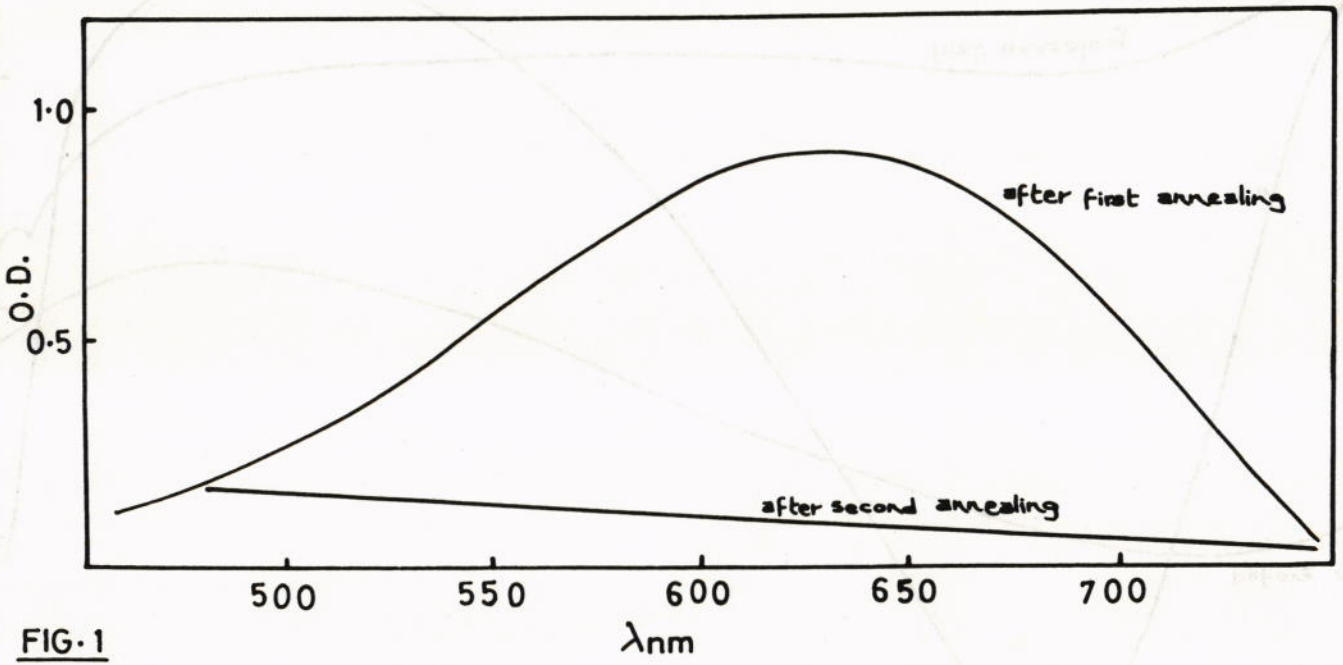
1·0
0·5
O.D.
after first annealing
after second annealing
500
550
600
650
700
λnm

FIG·1

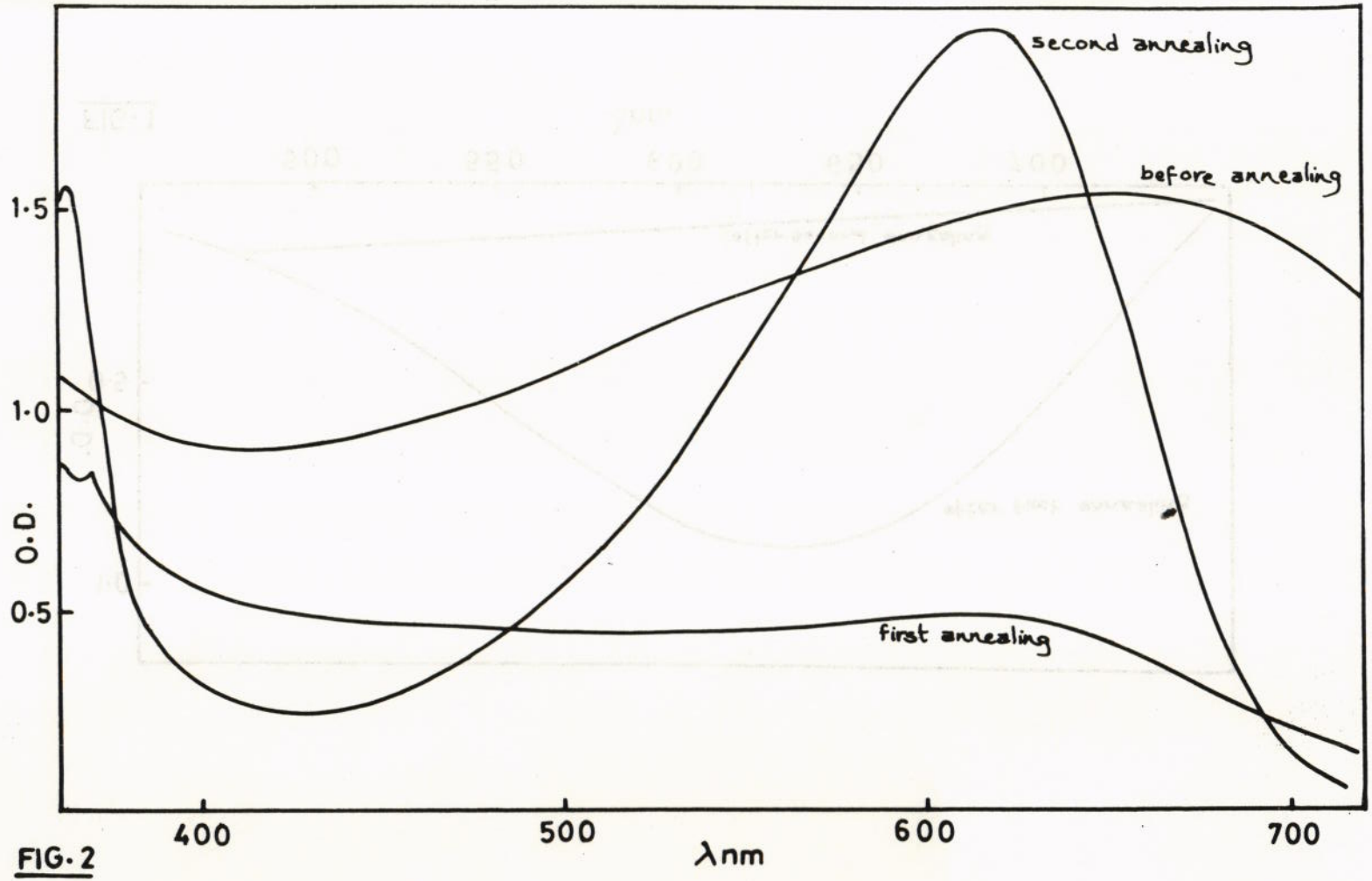
second annealing
before annealing
first annealing
1·5
1·0
0·5
O.D.
400
500
600
700
λnm

FIG·2

610 - 620 nm appeared, which increased in intensity after further annealing. At the same time another weak absorption at 363 nm appeared. The 640 nm absorption is assigned either to the trapped electron with some benzophenone negative ion formed by direct attachment of the electron to the benzophenone molecule or to the benzophenone negative ion alone. The 620 nm absorption is attributed to the benzophenone negative ion, formed through an anionic electron transfer from the isopropanol radical anions. The isopropanol radicals which are formed during the irradiation are ionized in the highly alkaline medium. The following reactions are proposed;

$$(CH_3)_2\dot{C}H\ OH \rightsquigarrow (CH_3)_2 - \dot{C} - OH \qquad \ldots\ldots\ldots(2)$$

$$(CH_3)_2\dot{C}OH + {}^{-}OH \rightarrow (CH_3)_2 - \dot{C} - O^{-} \qquad \ldots\ldots\ldots(3)$$

$$\text{then } (CH_3)_2\dot{C}-O^{-} + (C_6H_5)_2\,CO \rightarrow (C_6H_5)_2\dot{C}O^{-} + (CH_3)_2CO \qquad \ldots\ldots(4)$$

The absorptions are similar to those obtained by Adams et al. [18, 19] .

The 363 nm absorption is assigned to the OH or O^{-} adduct to the aromatic ring. In the liquid state Adams et.al. [19] have found an increase in the acetone yield product, which support the above anionic electron transfer.

(b) For the photobleached samples, after photobleaching the trapped electron, only a weak absorption was left at 640nm. On thermally annealing, the same results as in (a) were obtained and explained on the same basis as shown in Fig.(3).

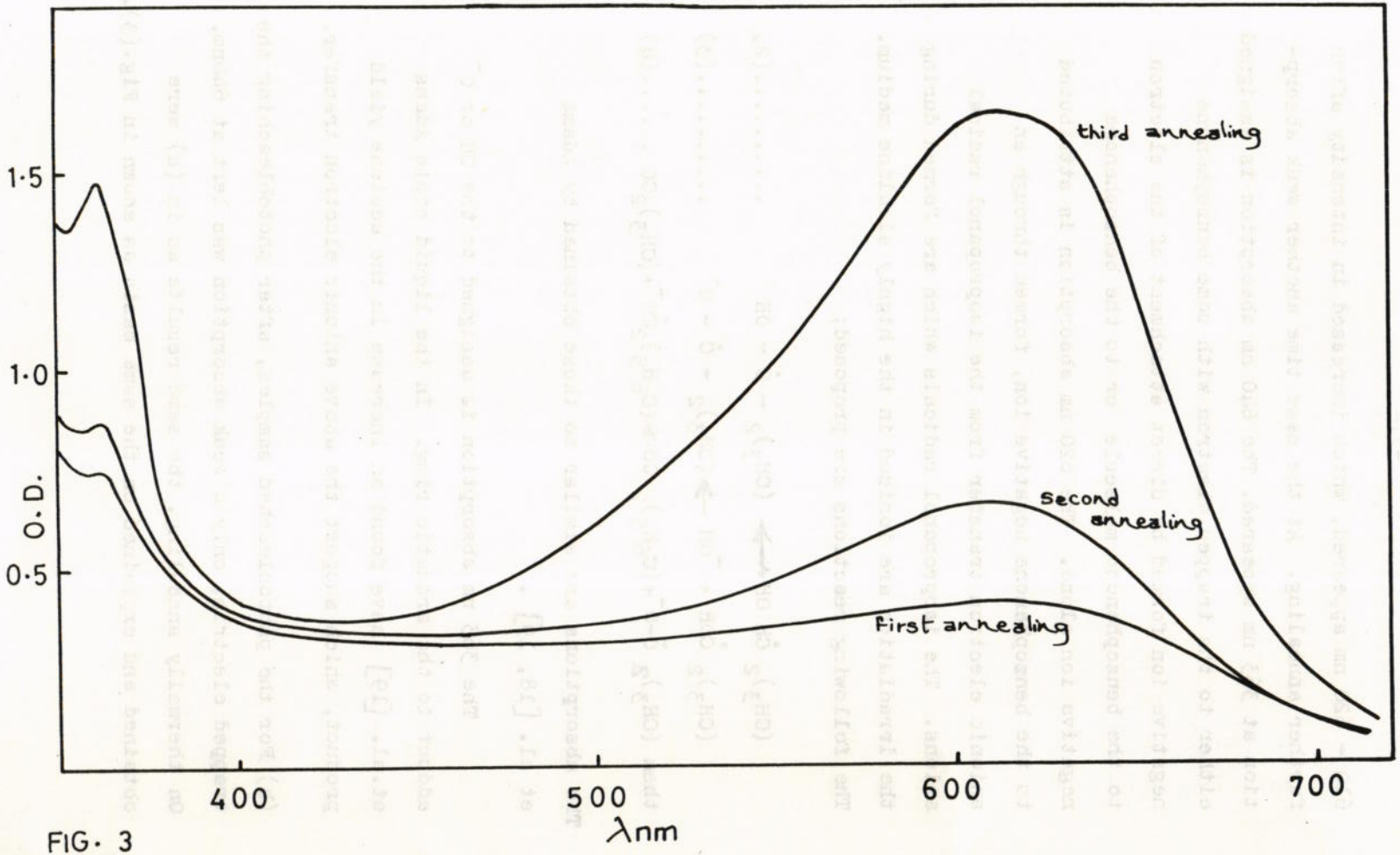
third annealing
second annealing
First annealing
1·5
1·0
0·5
O.D.
400
500
600
700
λnm

FIG. 3

3.) γ-radiolysis of benzophenone in some other glasses at 77°K;

(a) Since benzophenone is only slightly soluble in 7M KOH, higher concentration of the material was prepared in 7M KOH by dissolving the solute in ethanol first. A weak and broad absorption at 605 nm was obtained after annealing the irradiated sample. This absorption is assigned to an overlapping between the two absorpticns (1) the trapped electron and (2) a transient for the benzophenone formed either by direct electron attachment or via anionic electron transfer from ethanol negative ion. The G value calculated for $(C_6H_5)_2 - \dot{C}-o^-$ is found to be about 0.6, since ethanol concentration was low, the low G value is expected.

(b) In basic methanol glass Fig.(4), 2×10^{-3}M benzophenone was γ-irradiated. A broad absorption at 585 nm was obtained which disappeared after the annealing and instead a new absorption at 610 nm was obtained. The first absorption is assigned to the trapped electron, which is similar to that obtained by Adams et.al. [20] and was assigned to the solvated electron in basic methanol solution. The second absorption is assigned to the benzophenone radical anion formed through anionic electron transfer from methanol radical anion formed during the irradiation.

$$\dot{C}H_2O^- + (C_6H_5)_2CO \longrightarrow (C_6H_5)\dot{C} - O^- + CH_2O \quad \ldots\ldots\ldots (5)$$

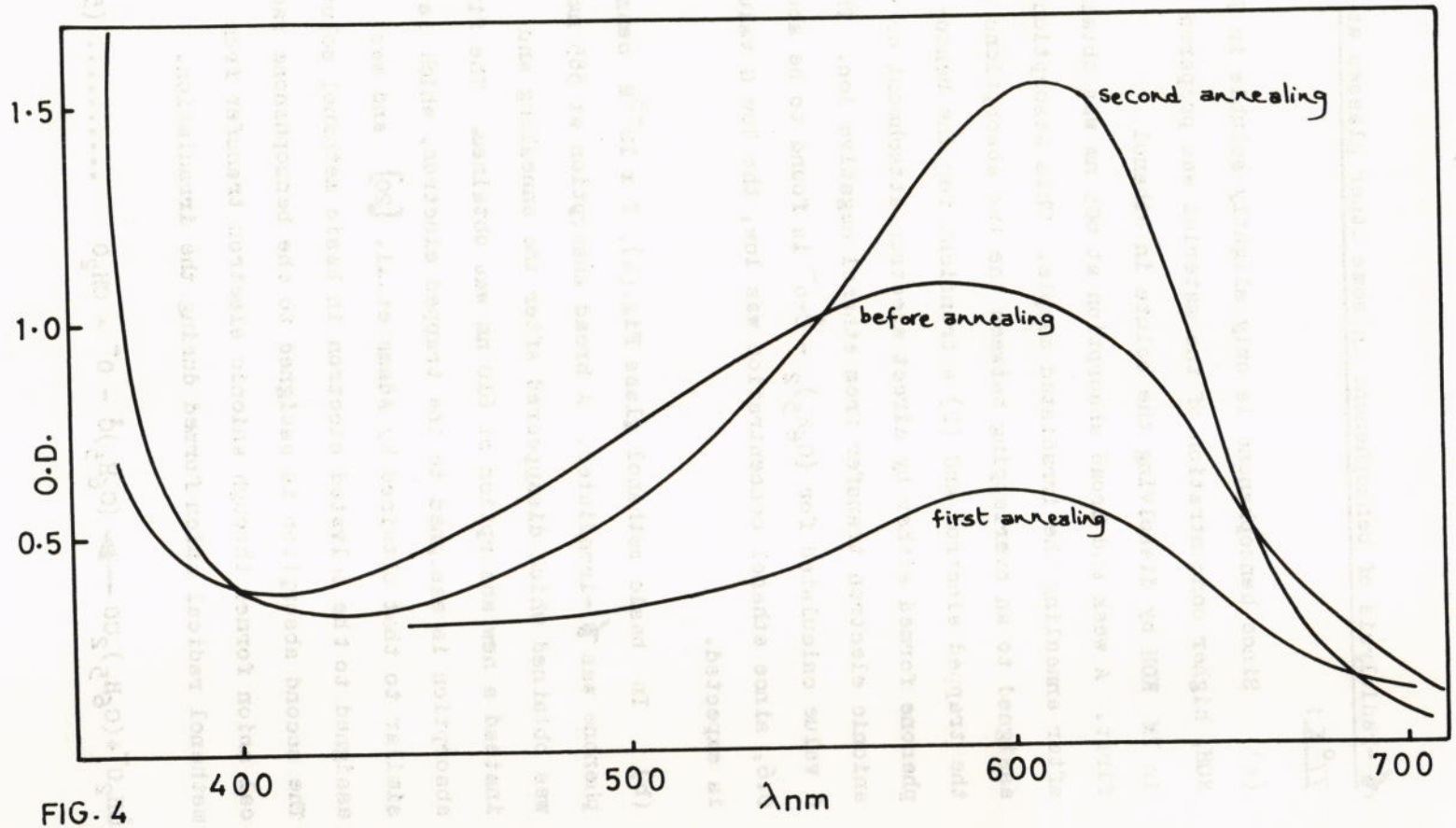
1·5
1·0
0·5
O·D.
second annealing
before annealing
first annealing
400
500
600
700
λnm

FIG. 4

The G $(C_6H_5)\dot{C}O^-$ is found to be about 1.1 which is almost identical to the one obtained in the case of basic isopropanol glasses.

(c) Using basic ethanol a very low yield was obtained for the benzophenone radical anion Fig. (5) formed in a similar manner as in (a). The G value is found to be about 0.5. This low G value may be due to the low melting point of the glass, at which the decay of the radical anion may occur.

(d) Benzophenone is found to behave similarly as in the above cases in basic normal propanol Fig.(6). In this medium the same 615 nm absorption is obtained after the thermally annealing process of the γ-irradiated sample. This absorption is again assigned to the benzophenone radical anion formed by the anionic electron transfer as shown below :

$$CH_3CH_2\dot{C}H\text{-}O^- + (C_6H_5)_2\,CO \longrightarrow (C_6H_5)_2\dot{C}\text{-}O^- + CH_3CH_2CHO \quad \ldots(6)$$

The G $(C_6H_5)_2\dot{C}O^-$ calculated in this medium is 1.04.

(e) The benzophenone radical anion is formed on irradiation of the solute in basic isobutanol at 77°K Fig.(7). A broad and weak absorption was obtained at 605 nm after the annealing. The formation of this radical anion is represented in the reaction below :

$$(CH_3)_2CH_2\,\dot{C}HO^- + (C_6H_5)_2\,CO \longrightarrow (C_6H_5)_2\dot{C}\text{-}O^- + (CH_3)_2CH_2CHO \ldots(7)$$

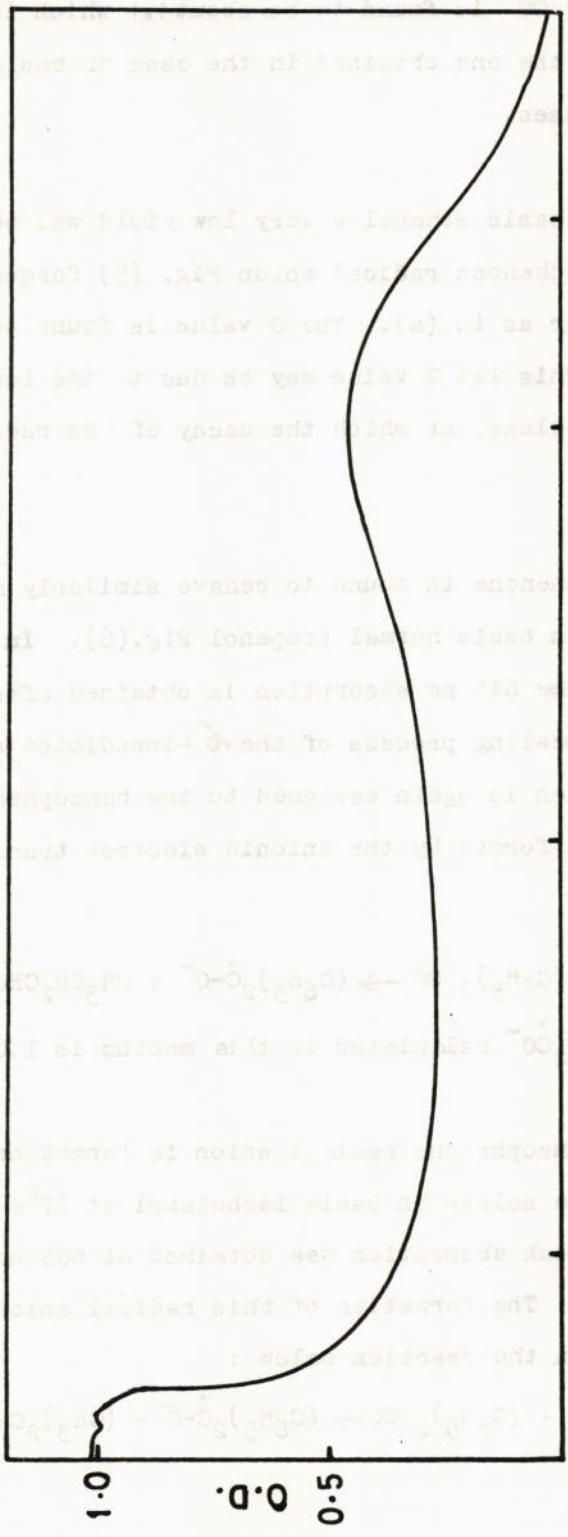

FIG·5

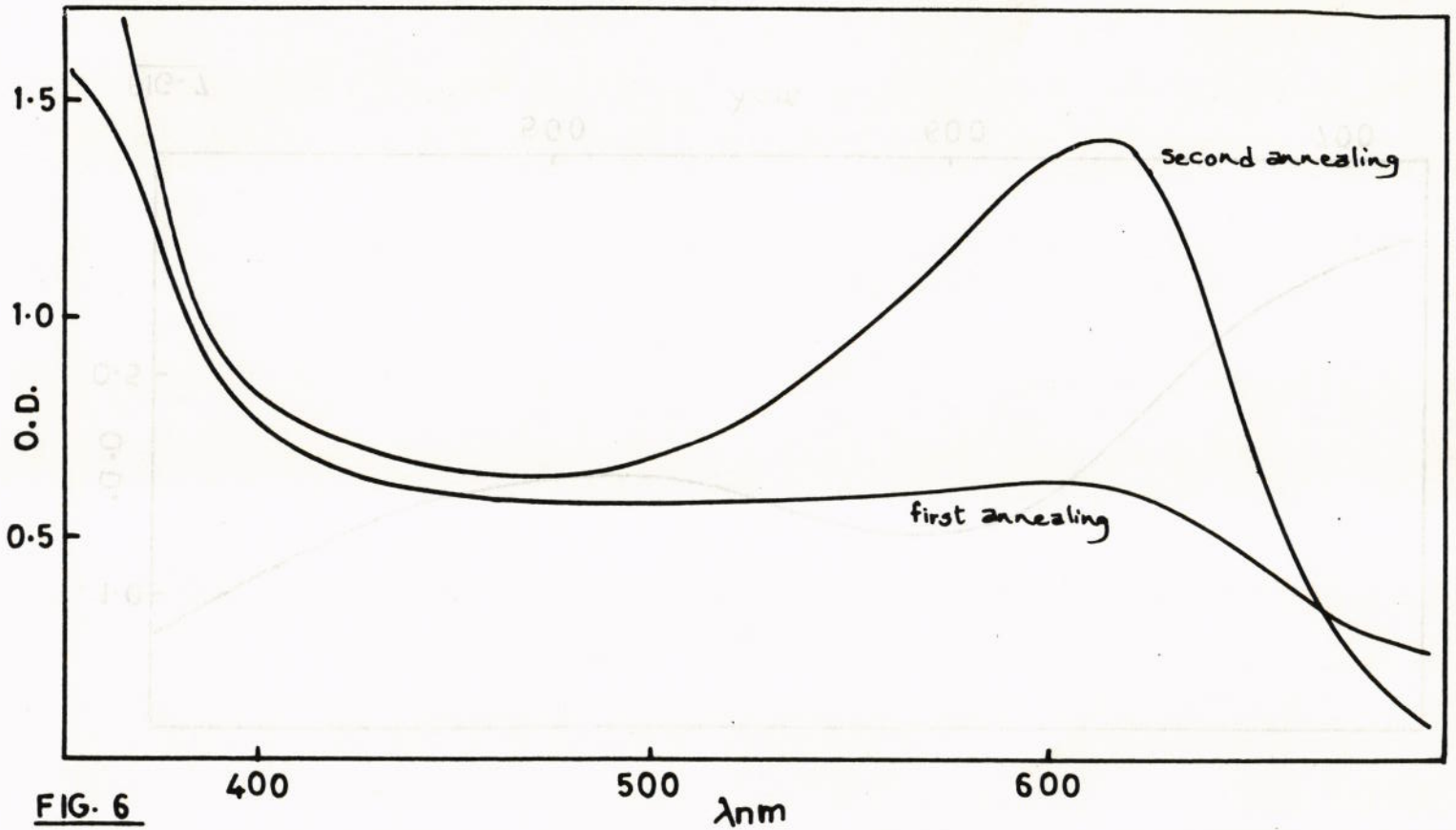

FIG. 6

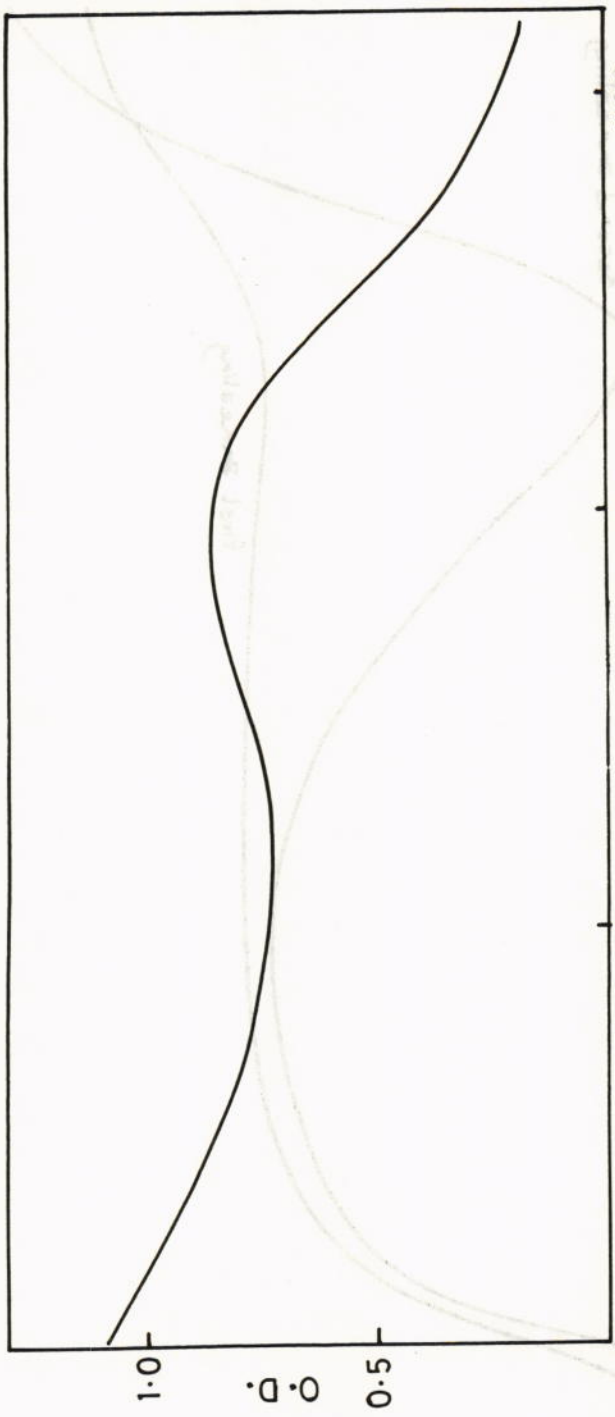

FIG. 7

The G value calculated for the $(C_6H_5)_2 \dot{C} - O^-$ in this medium is about 0.5. The glass is found to be the same as the ethanol one, of low melting point, which explains the low G value obtained.

(f) Benzophenone was γ-irradiated in neutral isopropanol glass Fig.(8), only a very weak absorption at 605 nm was obtained after the annealing process, which disappeared to give a new weak absorption at 554 nm. The 605 nm absorption is attributed to $(C_6H_5) \dot{C} - O^-$ formed by direct attachment. The 554 nm absorption is assigned to the neutralized form of the radical (the Ketyl radical) which may be formed through a neutralization process represented below :

$$(C_6H_5)\,\dot{C}O^- \xrightarrow{H^+} (C_6H_5)\,\dot{C}OH \qquad \ldots\ldots\ldots \quad (8)$$

This experiment gives more evidence for the formation of the benzophenone radical anion through anionic electron transfer process from the alcohol radical anions in the basic medium. From this experiment it is suggested that in neutral medium no alcohol radical anions are expected to be formed.

Effect of electron scavengers ;

The effects of (a) nitrous oxide, (b) oxygen and (c) SF_6 on the formation of benzophenone radical anion has been studied.

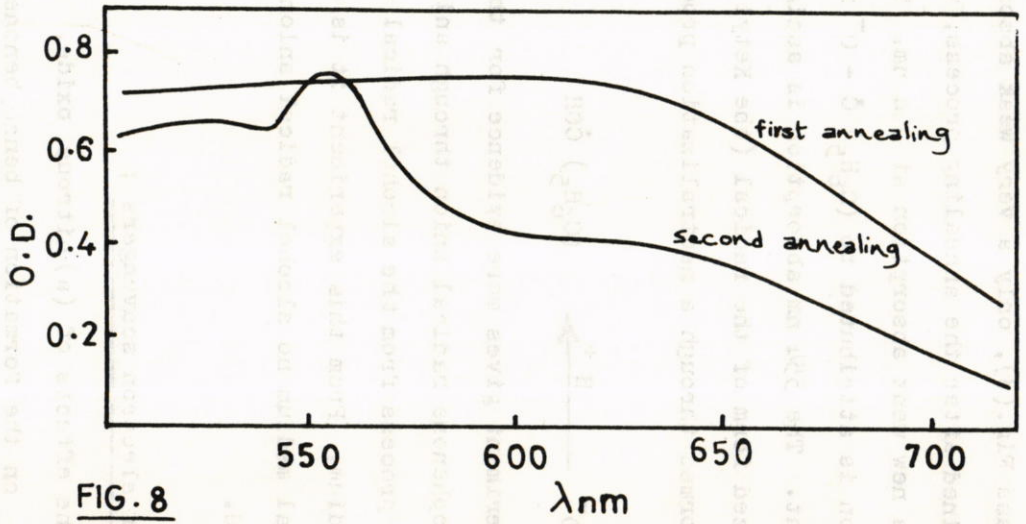
0·8
0·6
0·4
0·2
O.D.
first annealing
second annealing
550
600
650
700
λnm

FIG. 8

(a) It has been found that the addition of nitrous oxide to 10^{-3}M benzophenone decreases the yield product at 610 nm after the irradiation Fig. (9). The same results have been obtained in both photobleached and thermally annealed samples. From the above decrease a competition study was carried out by using different concentrations of nitrous oxide. The above decrease is assigned to the reaction of nitrous oxide with the already formed isopropanol radical anions. In other words, nitrous oxide competes with benzophenone to react with isopropanol radical anions.

$$N_2O + (CH_3)_2 \dot{C} - O^- \xrightarrow{K_9} N_2O^- + (CH_3)_2 \dot{C}O \quad \ldots\ldots (9)$$

and

$$(C_6H_5)_2CO + (CH_3)_2\dot{C}O^- \xrightarrow{K_{10}} (C_6H_5)_2\dot{C} - O^- + (CH_3)_2 CO \quad . \quad (10)$$

A plot was constructed between the optical density and the nitrous oxide concentration Fig. (10). From the above plot a linear relationship was obtained. Considering the expression used in the case of iodide and ethanol system in a similar competition in which $K_1 = K_2$. (slope of the straight line). It has been found in this experiment that $K_9 = K_{10}$.

(b) The presence of oxygen in high concentration is found to have the same effect on the formation of benzophenone radical anion. However the presence of 3 atmospheres of oxygen in the δ-irradiated sample of benzophenone stopped

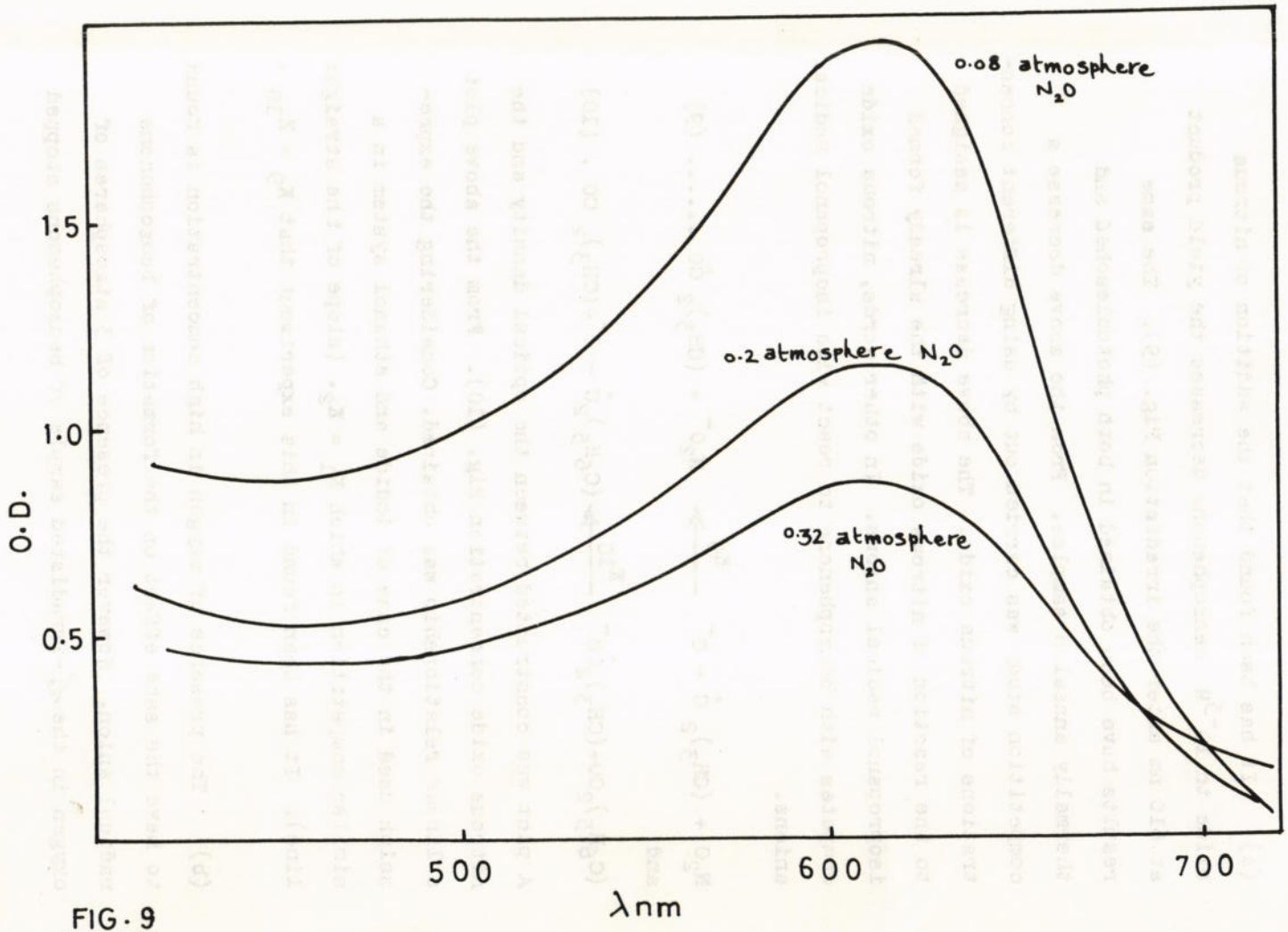
0.08 atmosphere
N_2O
0.2 atmosphere N_2O
0.32 atmosphere
N_2O
1.5
1.0
0.5
O.D.
500
600
700
λnm

FIG. 9

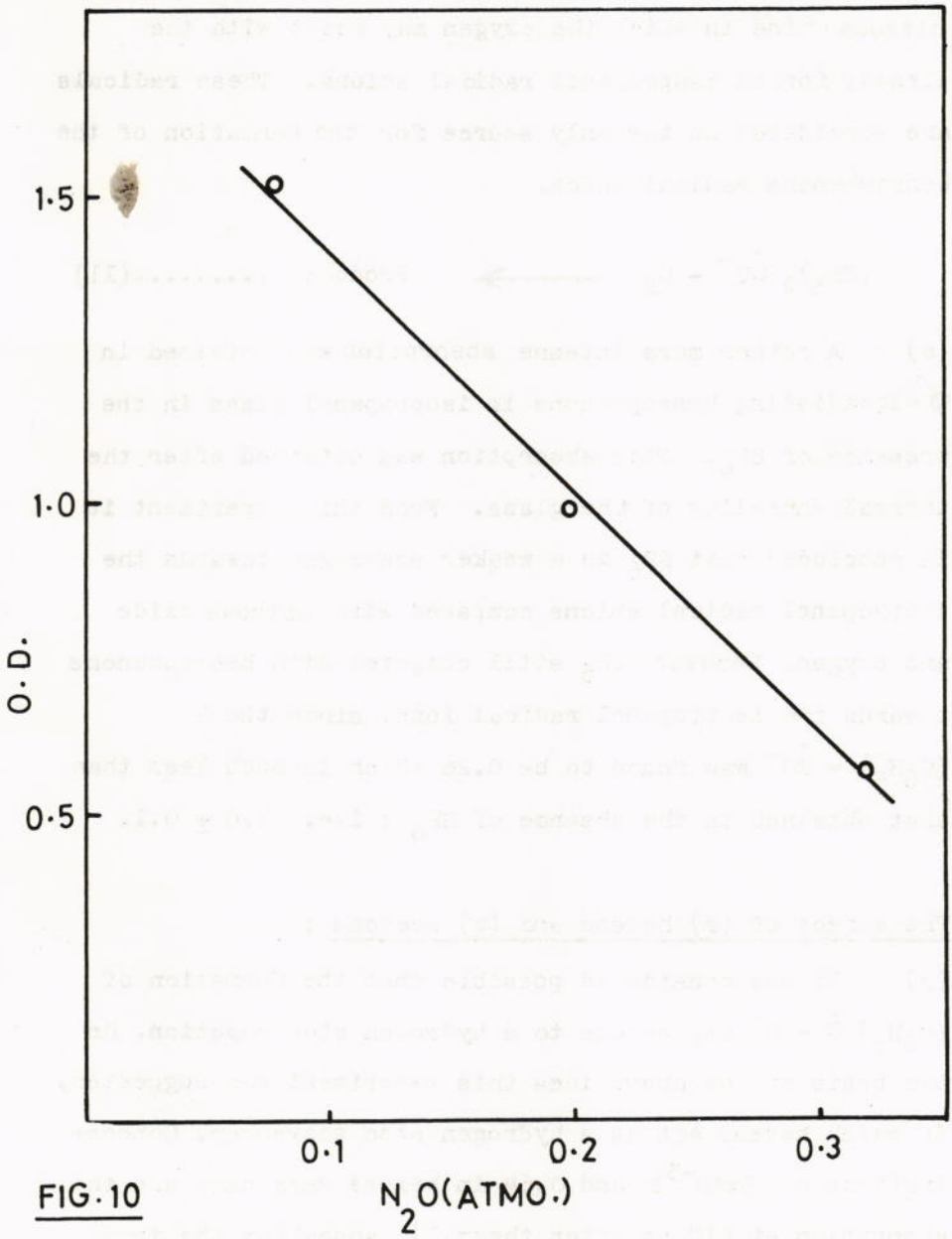

FIG·10

completely the formation of the benzophenone radical ion. This effect is attributed to the same behaviour found in nitrous oxide in which the oxygen may react with the already formed isopropanol radical anions. These radicals are considered as the only source for the formation of the benzophenone radical anion.

$$(CH_3)_2 \dot{C}O^- + O_2 \longrightarrow \text{Product} \quad \ldots\ldots\ldots(11)$$

(c) A rather more intense absorption was obtained in γ-irradiating benzophenone in isopropanol glass in the presence of SF_6. This absorption was obtained after the thermal annealing of the glass. From this experiment it is concluded that SF_6 is a weaker scavenger towards the isopropanol radical anions compared with nitrous oxide and oxygen. However SF_6 still competes with benzophenone towards the isopropanol radical ions, since the G $(C_6H_5) - \dot{C}O^-$ was found to be 0.28 which is much less than that obtained in the absence of SF_6 ; i.e. 1.0 ± 0.1.

The effect of (a) hexene and (b) acetone ;

(a) It was considered possible that the formation of $(C_6H_5)\dot{C} - O^-$ may be due to a hydrogen atom reaction. On the basis of the above idea this experiment was suggested, in which hexene act as a hydrogen atom scavenger. Concentrations of 5×10^{-3}M and 0.6M in hexene were used and the absorption at 610 nm after thermally annealing the irradiated sample was studied. The same product was obtained

in both cases with a G ($C_6H_5)_2\dot{C} - O^-$ 1.2, which is higher than expected. This increase in the G value is assigned to the low dose given to the sample which was within the range of the linearity of the yield dose plot. This experiment excluded reaction of hydrogen atom.

(b) It has been stated by Adam's et.al. [6] that the charge transfer phenomena occur between ketones takes place from acetone to benzophenone ;

$$\text{Acetone}^- \longrightarrow \text{Benzophenone}^-$$

However a mixture of 10^{-3}M benzophenone and 0.2M acetone was γ-irradiated in basic isopropanol glass at 77°K Fig.(11). A product absorbing at 615 nm was obtained after annealing of the sample. This product was found to be weaker than that obtained in the absence of acetone. The G $(C_6H_5)_2\dot{C}O^-$ calculated is about 0.8, which is low compared with the absence of acetone. This decrease is attributed to the fact that acetone is a stronger electron scavenger than benzophenone. In this experiment the charge transfer may take place between the isopropanol radical anions and the acetone molecules in the first annealing process. Then in the second annealing process there may be a charge transfer from acetone to benzophenone and at the same time one cannot exclude the decay of some of these radicals by two successive annealings. By doing so a loss in the radical anions causes the decrease in the

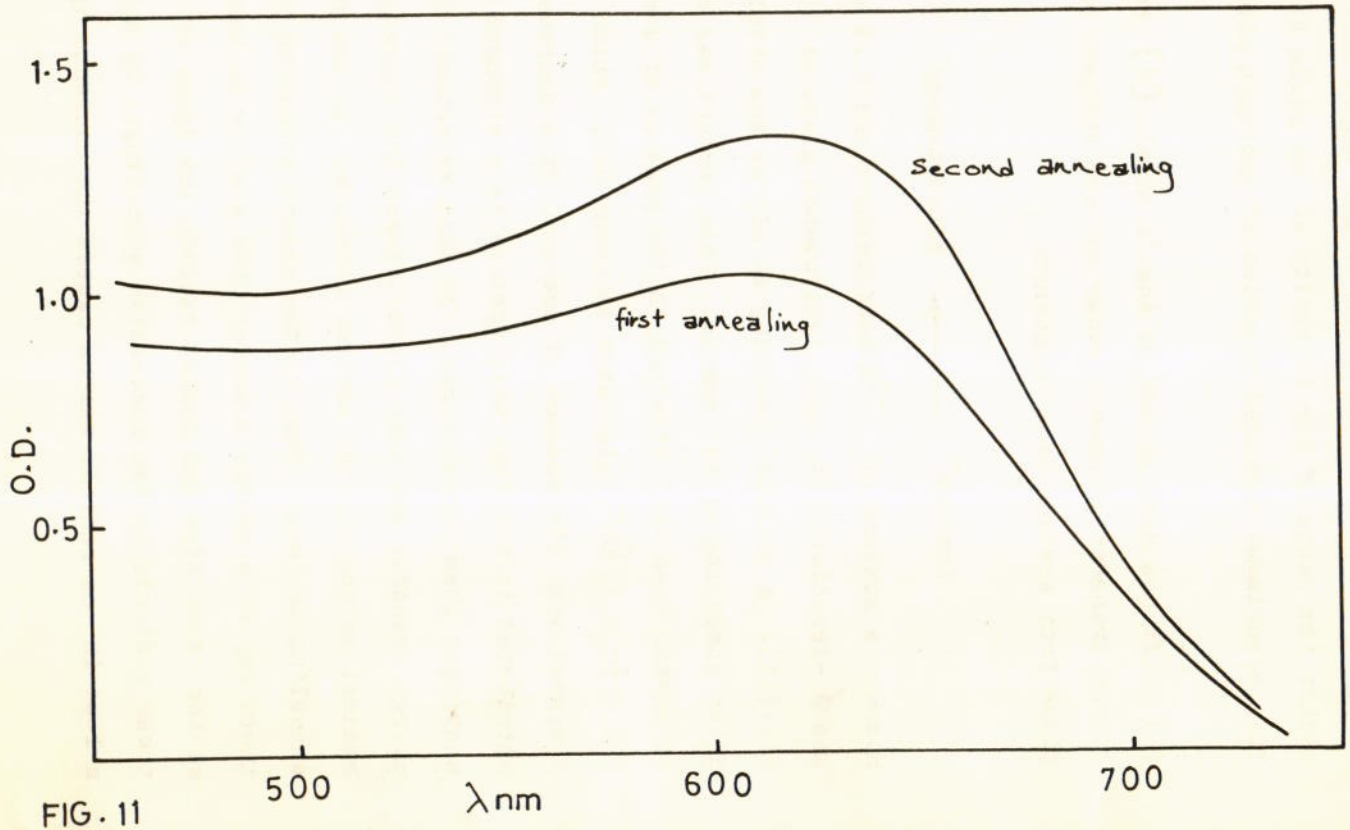

FIG. 11

G $(C_6H_5)_2 \dot{C} - O^-$ in this medium.

$(CH_3)_2CO + (CH_3)_2 - \dot{C} - O^- \rightleftharpoons$ Product .....(12)

Product + $(C_6H_5)_2CO$ $(C_6H_5)_2 \dot{C}O^-$ .....(13)

or

Product $\xrightarrow{160^oK}$ decay .....(14)

6.) <u>γ-irradiation of benzophenone in neutral methanol - water mixture glass at 77^oK ;</u>

When $10^{-3}M$ benzophenone was γ-irradiated in a neutral methanol - water mixture (80 % methanol + 20 % water), three different overlapping absorptions located at 605 nm, 552 nm and 525 nm were obtained Fig.(12). The 605 nm absorption is assigned to the directly formed benzophenone radical anion in the glass. After thermally annealing the sample, the 605 nm absorption disappeared and at the same time the 552 nm and 525 nm absorptions increased in intensity. The 552 nm and 525 nm absorptions are attributed to the benzophenone Ketyl radical (the neutralized form) and both absorptions belong to the same species, absorbing at two different wavelengths, since both absorptions were increased in intensity and decayed at the same time. The increase in the absorptions (i.e. 552 nm and 525 nm) is attributed to a neutralization process taking place between the H^+ formed in the neutral glassy sample and the initially formed benzophenone

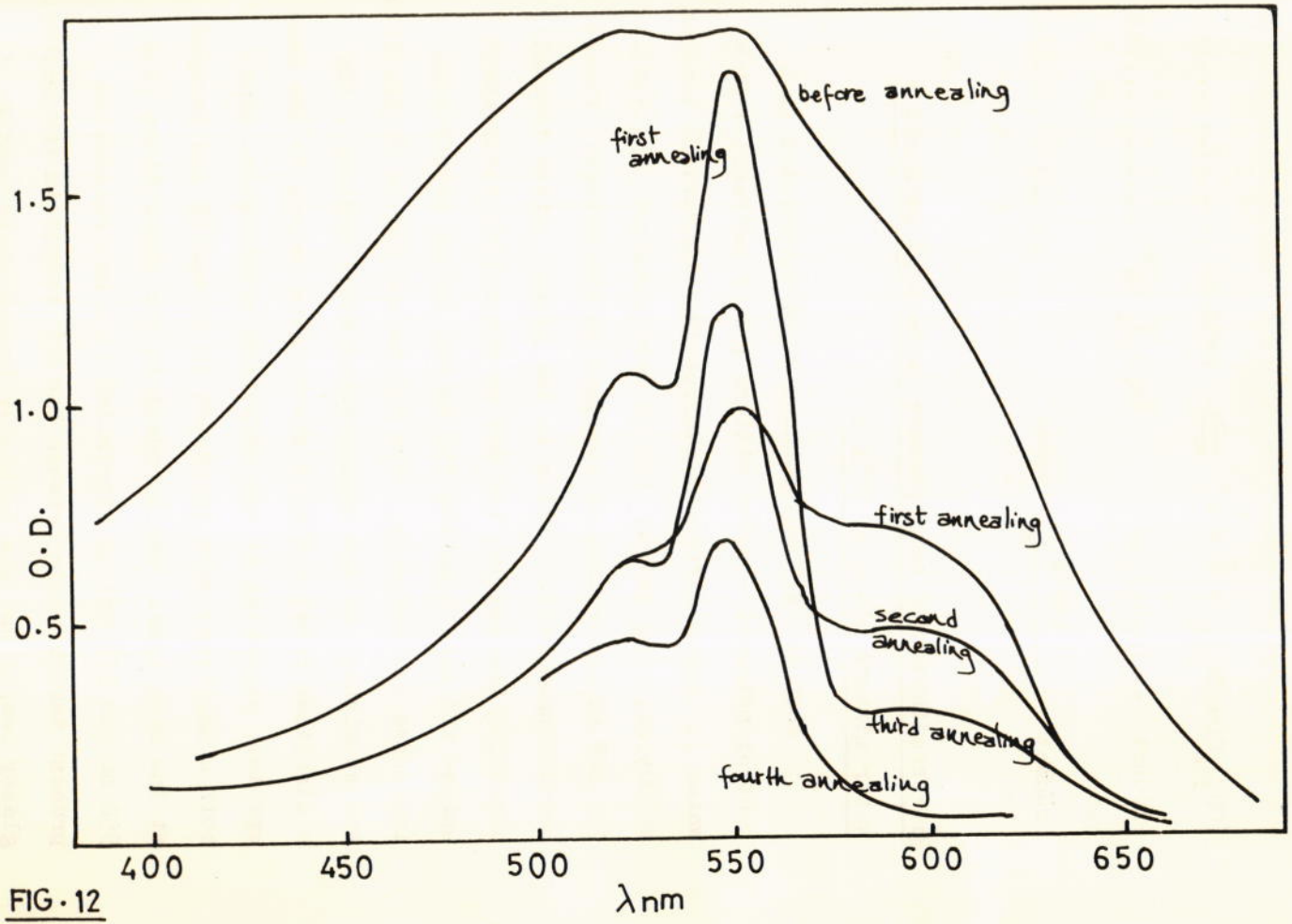
before annealing
first annealing
first annealing
second annealing
third annealing
fourth annealing
1·5
1·0
0·5
O·D·
400
450
500
550
600
650
λnm

FIG·12

radical anion. However, it has been shown by Beckett et.al [28] that the PK_a of the following equilibrium ;

$$(\phi)_2 \dot{C}O^- \rightleftharpoons (O)_2 \dot{C}OH \qquad \text{.....(15)}$$

is 9.2. Since the PK_a of the medium in which this experiment was carried out is much higher, a shift in the equilibrium towards the right is expected and the benzophenone Ketyl radical is the only species expected in such a medium. The G value for the neutral form of the Ketyl radical at 552 nm is calculated and found to be about 0.9.

REFERENCES

(1) Ronayne, Guarino and Hamill, J.Am. Chem. Soc., 84, 4230, (1962).

(2) Dainton, Keene, Kemp, Salmon and Teply, Proc. Chem. Soc. 1265. (1964).

(3) Dainton, Salmon and Teply, Proc. Roy. Soc., A.186, 27 (1965).

(4) Dainton, Salmon and Wardman, Chem. Commun., 1175 (1968).

(5) A. Shuttleworth, Ph.D. Thesis, Newcastle Upon Tyne (1969).

(6) J.A. Brivati, M.C.R. Symons, D.J.A. Tinling, H.W. Wardale and D.O. Williams, Chem. Commun., 402 (1965).

(7) I.A. Taub and K. Eiben (Private Communication).

(8) J.A. Brivati, M.C.R. Symons, D.J.A. Tinling, H.W. Wardale and D.O. Williams, Trans. Fard. Soc., 63, 212 (1967).

(9) B.G. Ershov and A.K. Pikaev (Private Communication).

(10) G. Czapski and L. Dorfman, J. Phys. Chem., 68, 1169 (1964).

(11) V.N. Shubin, V.A. Zhigunov, V.I. Zolotarevsky, and P.I. Dolín, Nature, 212, 1002 (1966).

(12) G. Nilson, H.C. Christensen, J. Fenger, P. Pagsberg and S.O. Nielson, Abstracts Eighth Int. Free Radical Symp., Novosibirsk, U.S.S.R. (1967).

(13) R. Livingstone, H. Zeldes and E.H. Taylor, Phys. Rev., 94, 725 (1954).

(14) H. Zeldes and R. Livingstone, Phys. Rev., 96, 1702 (1954).

(15) R. Livingstone, H. Zeldes and E.H. Taylor, Discussion Farad. Soc., 19, 166 (1955).

(16) T. Henriksen, Radiation Res., 23, 63 (1964).

(17) M.S. Matheson and B. Smaller, J. Chem. Phys., 23, 521 (1955).

(18) T. Trammel, H.Zeldes and R. Livingstone, Phys. Rev., 10, 630 (1958).

(19) R. Livingstone, J. Chem. Educ., 36, 349 (1959).

(20) R. Livingstone and A.J. Weinberger, J. Chem. Phys., 33, 499 (1960).

(21) J. Kroh, B.C. Green and J.W.T. Spinks, Nature, 189, 654 (1961).

(22) J. Kroh, B.C. Green, and J.W.T. Spinks, Cand J. Chem., 40,413 (1962).

(23) P.N. Moorthy and J.J. Weiss, J. Chem. Phys., 42, 3121, (1965).

(24) P.N. Moorthy and J.J. Weiss, J. Chem. Phys., 42, 3127 (1965).

(25) R.A. Zhitnikov and A.L. Orbell, Fiz. Tverd. Tela, 7, 3522 (1965).

(26) V.N. Belevskii and L.T. Bugaenko, Zh. Fiz. Khim, 39, 2589 (1965).

(27) V.N. Belevskii, L.T. Bugaenko and V.B. Golubev, Dok. 1.Akad, Nauk, S.S.S.R. 168, 122 (1966).

(28) B.G. Ershov and A.K. Pikaev, Dokl. Akad., Nauk, S.S.S.R, 169, 616 (1966).

(29) S.K.Ismail, Al-Mustansiriyah J. of Science, Vol.3. (1968).

(30) S.K. Ismail, Al-Mustansiriyah J. of Science, Vol.4, No.1(1979).

AMINO PYRIDNE AND RELATED COMPOUNDS PART I PREPARATION AND CONDENSATION OF ETHYL N-2-PYRIDYL FORHIMIDATES WITH SOME ALIPHATIC AND AROMATIC AMINES

Khalid S. Al-Dulaimi*, Adil S. Abdul-Razzak**
a n d
Abdul-Jabbar A. Mukhles***

Aminopyridine and its methyl derivatives are condensed with ethyl orthofomate in acid medium to give the corresponding formidates (I). The latter have been found to react at room temperature with some aliphatic and aromatic amines with different rates giving substituted unsymmetrical formamidines (II).

I N T R O D U C T I O N

There is an extensive amount of data on the preparation and reaction of imidates of aromatic amines such as amiline [1]. However, the imidates of hetrocyclic amines such as aminopyridine have attracted little attention.

It has been reported that 2-Aminopyridine and its derivatives condense with ethyl orthoformate under reflux to give N-N-dipyridyl formamidine [2]. N,N bis (halo-dipyridyl formamidines [3]. and N,N bis (nitrodipyridyl formamidine [4]. Respectively. All these are symmetrical formamidines.

* Now at the Department of Bio-Medical Chemistry, College of Medicine, Al-Mustansiriyah University.

** Now at the Department of Chemistry, College of Education, University of Baghdad.

*** Now at the Department of Chemistry, College of Education, Al-Sulaimaniah University.

Al-Mustansiriyah Journal of Science vol. 4 No. 1 (1979).

RESULTS AND DISCUSSION

In the present work we show that 2-Aminopyridine and its methyl derivatives react with ethylorthoformate in acid medium forming the formimidates (I). Some of these compounds were recently prepared by Attar-Bashi [5], similar to those reported earlier by Robert [6], using aniline. Bashi attempted to treat these esters with different alcohols and reported that no transesterfication product could be isolated, he suggested that the p-electrons on the nitrogen atom in the pyridine ring has a role in preventing the transesterfication reaction.

In our work we prove that these formimidates could undergo condensation reaction at room temperature with aromatic and aliphatic amines to give unsymmetrical amidines (II). The rate of condensation was found to depend on the position of the methyl group on the pyridine nucleus, thus the reaction was extremely alow (low yield) when the methyl group was in 3-Position in contrast to the fast reaction observed when the methye group was in any of the remaining positions. This observation could be explained on the ground of steric effect of the methyl group. All these compounds are fully characterized by their spectra. (i.r., n.m.r.).

The purpose of preparing these types of compounds is due to their biological activity. However, we confirmed in a separate report that N-cyclohexyl N-6-methyl-2pyridyl formimidine has an anticholinesterase action on isolated guinea pig iluem, isolated rectus abdominis and on both rabbit and frog heart [7].

EXPERIMENTAL

Unless etherwise stated, i.r. spectra were measured with a unicam SP 200 instrument for solutions in cholroform, n.m.r. spectra with Varian A-60 instrument for solutions in deuterie-chloroform containing tetramethysilane as an internal standard.

Microanalytical samples were analysed in West Germany by Max Plank Institute, Ruhr. m.p.s. were determined in open capillary tubes.

GENERAL PROCEDURE FOR THE PREPARATION OF ETHYL N-2PYRIDYL FORMIMIDATES:-

A mixture of the 2-aminopyridine (0.5 mole), ethyl orthoformate (0.75 mole), and hydrochloric acid (0.3 gm) was placed in a 250 ml flask and he ated on an oil bath. The ethanol was removed from the reaction flask as soon as it was formed, 54-56 ml (theoretical 58 ml) ethanol was collected. The desired products were distilled under reduced pressure (cf. Table 1).

GENERAL PROCEDURE FOR THE PREPARATION OF N-ALKYL, N-2-PYRIDYL-FORMAMIDINES:-

Ethyl N-2-pyridyl-formimidates (I) was mixed with equimolar quantity of the amines. The mixture was vigorously shaken for a certain period of time and left at room temperature until the reaction is complete. A white solid of N-alkyl N-2pyridyl formamidine (II) was formed. The time required for the reaction depends upon the type of the amines used and the structure of the ethyl N-2-pyridylformimdates (cf. tables 2, 3, and 5). The solid was washed with a small amount of petroleumether to remove any remaining starting material. filtered and recrystallized from ether or chloroform.

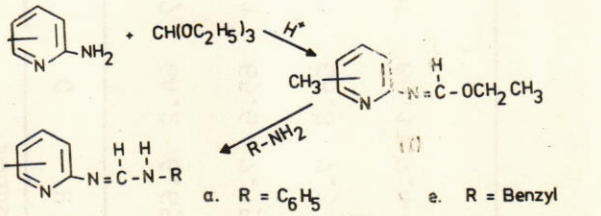

(II)

a. R = C_6H_5
b. R = C_6H_4-CH_3-m
c. R = C_6H_4-OCH_3-m
d. R = C_6H_4-Cl-m
e. R = Benzyl
f. R = Cyclohexyl
g. R = Cycloheptyl

TABLE 1. Ethyl N-2-pyridylformimidates

Type of pyridine	B.P. (mm Hg) °C	Yield (%)	nD^{20}	Formula	Calc. (%)			Found (%)		
					C	H	N	C	H	N
2-Amino-Pyridine	120/20	52.0	1.5234	$C_8H_{10}N_2O$	64	6.7	18.7	64.2	6.65	18.5
2-Amino-3-Methylpyridine	130/15	54.7	1.5191	$C_9H_{12}N_2O$	65.9	7.3	17.1	65.6	7.15	17.2
2-Amino-5-Methylpyridine	130/12	51.2	1.5223	$C_9H_{12}N_2O$	65.9	7.3	17.1	65.8	7.3	17.4
2-Amino-6-Methylpyridine	120/20	50.8	1.5244	$C_9H_{12}N_2O$	65.9	7.3	17.1	66.1	7.4	16.9

TABLE 2. N-ALKYL, N -2pyridylformamidines

Compound	M.P. °C	Yield (%)	Time required	Picrate derivatives	Formula	Calc (%)			Found (%)		
						C	H	N	C	H	N
IIa	116-7	73.5	5 minutes	214-5°C	$C_{12}H_{11}N_3$	73.1	5.6	21.3	73.1	5.5	21.1
IIb	139-40	68.9	Overnight	210-1	$C_{13}H_{13}N_3$	73.9	6.2	19.9	73.6	6.4	20.0
IIc	90.1	63.7	Overnight	212-3	$C_{13}H_{13}N_3O$	68.7	5.7	18.5	69.0	5.6	18.6
IId	145-6	63.8	5 minutes	202-3	$C_{12}H_{10}N_3Cl$	62.3	4.3	18.2	62.1	4.2	18.4
IIe	70-1	75.5	35 days	152-3	$C_{13}H_{13}N_3$	73.9	6.2	19.9	74.0	6.1	20.1
IIf	84-5	75.2	5 minutes	187-8	$C_{12}H_{17}N_3$	70.9	8.4	20.7	70.6	8.2	20.9
IIg	-	negative	-	-	-	-	-	-	-	-	-

TABLE 3. N-Alky, N (3-methyl-2-pyridy) formamidines

Compound	M.P. °C	Yield (%)	Time required	Picrate Derivatives	Formula	Calc. (%)			Found (%)		
						C	H	N	C	H	N
IIa	133-4	16.6	9 days	180-1°	$C_{13}H_{13}N_3$	73.9	6.2	19.9	74.1	6.1	20.0
IIb	116-7	15.5	3 days	191-2	$C_{14}H_{15}N_3$	74.7	6.7	18.7	74.8	6.7	18.9
IIc	-	Negative	-	-	-	-	-	-	-	-	-
IId	-	Neg.	-	-	-	-	-	-	-	-	-
IIe	-	Neg.	-	-	-	-	-	-	-	-	-
IIf	-	Neg.	-	-	-	-	-	-	-	-	-
IIg	-	Neg.	-	-	-	-	-	-	-	-	-

TABLE 4. N-Alkyl, N (5-methyl-2-pyridyl) formamadines

Compound	M.P. °C	Yield (%)	Time required	Picrate Derivatives	Formula	Calc (%)			Found (%)		
						C	H	N	C	H	N
IIa	130-1	73.8	5 minutes	249-50°	$C_{13}H_{13}N_3$	73.9	6.2	19.9	73.7	6.3	19.9
IIb	144-5	72.7	5 minutes	163-4	$C_{14}H_{15}N_3$	74.7	6.7	18.7	74.6	6.7	18.9
IIc	140-1	69.5	15 minutes	160-1	$C_{14}H_{15}N_3O$	69.7	6.2	17.4	69.8	6.3	17.4
IId	151-2	75.0	5 minutes	235-6	$C_{13}H_{12}N_3Cl$	63.7	4.9	17.1	63.9	4.8	17.0
IIe	109-10	75.5	5 minutes	168-9	$C_{14}H_{15}N_3$	74.7	6.7	18.7	74.7	6.6	18.6
IIf	97-8	70.8	3 days	158.9	$C_{13}H_{19}N_3$	71.9	8.8	19.3	72.0	8.6	19.3
IIg	74-5	54.0	9 days	142-3	$C_{14}H_{21}N_3$	72.7	9.1	18.2	72.6	9.3	18.2

TABLE 5. N-Alkyl, N (6-methyl-2-pyridyl) formamidines

Compound	M.P. °C	Yield (%)	Time required	Picrate Derivatives	Formula	Calc. (%)			Found (%)		
						C	H	N	C	H	N
IIa	104-5	71.8	5 minutes	188-9	$C_{13}H_{13}N_3$	73.9	6.2	19.9	73.7	6.1	20.0
IIb	109-10	77.3	5 minutes	153-4	$C_{14}H_{15}N_3$	74.7	6.7	18.7	74.8	6.7	18.8
IIc	89-90	61.1	20 minutes	184-5	$C_{14}H_{15}N_3O$	69.7	6.2	17.4	69.6	6.3	17.2
IId	137-8	72.5	1 minute	186-7	$C_{13}H_{12}N_3$ Cl	63.7	4.9	17.1	63.7	5.0	17.2
IIe	112-3	67.8	5 minute	164-5	$C_{14}H_{15}N_3$	74.7	6.7	18.7	74.5	6.9	18.8
IIf	72-3	70.4	1 hour	192-3	$C_{13}H_{19}N_3$	71.9	8.8	19.3	71.7	8.8	18.4
IIg	Negative	-	-	-	-	-	-	-	-	-	-

REFERENCES

1. Robert Roger and Douglas G. Neilson. Chem. Review 61, 179 (1961).

2. Katayanagi. J. Pharm. Soc. Japan, 68, 228 (1948); C.A., 48, 4545 (1954).

3. Takahashi, Saikachi, Goto and Stake. J. Pharm. Soc. Japan, 64, No. 11A, 55 (1944); C. A. 45, 8530 (1951).

4. Takahashi, Senda and Zenro, J. Pharm. Soc. Japan, 69, 104 (1949); C. A., 44, 3450 (1950).

5. M. Attar-Bashi. Bull. Coll. Sci. Vol. 17, No. 2, (1976).

6. R. M. Roberts. J. Am. Chem. Soc., 71, 3848 (1949).

7. T. Mahmood and K. Sultan.
Ann. Coll. Med. Mosul, 8, 103 (1977).

APPLICATION OF THE ELECTRICAL PROSPECTING METHOD TO EVALUATE THE SHALLOW FORMATIONS IN "ABU MINA BASIN"

Talaat A. Abdel-Latif*, Mokhtar A. Sayed*

and

Salah E. Khalil**

A B S T R A C T

The D.C. Resistivity method is applied for studying the shallow formations in a desert area lying in the northwest of the Nile Delta. The area is looked forward as having some agricultural potentialities. The measurement and interpretation of 267 resistivity soundings indicated that the Holocene alluvial deposits found on the surface consist actually of two layers, an upper thin layer having a thickness of 0.5 to 2 m and resistivity of 10 to 400 Ohm.m and a wet layer varying in resistivity from 3 to 12 Ohm.m. The underlying Pleistocene lagoonal deposits were found to have a thickness ranging from 10 to 30 m and a resistivity ranging from 5 to 25 Ohm.m. The thickness distributions are given in the form of isopach maps. Analysis of the isopach anomalies having different amplitudes gave the area percentage for the different thickness ranges. A tentative soil map is given and the significance of the geophysical results is discussed in relation to land use.

INTRODUCTION

This study presents an example of the successful use of one of the electrical prospecting methods, namely the resistivity sounding method, for the determination of some of the parameters

* Desert Institute, Cairo, Egypt.
** Suez Canal University, Egypt.

characterizing the alluvial deposits which cover the surface of Abu Mina Basin as well as the underlying lagonnal deposits. The first formation is regarded to be reclaimable for agricultural purposes while the other is investigated for its clay and high salt contents which may have a direct effect on the cultivation and irrigation potentialities of the soil. The area is a desert one laying in the northwest of the Nile Delta (Fig. 1) between longitudes 29° 25' E, 29° 45' E and latitudes 30° 40' N and 30° 55' N. The ground elevation varies between 10 and 50 m above sea level. The area is about 500 sp.km. and lies within the Desert lands looked forward for agricultural expansion projects.

GENERAL GEOLOGIC FEATURES

The area occupies the northeastern extrimities of the Marmarica Plateau and is characterized by simple topography. The surface is a plain covered with the Holocene alluvial deposits which consist of quartz sand, clay and calcareous materials, derived originally by water action from the adjacent rocks. Drilling in the area showed that these alluvial deposits are underlain by the Pleistocene lagoonal deposits which consist of clay, fine sand and gypsum. Underlying the lagoonal depsits are the deltaic deposits composed of sandstone, gravelly sand and gravel, followed downward by the Pleiocene clay.

RESISTIVITY MEASUREMENTS AND INTERPRETATION

The field measurements included 267 shallow resistivity soundings. The sounding stations were arranged along a grid pattern with a grid spacing of one kilometer as shown in (Fig.2) The spreading of the current line was within 200 m which was found enough to pick up the effect of the lower boundary of the

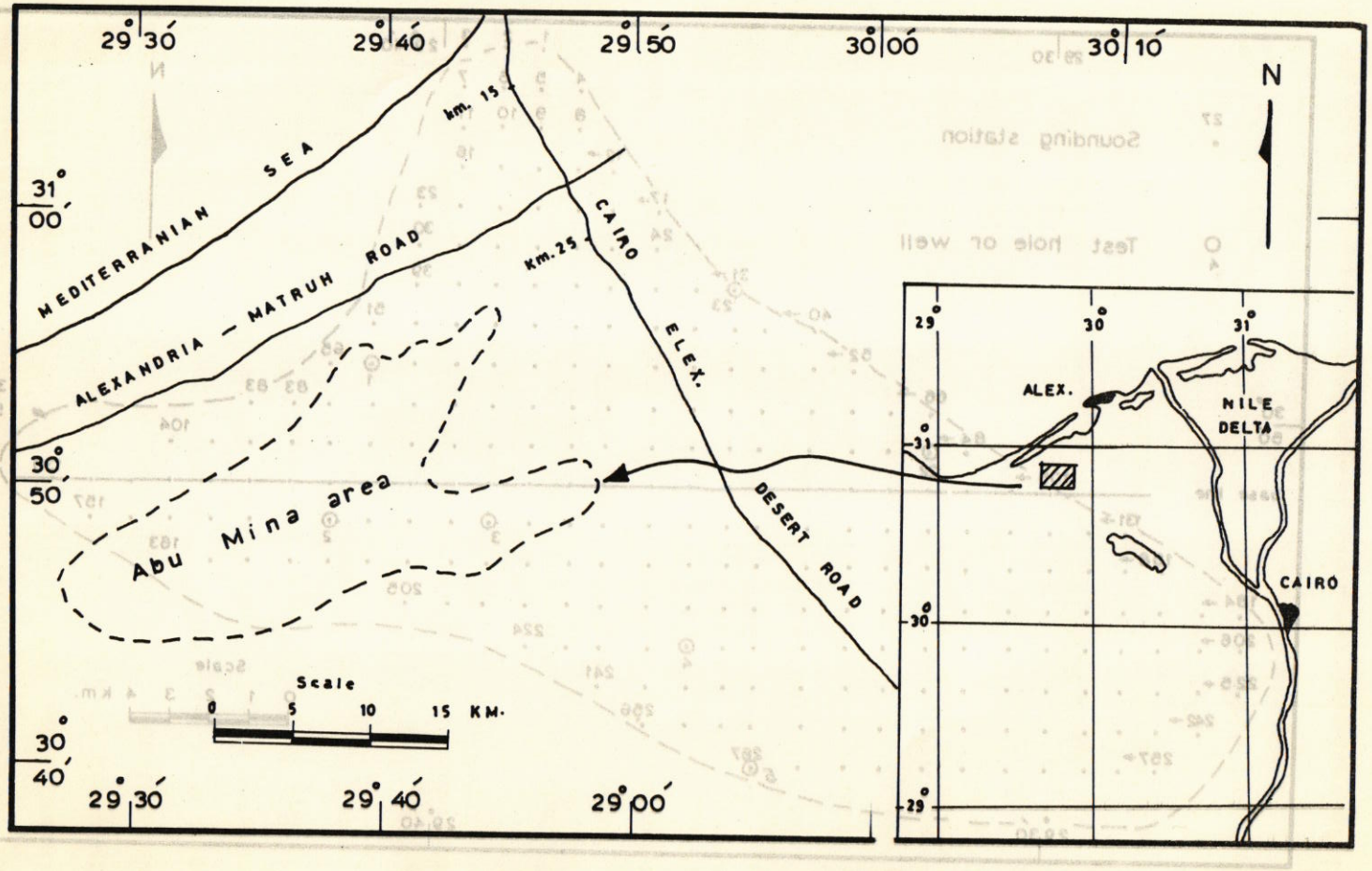

FIG.(1) A LOCATION MAP OF THE STUDIED AREA

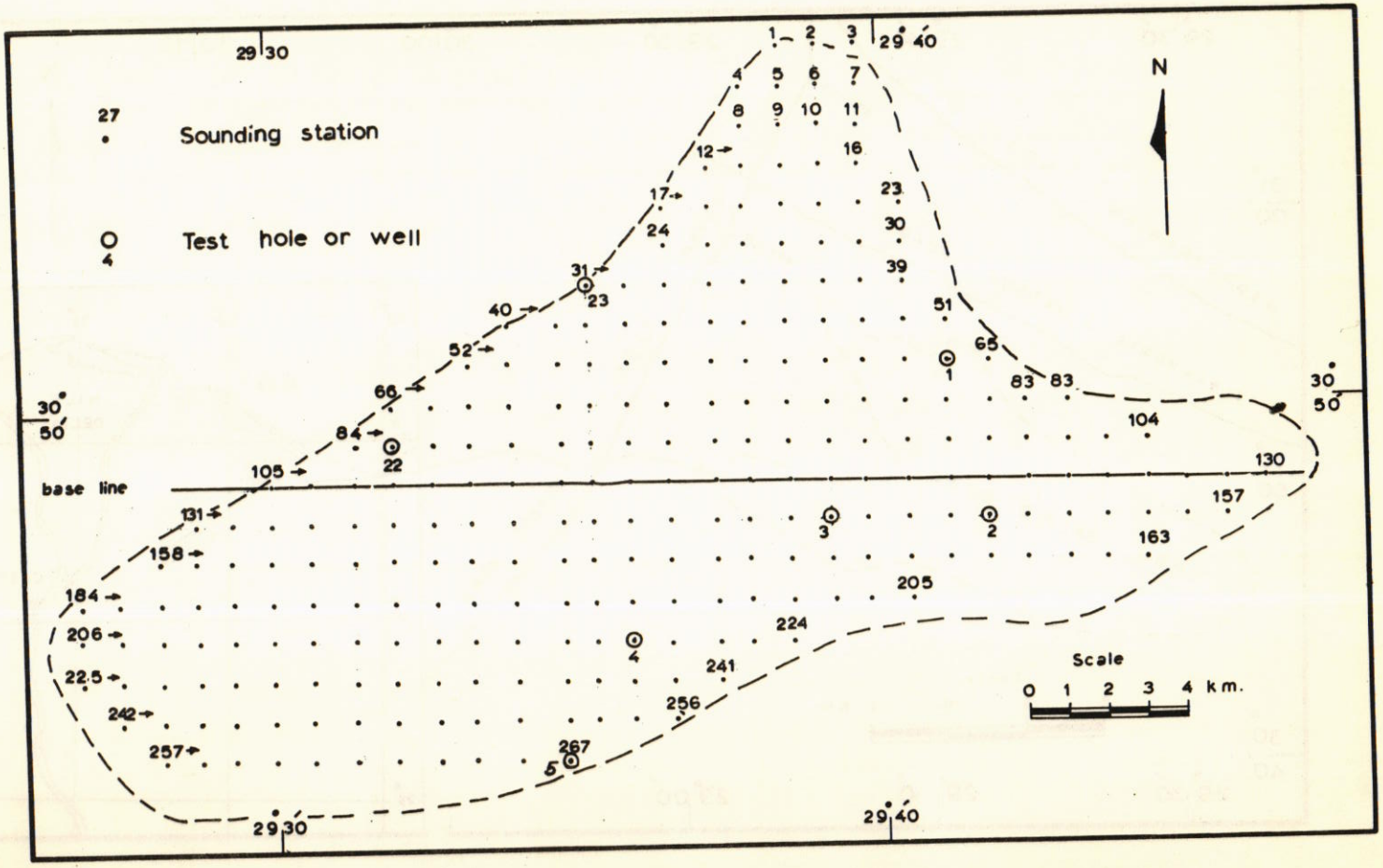

FIG. (2) A LAYOUT OF THE ELECTRICAL RESISTIVITY SURVEY

lagoonal depsits. Measurement of the potential difference and current intensity was made by means of the Russian electronic potentiometer, type 3CK-1. The Schlumberger electrode configuration was used in carrying out the field survey according to which the apparant resistivity is calculated through the following equation:

$$\rho_a = K.\frac{\Delta V}{I} \text{ Ohm.m.}$$

where,

ρ_a is the apparent resistivity

ΔV is the potential difference in millivolts.

I is the current intensity in milli Amperes and

K is a geometrical constant related to the spacings of the current and potential electrodes.

The field date were plotted in the form of resistivity sounding curves relating the apparent resistivity ρ_a to the apparent depth represented by half the current electrode spacing AB/2.

Interpretation of the 267 resistivity sounding curves was carried out using the curve matching method with the object of getting the formation resistivity and depth of the different rock layers encountered in the survey. Use was made in this respect of the family of theoritical master curves of Pilaev [1] and Vnii-Geophysica [2] .

The sounding curves obtained for stations 64, 151, 147, 220, 267, 85 and 31 were correlated with the 7 wells drilled at the same respective Iocations, namely well 1, 2, 3, 4, 5, 22 and 23. This correlation was found necessary to minimize the effect of the

principle of equivalence, on one hand, and to get the resistivity ranges for both the alluvial and lagoonal deposits on the other. Knowing such resistivity values makes it possible to follow any of the two formations in the different parts of the area through the interpreted resistivity sounding curves.

The results of correlation showed out that:-

(1) The alluvial deposits are geoelectrically recognized to be consisting of two layers; an upper dry thin layer forming the soil cover in the area and a lower one with a relatively greater thickness which contains some water content. The later is referred here to as the "wet" alluvial layer.

(2) The formation resistivities of the alluvial and lagoonal deposits are as follows:-

Formation	Resistivity range (Ohm.m)
Dry alluvial deposits	10 - 400
Wet alluvial deposits	3 - 12
Lagoonal deposits	5 - 25

RESULTS AND DISCUSSION

In the following each of the mentioned formations is evaluated as to its configuration and characteristics.

1. Dry alluvial depostis

The thickness of this layer was found to vary from about 0.5 m to 2 m. as shown by the isopach contour map of (Fig. 3). Relatively thick lenses of these deposits are found in the middle of the basin. The calculation of the areal extention of

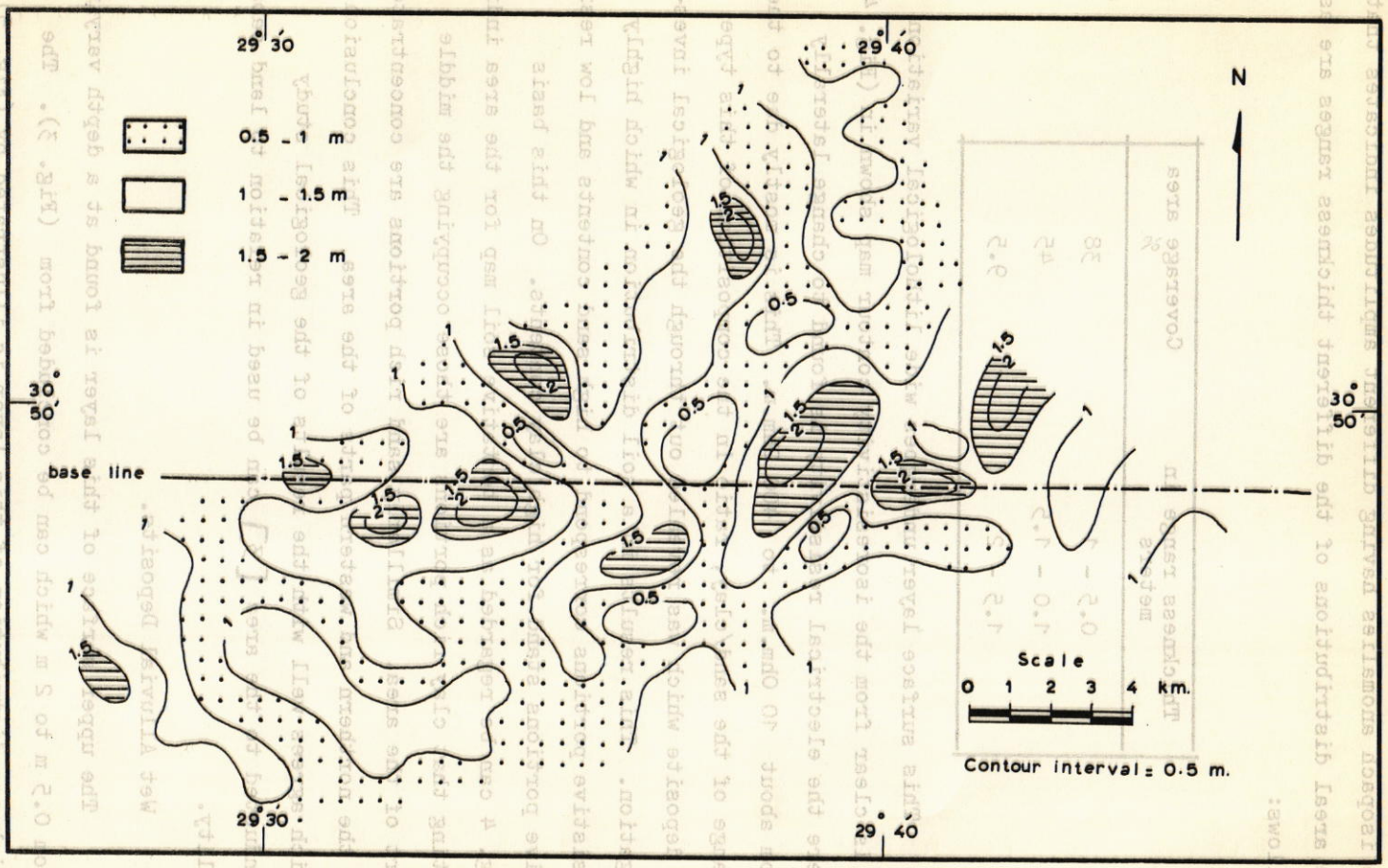

FIG.(3) AN ISOPACH CONTOUR MAP FOR THE DRY SECTION OF ALLUVIAL DEPOSITS

the isopach anomalies having different amplitudes indicates that the areal distributions of the different thickness ranges are as follows:

Thickness range in meters	Coverage area %
0.5 - 1	38
1.0 - 1.5	45
1.5 - 2	9.5

This surface layer undergoes wide lithological variation as is clear from the isoresistivity contour map shown in (Fig. 4) where the electrical resistivity is found to change laterally from about 10 Ohm.m. to 400 Ohm.m. This is mostly due to the change of the sand/clay, ratio in the composition of this type of deposite which was revealed out through the geological investigation. This results in a soil distribution in which highly resistive portions correspond to high sand contents and low resistive portions stand for high clay contents. On this basis Fig. 4 can be regarded as a tentative soil map for the area indicating that clay rich portions are those occupying the middle part of the area. Simillarly sand rich portions are concentrated in the northern and western parts of the area. This conclusion which agrees well with the results of the geological study conducted to the area [3] can be used in relation to land cabability.

2. Wet Alluvial Deposits.

The upper surface of this layer is found at a depth varying from 0.5 m to 2 m which can be concluded from (Fig. 3). The thickness distribution of this layer is illustrated by (Fig. 5) which indicates that it changes from 5 to 20 m, i.e. about 10 times

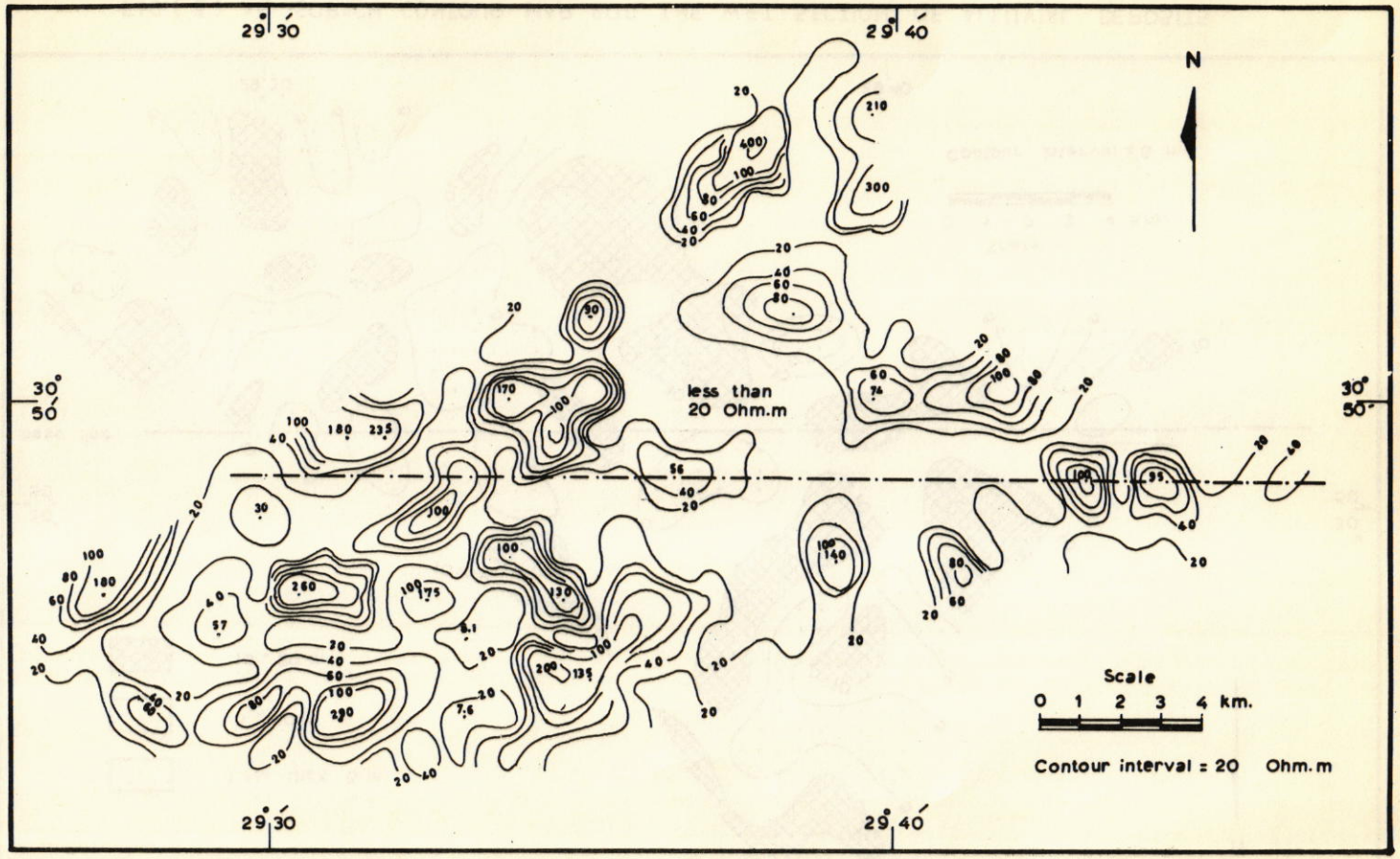

FIG.(4) AN ISO-RESISTIVITY CONTOUR MAP FOR THE DRY ALLUVIAL DEPOSITS

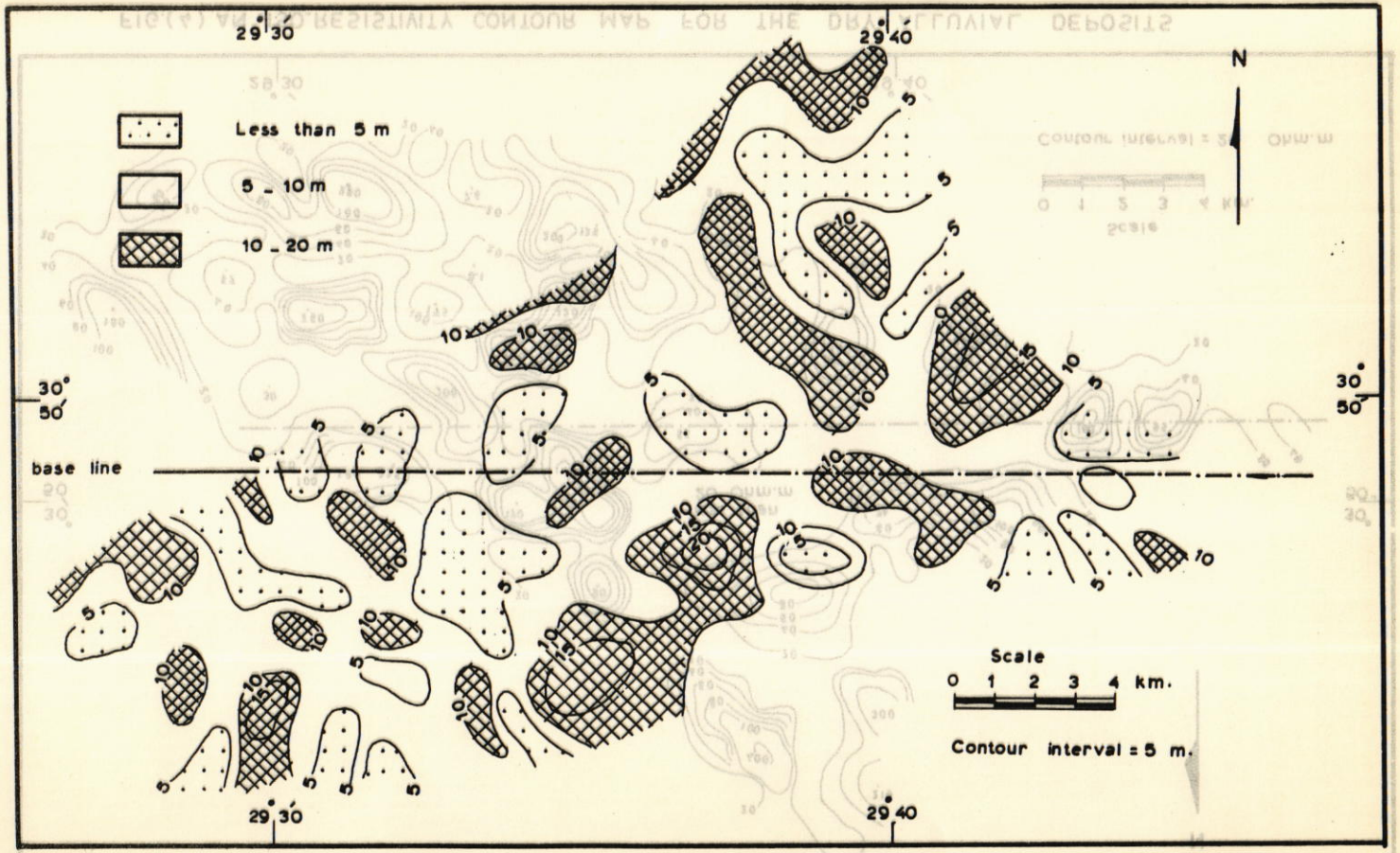

FIG.(5) AN ISOPACH CONTOUR MAP FOR THE WET SECTION OF ALLUVIAL DEPOSITS

as the dry section of the alluvial deposits. Although no particular trend is ovserved in this thickness distribution, it can be stated that in most parts of the area the thickness of this layer is from 10 to 20 m. Area calculation for the isopach anomalies indicates the following:

Thickness range in in meters	Area Percentage
Less than 5	25.5
5 - 10	26.0
10 - 20	47.2

3. Lagoonal Deposits.

This layer is recognized as the third geoelectrical layer underlying the wet alluvial deposits. It varies is thickness from 10 m to about 30 m as shown in (Fig. 6)and in depth from 5.5 to 22.5 m from the surface. The thickness distribution is given below and shows that in most parts of the area the thickness of the lagoonal deposits lines between 210 and 20 m.

Thickness range in meters	Area percentage
Less than 10	3
10 - 20	56
20 - 30	38

It is obvious that the lagoonal deposits lies deep enough below the soil and consequently do not introduce any difficulty for land use through the irrigation, drainage or cultivation processes as far as the soil salinity is concerned.

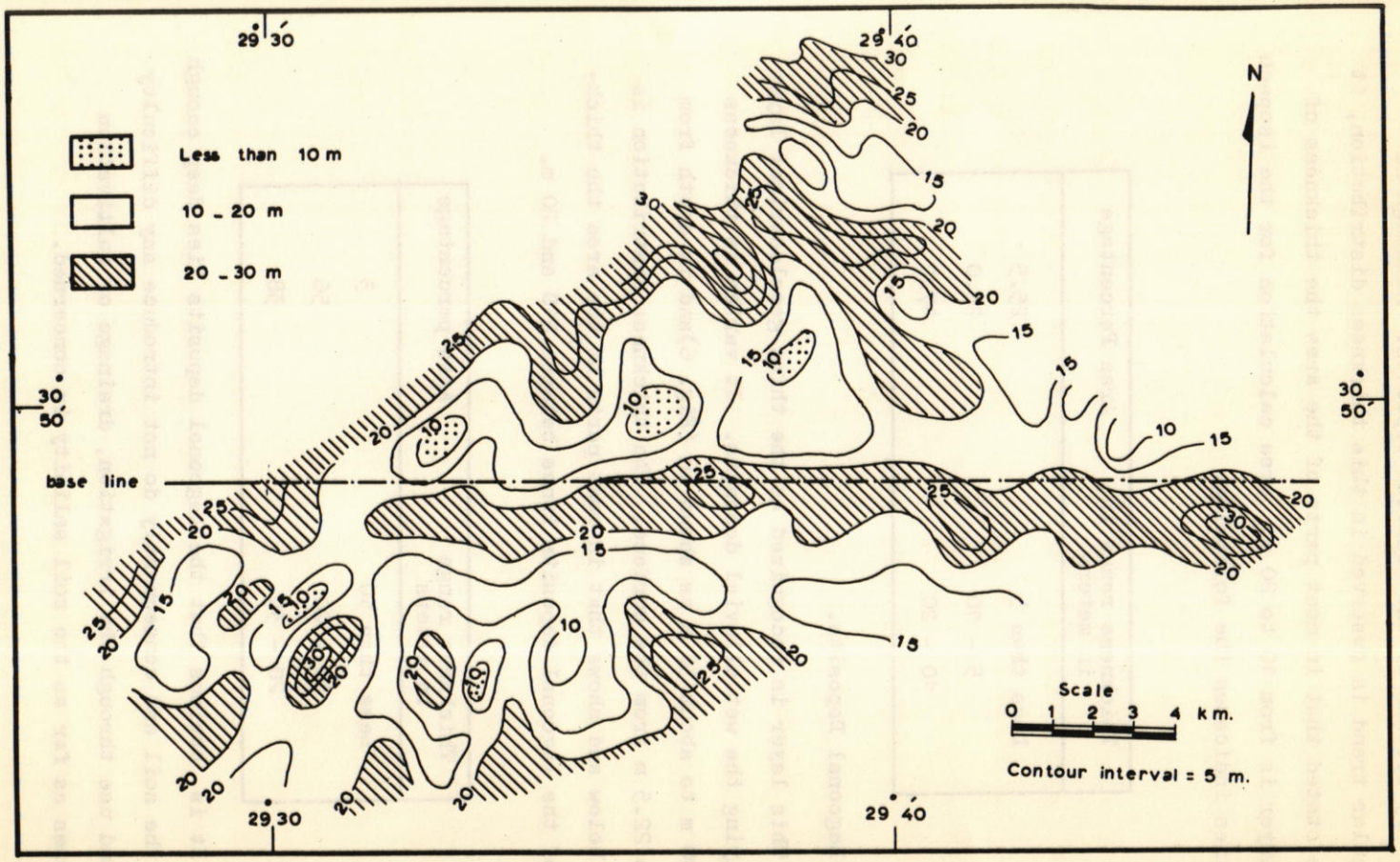

FIG.(6) AN ISOPACH CONTOUR MAP FOR THE LAGOONAL DEPOSITS

These deposits, however, being enriched in salt contents, represent a source of salt contamination for surface water that may percolate to the ground water lying below within the deltaic deposits.

SUMMARY AND CONCLUSIONS

The area of Abu Mina Basin has been geoelectrically investigated by means of 267 resistivity soundings with the purpose of evaluating some of the shallow formations in relation to cultivation and irrigation processes. The qualitative and quantitative interpretation of the field data indicated that:

1. The Holocene alluvial deposits found on the surface consist geoelectrically from two layers. The Upper layer is thin, dry and varying idely in resistivity due-mostly-to the lateral variation in the sand/clay ratio. It changes in thickness from 0.5 m to 2 m and in res. from 10 to 400 Ohm.m. The lower layer contains some water content and has a thickness range of 5 to 20 m. and resistivity varying from 3 to 12 Ohm.m.

2. The underlying layer consisting of the Pleistocene lagoonal deposits vary in thickness from 10 to 30 m and in resistivity from 5 to 25 Ohm.m.

3. The middle part of the basin has a clay rich soil while the northern and western parts are occupied by sand rich soil. This is illustrated by a tentative soil map.

4. The lagoonal deposits which are enriched in gypsum have no effect on the soil as they lie far enough below the surface but

they may affect the quality of ground water within the underlying deltaic deposits as they would enrich the surface water percolating down to the water table in salt content.

The analysis of the thickness anomalies having different amplitudes indicated that:

1. On the surface the dry alluvial deposits having a thickness of 1 to 1.5 m cover a majority of 45 % of the area.
2. In the subsurface, wet alluvial deposits with a thickness of 10-20 m cover 47.2 % followed downward by a 10 to 20 m thick layer of lagoonal deposits covering 56 % of the subsurface area.

REFERENCES

(1) A.M. Pilaev. Manual for the interpretation of vertical electrical sounding curves. Moscow (in Russian, (1948).

(2) Vnii Geofizica. Album Poletak elektricheskov zondirovaniya dka trakhaloinikh gorizontalnovo odnorodrikh, Razrezof, Moscow (in Russian, (1963.

(3) S. Attia. Petrology and Soil genesis of the Quaternary deposits in the region west of the Nile Delta. Ph.D. thesis, Faculty of Science, Ain Shams University, (1975).

-0-0-0-0-0-

APPLICATION OF X-RAY DIFFRACTION TO STUDY THE INTERDIFFUSION IN THE RBI-KI SOLID SOLUTION

Yasseen N. Obaid*

A B S T R A C T

Interdiffusion in the RbI-KI solid solution has been studied over 575°C. The Boltzmann-Matano method is employed to compute diffusivities from concentration vs. penetration curves measured with sectioning and radiocristallographic analysis. It is found that the interdiffusion coefficient is concentration-dependent inspite of the fact that KI-RbI is a nearly ideal thermodynamic system.

INTRODUCTION

In recent years, the studies of diffusion of one element into another, especially of the same group of periodic table, have become important due to advances in solid state devices in electronics and other applications.

In a previous work, [1] a solid state system, $RbAg_4I_5$-KAg_4I_5 has been studied in connection with interdiffusion.

The KI-RbI has been chosen for a similar study because it is almost an ideal thermodynamic system and also because the lattice parameters, a_o, are well known (a_o is equal to 7.340Å for pure RbI, and 7.065 Å for pure KI).

* Physics department, College of Education, Al-Mustansiriyah University, Baghdad - IRAQ.

The relation between the interdiffusion coefficient ($\bar{D}$) and the concentration (c) for NaI-KI has been studied by Haget [6] where it shows a peak at c=0.55 which becomes more pronounced as the temperature increases.

In the case of KI-RbI, Bonpunt [3], have studied the same phenomenon at four different temperatures, the curves which they have obtained do not show a regular behavious, as there are more than one peak, and the peaks show some shift at different temperatures. The irregular behavious of this substance makes it interesting to examine the relation at other temperatures in order to study the details of this relation and try to find some explanation to the factors producing this irregularity.

EXPERIMENTAL METHOD

(a) Preparation of sample for Crystallographic Analysis

KI and RbI salts of high purity were commercially obtained from Merck. One of these salts was taken and pressed into a cylindrical pellet of 16 mm in diameter, and the other salt was placed directly over the pellet in the same matrix and compressed by a pressure of 5 Tons/cm^2, resulting in a uniform cylindrical sample of KI RbI solid solution of 16 mm in diameter and 10-15 mm in length.

The cylindrical sample was heated in an automatic controlled furnace at a temperature 575°C for a period ranging from 50 hrs to 108 hrs. The constant temperature of the furnace was monitered by Cr-Al thermocouple of accuracy $\pm$ 1°C. In order to minimise the thermal gradient effect of Interdiffusion, the cylindrical sample was enclosed in a metallic block and the

sample temperature was recorded by another Cr-Al thermocouple in contact with the sample.

Figure 1 gives the thermal diagram of KI-RbI sample.

After the thermal processing of the sample, it was immediately quenched and the edges of the pellets were rounded off in order to eliminate the surface diffusion effects. Thin sections prependicular to the direction of diffusion were cut with the help of ultramicrotome 20-30 μm thick and the progress of the knife edge could be observed with a precision of 1 μm with the help of micrometric screw of the mictotome. The requirements of the crystallographic analysis needed sample sections of 20-30 μm thick.

X-ray Analysis of KI_z RI_{I-z} solid solution

The Interdifussion of the samples of KI RbI results in the formation of a continuous solid solution. X-ray powder diffractometer has been used to follow the interpenetration by determining the concentration of each layer. Cu $K_{\alpha 1}$ and $K_{\alpha 2}$ X-rays of wavelength (λ = 1.54051 A°) have been used to study the parameters in the sample.

Scanning rate of 2θ (1/20 per minute) was used to get more precise results. Experimental values have been corrected by using internal standard of Si or Al, and with the help of correction charts corresponding to Cu $K_{\alpha 1}$ wavelength of 1.54051 $\mathring{A}$.

The (400) reflection have been chosen to determine the concentration which passes from an angle $\theta = 24.78^{\circ}$ for pure RbI to $\theta = 25.86^{\circ}$ for pure KI.

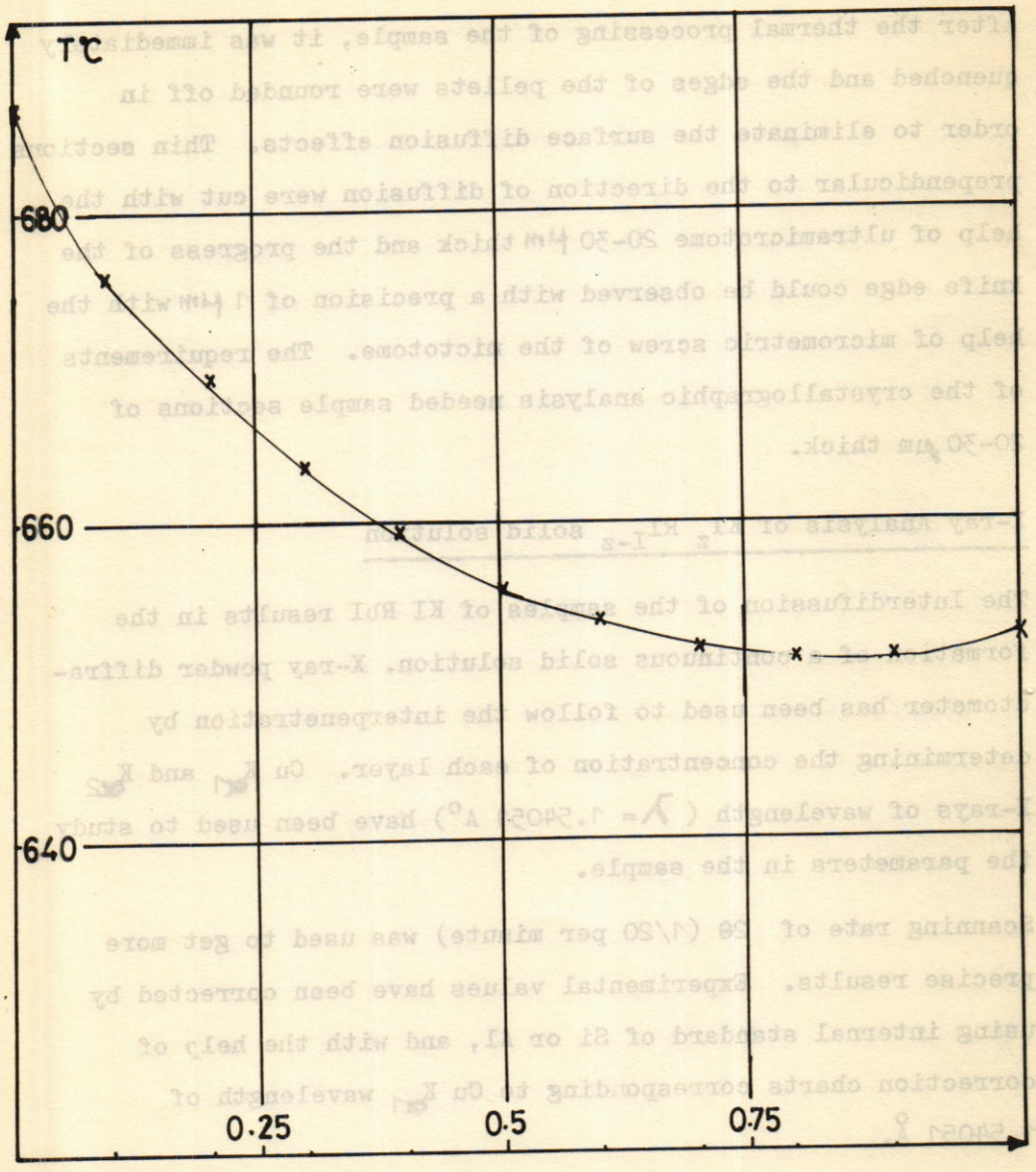

Figure 1. Thermal diagram of KI RbI solid Solution. Melting point of KI is 687°C and melting point of RbI is 653°C.

Quartz has been used as internal standard (112) reflection at an angle $\Theta = 25.06^{\circ}$

Another (200) reflection passes from $\Theta = 12.10^{\circ}$ to 12.58° for pure $Z_{RbI} = 1$ and $Z_{RbI} = 0$, when the 101 reflection Quartz with $\Theta = 13.32^{\circ}$ has been taken. In this analysis atomic concentrations have been determined with an accuracy of $\pm$ .01%

R E S U L T S

Lattice parameters obtained by the crystallographic analysis of the $KI_z\ RbI_{1-z}$ solid solution are given in table 1. The parameter a_o for pure KI is equal to 7.065 $\pm$ .001 A° and for pure RbI is equal to 7.340 $\pm$ .002 $\mathring{A}$ where the corresponding values obtained by L. Ponpunt [2] are 7.064 $\pm$ .0015 A° and 7.3475 $\pm$ .002 A° respectively. It is clear that our values are consistent with those previously reported.

Figures 2 and 3 give the graphs of the parameters for $K1_z\ RbI_{1-z}$ solid solution.

Table 1. Parameters (a_o) and volume (V) of unit cell

Composition z	a_o (A°)	V($A^{\circ 3}$)
0	7.340	396.22
0.1	7.322	392.63
0.2	7.296	388.36
0.25	7.285	386.15
0.3	7.267	383.84
0.4	7.238	379.19
0.5	7.210	374.84
0.6	7.183	370.72
0.7	7.154	366.28
0.75	7.149	365.45
0.8	7.124	361.57
0.9	7.094	356.99
1.0	7.065	352.72

The Interdiffusion of $KI_z\ RbI_{1-z}$ solid solution has been studied at a constant temperature of 575°C for a period varying

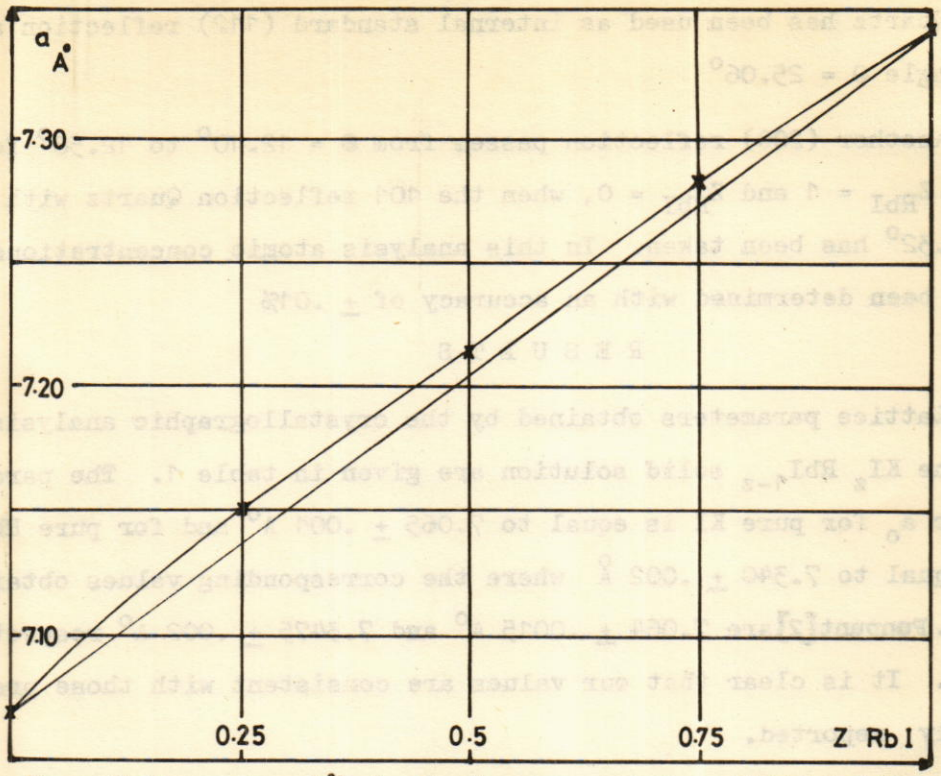

Figure 2. Parameter $a_o(A^\circ)$ of unit cell and concentration of KI-RbI Solid solution

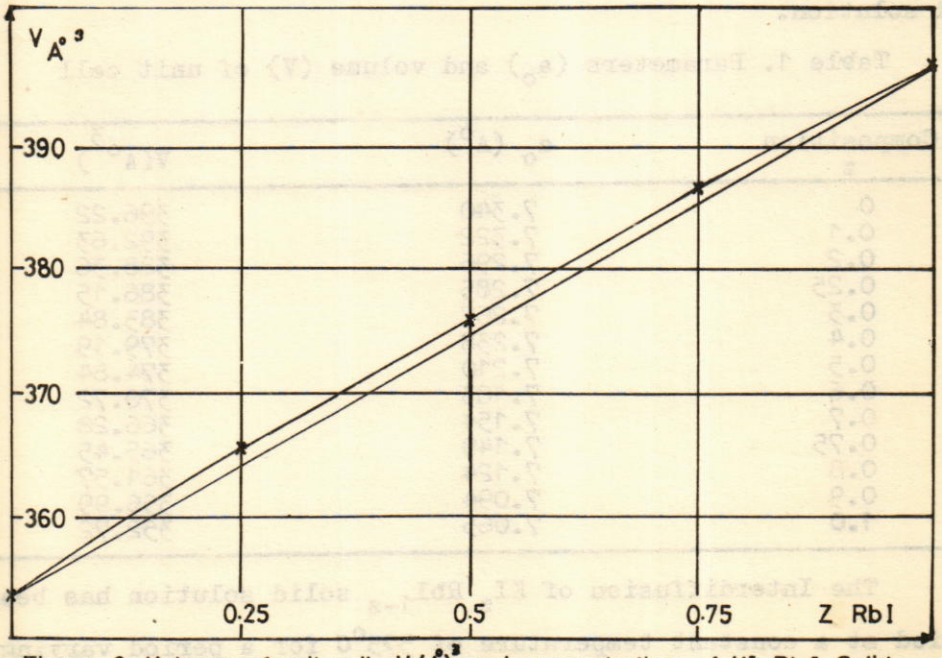

Figure 3. Volume of unit cell $V(A^\circ)^3$ and concentration of KI-RbI Solid solution (c)

from 50 hrs to 108 hou. Figure 4 gives the distribution of concentration in Isothermal diffusion of KI-RbI solid solution. Figure 5 gives the values of penetration for different concentration according to Boltzmann-Matano relation. In the limit of experimental error, it is possible to apply Boltzmann's assumption, [4]

$$\lambda = X / \sqrt{t}$$

which is constant for fixed concentration C and temperature T, where X is the penetration. The reference plane X = 0, is the "Matano interface" defined by the condition,

$$\int_0^1 x \; dc = 0$$

The initial and boundary conditions are given by

$$t = 0, \quad C = 1, \text{ for } x > 0$$

and

$$C = 0, \quad \text{for } x < 0$$

and for the values $x = \pm \infty$, $\frac{dc}{dx} = 0$

The concentration of Matano interface has been found to be constant.

$$C_M = 0.550 \pm 0.015 \quad \text{for RbI}$$

With these conditions, it has been possible to use the graphical method of Boltzmann- Matano [5] to obtain the Interdiffusion Coefficients, $\bar{D} = \frac{-1}{2} \left(\frac{dx}{dc}\right) \int_0^c x \; dc$

We have used the long curve to compute the value of $\bar{D}$ with the accuracy which varies from 5% to 15%. Table 2 gives the Interdiffusion Coefficient $\bar{D}$ at a constant temperature of 575° C.

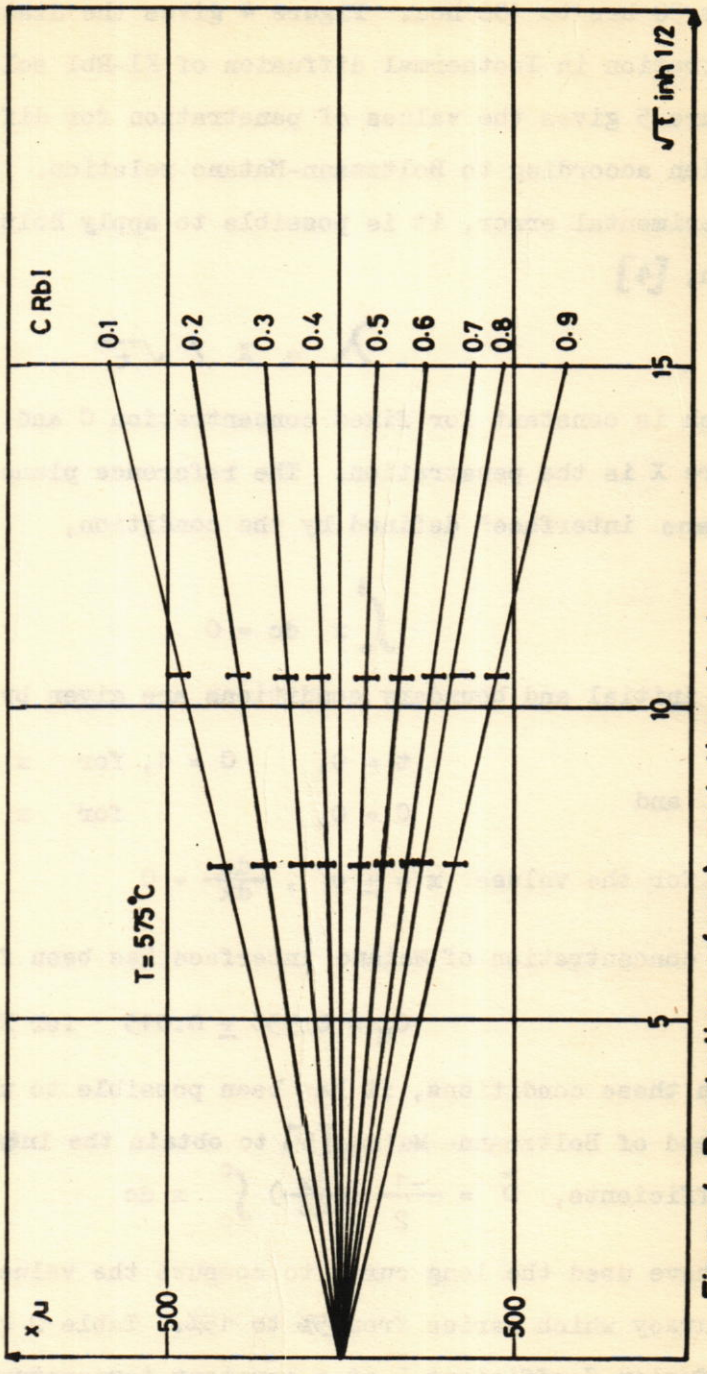

Figure 4. Penetration x (μm) and time in hrs

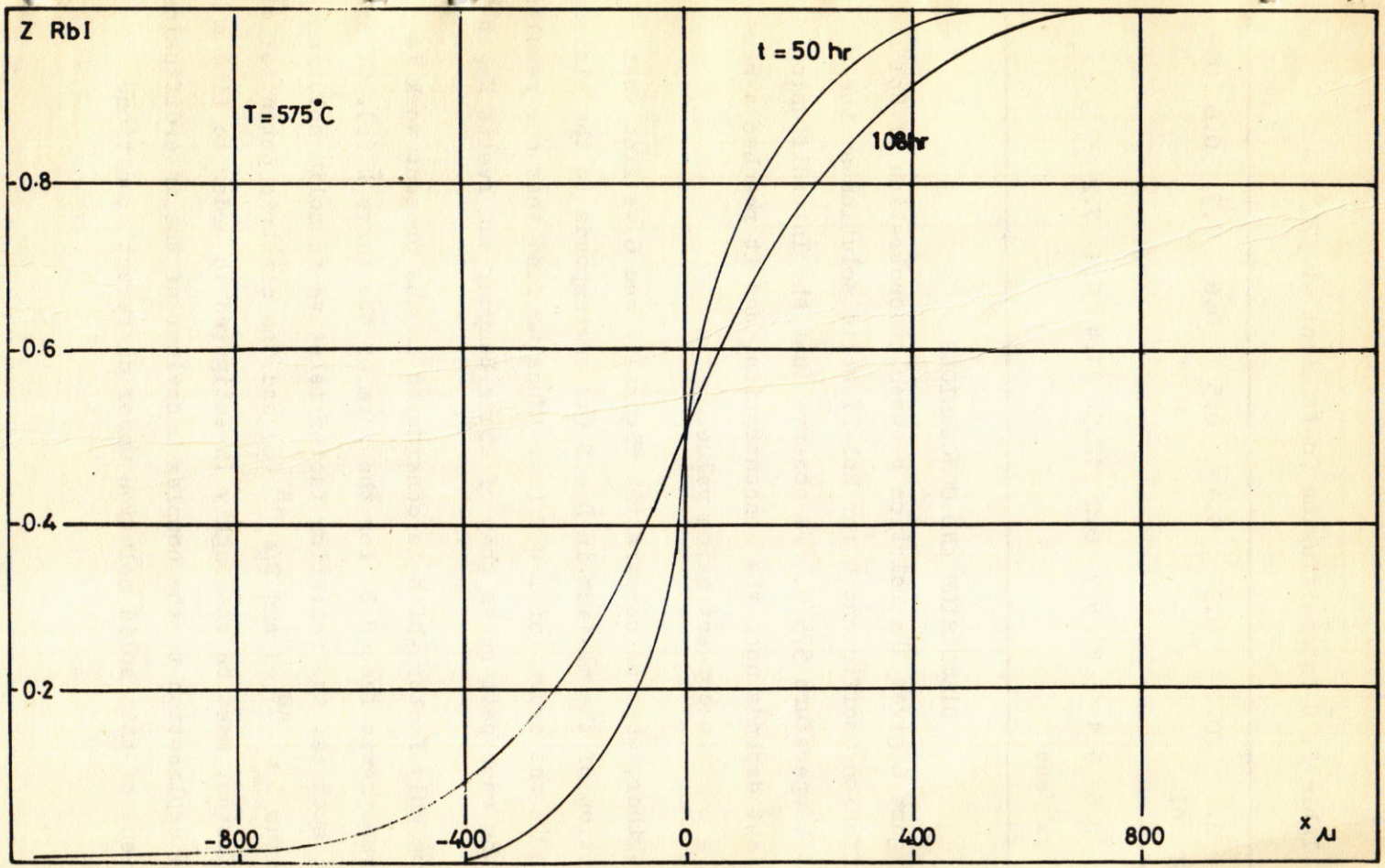

Figure 5. Curve of penetration x (μm) and concentration for time 50 hrs and 108 hrs at temperature 575 °C

Table 2, $\bar{D}$ Interdiffusion Coefficient at 575°C

C mole of RbI	0.1	0.2	0.3	0.4	0.5	0.6	0.7	0.8	0.9
$D10^{-10} cm^2/sec$	6.6	7.1	5.8	5.7	6.2	12.5	11.4	9.1	7.2

DISCUSSION AND CONCLUSIONS

Figure 6 gives the relation between concentration of RbI and Interdiffusion Coefficient $\bar{D}$ for RbI-KI solid solution at the constant temperature 575°C. We observe that the Interdiffusion coefficient depends upon the concentration, and it reaches a maximum at a certain concentration value.

Further, when we compare the Figures 2 and 6 we find that the position of the maximum in $\bar{D} = f(z)$ corresponds to the minimum position in the cruve for $T = f(z)$. Thus we find that our results follow the same pattern as that of Louis Bonpunt and Yvette Haget [3].

The only factor which is considered in the present work is the thermodynamic factor ϕ for the form of the curve $\bar{D}(c)$. Other factors, such as: the radiation factor relative to solid solution homogenious $D_A^{*\,AB}(c)$ and $D_B^{*\,AB}(c)$ and the electric potential of the diffusion, must be thoroughly investigated in order to find a complete explanation to the complex behaviour of the interdiffusion coefficient of this solid solution under different conditions.

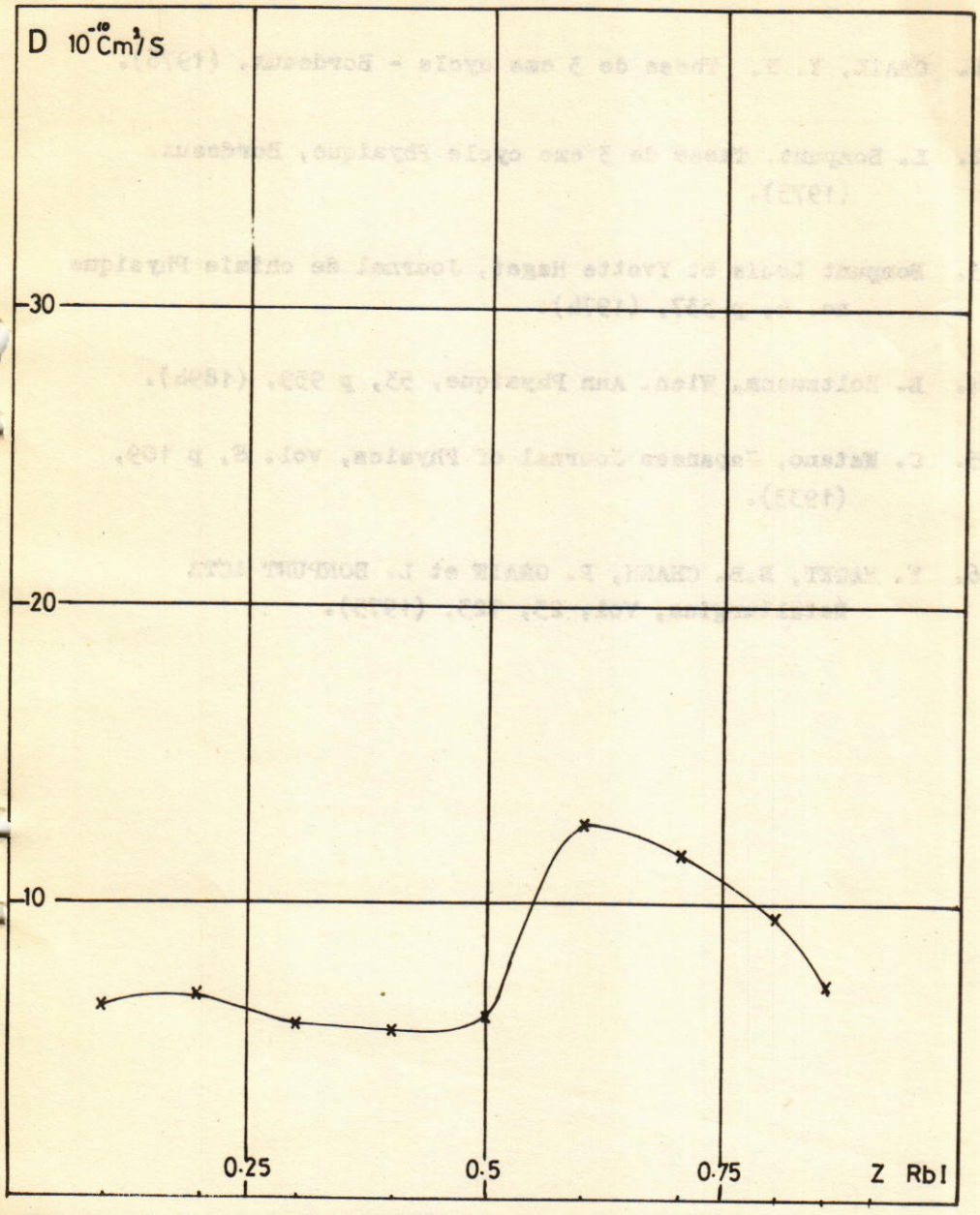

Figure 6. Curve of interdiffusion coefficient and concentration of solid solution KI-RbI

REFERENCES:-

1. OBAID, Y. N. These de 3 eme cycle - Bordeaux. (1976).

2. L. Bonpunt, These de 3 eme cycle Physique, Bordeaux. (1973).

3. Bonpunt Louis et Yvette Haget, Journal de chimie Physique no. 4, p 537, (1974).

4. L. Boltzmann, Wien, Ann Physique, 53, p 959, (1894).

5. C. Matano, Japanese Journal of Physics, vol. 8, p 109, (1933).

6. Y. HAGET, N.B. CHANH, P. GRAIN et L. BONPUNT ACTA Metallurgica, Vol, 23, 723, (1975).

A DUAL-MODEL OF HADRONS BEYOND THE NARROW WIDTH APPROXIMATION

A.K. Bassiouny*

A B S T R A C T

A dual-model of hadrons in the form of infinite series of Veneziano-type amplitude is introduced. Regge asymptotic behaviour is obtained independant of the usual assumption of straight-line trajectories. The possibility of increasing total scattering cross-section with the energy and the behaviour of $\frac{d\sigma_{el}}{dt}$ in the diffraction region are discussed.

INTRODUCTION

The dual-resonance model has succeeded in giving expressions for the scattering amplitude in a consistant mathematical scheme [1]. However, it is based on a real scattering matrix with poles on the real axis corresponding to infinitely-narrow resonances, or equivalently straight-line Regge trajectories. This assumption, which is fundamental for the derivation of the asymptotic Regge behaviour, gives rise to an internal inconsistancy of the model, since the resonant state must have a finite lifetime corresponding to non-zero width. In order to take into account the existance of resonant states with finite lifetime, we must drop the assumption of straight-line trajectories, [2], [3]. To construct an amplitude which satisfies unitarity, we introduce here an infinite series, each term of which is of Veneziano-type amplitude.

---

* Department of Physics, College of Science, Al-Mustansiriyah University, Baghdad - IRAQ.

Al-Mustansiriyah Journal of Science, Vol. 4, No. 1 (1979).

SCATTERING AMPLITUDE

The (s,t) scattering amplitude for spinless particles which satisfies the constraints:

1) crossing symmetry $A(s,t) = A(t,s)$

2) $A(s,t)$ is a superposition of terms of Veneziano-type cannot be uniquely determined. A simple representation of the amplitude satisfying these requirements is:

$$A(s,t) = \lambda \sum_{l,m=0}^{\infty} \frac{\Gamma(-\alpha(t)+l)\,\Gamma(-\alpha(s)+m)}{\Gamma(-\alpha(s)-\alpha(t)+l+m)\,l!\,m!} \left(\frac{s}{a}\right)^{l} \left(\frac{t}{a}\right)^{m} \quad \text{------ (1)}$$

Where (s), (t) are Regge trajectories, and and a are constants.

The amplitude (1) can be also written in integral form.

In fact,

$$A(s,t) = \sum_{l,m} \int_0^1 x^{-\alpha(t)-1+l} (1-x)^{-\alpha(s)-1+m} \frac{1}{l!m!} \left(\frac{s}{a}\right)^{l} \left(\frac{t}{a}\right)^{m} dx$$

$$= e^{t/a} \int_0^1 x^{-\alpha(t)-1} (1-x)^{-\alpha(s)-1} e^{\left(\frac{s}{a}-\frac{t}{a}\right)x} dx \quad \text{where} \begin{pmatrix} \mathrm{Re}\,\alpha(s) < 0, \\ \mathrm{Re}\,\alpha(t) < 0 \end{pmatrix}$$

$$= e^{t/a} B(-\alpha(t), -\alpha(s))\, F\left(-\alpha(t), -\alpha(s)-\alpha(t), \frac{s-t}{a}\right) \quad \text{-----(2)}$$

where $F\left(-\alpha(t), -\alpha(s)-\alpha(t), \frac{s-t}{a}\right)$ is the confluent hypergeometric function and $B(-\alpha(t), -\alpha(s))$ in the Euler's function.

The integral representation (2) defines the amplitude $A(s,t)$ as analytic function of t for fixed real s regular for Re $\alpha(t)$

Anelytic continuation of the confluent hypergeometric function and Euler's function define an amplitude, which has the same singularities as $\alpha(t)$, together with simple poles when $\alpha(t)$ is integer. The same behavious is obtained in the s-plane for fixed real t.

REGGE ASYMPTOTIC BEHAVIOUS

Another function closely related to the confluent hypergeometric function is U (a,c,z) defined by the integral:

$$U(a,c,z) = \frac{1}{\Gamma(a)} \int_0^\infty e^{-zx}\, x^{a-1}\, (1+x)^{c-a-1}\, dx \qquad \text{------ (3)}$$

It has a left cut in the Z-plane, and the asymptotic behaviour

$$U(a,c,z) \sim z^{-a} \quad \text{as } |z| \to \infty \qquad \text{------ (4)}$$

Using the relation (4):

$$F\left(-\alpha(t), -\alpha(s)-\alpha(t), \frac{s-t}{a}\right) = \frac{\Gamma(-\alpha(s)-\alpha(t))}{\Gamma(-\alpha(s))} e^{-i\pi\varepsilon\alpha(t)}$$

$$U\left(-\alpha(t), -\alpha(s)-\alpha(t), \frac{s-t}{a}\right) + \frac{\Gamma(-\alpha(s)-\alpha(t))}{\Gamma(-\alpha(t))} e^{\frac{s-t}{a}}$$

$$e^{i\varepsilon\pi\alpha(s)}\; U\left(-\alpha(s), -\alpha(s)-\alpha(t), \frac{t-s}{a}\right)$$

Where $\varepsilon = \pm 1$ if $\mathrm{Im}\,(s-t) \gtrless 0$. ------ (5)

and fixing t by a real negative value, then the asymptotic behaviou of the amplitude when $s + i\varepsilon \to \infty$ is

$$A(s,t) \sim \lambda\, e^{t/a}\, \Gamma(-\alpha(t))\, \left(\frac{-s}{a}\right)^{\alpha(t)}$$

$$+ \lambda\, e^{s/a}\, \Gamma(-\alpha(s))\, \left(\frac{s}{a}\right)^{\alpha(s)} \qquad \text{-------(6)}$$

Similarly the (u,t) amplitude has the following asymptotic behaviour:

$$A(u,t) \sim \lambda\, e^{t/a}\, \Gamma(-\alpha(t))\, \left(\frac{s}{a}\right)^{\alpha(t)} + \lambda\, e^{u/a}\, \Gamma(-\alpha(u))\, \left(\frac{-s}{a}\right)^{\alpha(u)}$$

The full amplitude is then:

$$A = A(s,t) + A(u,t) \underset{s+i\varepsilon\to\infty}{\sim} \lambda\, e^{t/a}\, \Gamma(-\alpha(t))\, \left(1 + e^{-i\pi\alpha(t)}\right)$$

$$\left(\frac{s}{a}\right)^{\alpha(t)} + \lambda\, e^{s/a}\, \Gamma(-\alpha(s))\, \left(\frac{s}{a}\right)^{\alpha(s)} \qquad \text{--------(7)}$$

where at fixed t and $s \to \infty$ $A(s,u) \to 0$.

We notice that the first term is the Regge asymptotic behaviour, where the trajectory $\alpha(t)$ is not essentially a straight line.

Assuming that Im $\alpha(s) \ll |\text{Re}\,\alpha(s)|$ as $s \to \infty$ we get

$$\text{Im} \cdot A \sim \frac{\lambda \pi e^{t/a}}{\Gamma(1+\alpha(t))} \left(\frac{s}{a}\right)^{\alpha(t)} + \lambda e^{s/a}\, \text{Im} \cdot \alpha(s) \left(\frac{s}{a}\right)^{\text{Re}\,\alpha(s)}$$

$$\left[\Gamma(-\text{Re}\,\alpha(s)) \ln \frac{s}{a} - \Gamma'(-\text{Re}\,\alpha(s))\right]$$

Using the optical theorem, the total scattering cross-section is:

$$\sigma_T = \frac{1}{s}\,\text{Im}\,A \sim \frac{\lambda\pi}{\Gamma(1+\alpha(0))}\left(\frac{s}{a}\right)^{\alpha(0)-1} + \lambda e^{s/a}\,\text{Im}\,\alpha(s)\left(\frac{s}{a}\right)^{\text{Re}\,\alpha(s)}$$

$$\left[\Gamma(-\text{Re}\,\alpha(s)) \ln \frac{s}{a} - \Gamma'(-\text{Re}\,\alpha(s))\right] \qquad \text{-------(8)}$$

If we assume pomeron - exchange i.e. $\alpha(0) = 1$, then the first term gives constant cross-section, while the contribution of the second term depends on the behaviour of Im $\alpha(s)$ and Re $\alpha(s)$ If Im $\alpha(s) \to 0$ as $s \to \infty$, then the second term vanishes, and the total cross-section is constant. However if Im $\alpha(s)$ tends to a positive constant, the total cross-section will increase again with the increase of energy, i.e. σ_T will have a minimum, a fact which is experimentally seen for pp-reaction [5]

DIFFRACTION REGION

Another important result of the model is that it also explains the behavious of $\frac{d\sigma_{el}}{dt}$ in the diffraction region [6]. In fact, in the neighbourhood of $t = 0$:

$$\frac{d\sigma_{el}}{dt} \sim \frac{1}{s^2}|A|^2 \sim \left(\frac{d\sigma_{el}}{dt}\right)_{t=0} e^{2t/a} \left(\frac{s}{a}\right)^{2\alpha(t)-2}$$

$$= \left(\frac{d\sigma_{el}}{dt}\right)_{t=0} e^{bt} \qquad \text{------(9)}$$

where the exponential slope $b = \frac{2}{a} + 2\alpha'(0) \ln \frac{S}{a}$ is positive provided that $a > 0$.

As seen the diffraction peak shrinks with the increase of S. If $\alpha'(0)=0$ i.e. the case of pomeron-exchange, then b as experiments show will be independant of s. For almost all reactions the exponential slope $b \sim 5 - 10$ (Gevic)$^{-2}$ and hence the parameter $a \sim 0.2\text{-}0.4$ (Gevic)^{2}.

RESONANCES

The scattering amplitude A (s,t) has simple poles when $\alpha(s) = n$ where n is a positive integer. The residue at the pole $S = S_m$ is given by:

$$R = \frac{(-)^{n+1}}{n!} \frac{\Gamma(-\alpha(t))}{\Gamma(-n-\alpha(t))} F\left(-n, -n-\alpha(t), \frac{t}{a} - \frac{S_n}{a}\right)$$

$$= \sum_{r=0}^{n} \binom{n}{r} \frac{\Gamma(\alpha(t)+n-r+1)}{\Gamma(\alpha(t))} \left(\frac{t}{a} - \frac{S_n}{a}\right)^r \qquad \text{-------(10)}$$

If $\alpha(t) = \alpha(0) + \alpha'(t)$ when $t < 0$ i.e. the trajectory is assumed to be linear only for negative values of t, then the residue is a polynomial of degree n corresponding to resonant states of spin $J \leq n$.

REFERENCES

1. G. Veneziano, Nuovo Cim. 57A, 190. (1968).

2. A. S. Di Giacomo, L. Fubini, Sertorio and G. Veneziano, Phys. Lett. 33B, 171 (1970).

3. C. E. De Tar, K. Kang Chug I-Tan and J. H. Wein Phys. Rev. D4, 425 (1971).

4. W. Magnus, E. Oberhettinger, R. Soni, Formulas and theorems for the special functions of mathematical physics.

5. U. Amaldi, Phys. Lett., B44, 112, (1973).

6. W. Rarita, R.J. Riddell Jr., C.B. Chiu, R.J.N. Phillips, Phys. Rev., 165, 1615, (1968).

-0-0-0-0-0-

DIELECTRIC PROPERTIES OF SOME OILS AT LOW FREQUENCY REGION

S.H.M. El-Sabeh*, K.N. Abd-El-Nour*, A.S.J. Al-Ani* and T.A. Al-Dhahir*

A B S T R A C T

The dielectric constant ϵ' and dielectric loss ϵ'' have been measured for some types of oils at different frequencies ranging from 70 Hz up to 10^5 Hz, at temperatures from 20°C to 80°C. The absorption region obtained is attributed to the surface changes of the interfaces of dielectric (Maxwell-wagner effect). The effect of sulfur on the dielectric properties of the samples are studied.

EXPERIMENTAL

The oil samples under test are either raw materials or products which are obtained from a petroleum refinery, [1]. The raw materials, diesel oil, gas oil and kerosene are extracted from crude oil directly by fractional distillation at different boiling ranges. The product samples, kerosene and A.T.K. (special fuel for aeroplanes) are obtained by hydrogenation of kerosene raw with hydrogen under certain conditions of temperature and pressure in the presence of catalyst. This process is used mainly to reduce sulfur compounds and mercaptans in the distillates, where this reduction is preferable in some uses of oils.

---

* Now at the Department of Physics, College of Science, Al-Mustansiriyah University, Baghdad - IRAQ.

Al-Mustansiriyah Journal of Science, Vol. 4, No. 1 (1979).

The measurements of dielectric constant ϵ' and dielectric loss ϵ'' are carried out at frequencies ranging from 70 Hz up to 10^5 Hz using a low frequency dekameter (WTW, type DK05) of the of the Schering bridge type.

The D-C conductivity of the samples are measured using multirange ammeter (Phywe) and E.H.T. power supply unit (Philip Haris LTD.). The accuracy of the measurements amounts to 2%. The temperature is controlled by using ultra thermostat.

RESULTS AND DISCUSSION

The data obtained for the dielectric loss ϵ'' versus log frequency for the different samples at three measured temperature 20°, 50° and 80°C are shown in Fig. (1). It is found that at this range of frequency, diesel oil shown the highest loss while kerosene (product) shows the lowest loss. This means that the dielectric loss increases with the increase of sulfur content in the sample. This is similar to that found in the case of natural rubber [2], the sammples containing more sulfur (natural rubber for sulf r vulcanizer) show higher losses.

The increase in ϵ'' at the low frequency region with the increase of sulfur content may be due to either the Maxwell Wagner effect or the direct current conductivity or both. The general aspects of Maxwell-Wagner effect were evaluated by Wagner [3]. This effect will not normally appear in homogenous liquid systems, but due to an a-c current which is in phase with the applied potential. This current results from the differences in the conductivities and dielectric constants of the substances composing the oil materials. A number of Maxwell-Wagner systems have been evaluated [4,5]. Corrections for conductivity have been made according to the equation [6],

$$\epsilon''_{\text{corrected}} = \epsilon''_{\text{observed}} - \frac{2\sigma}{f}$$

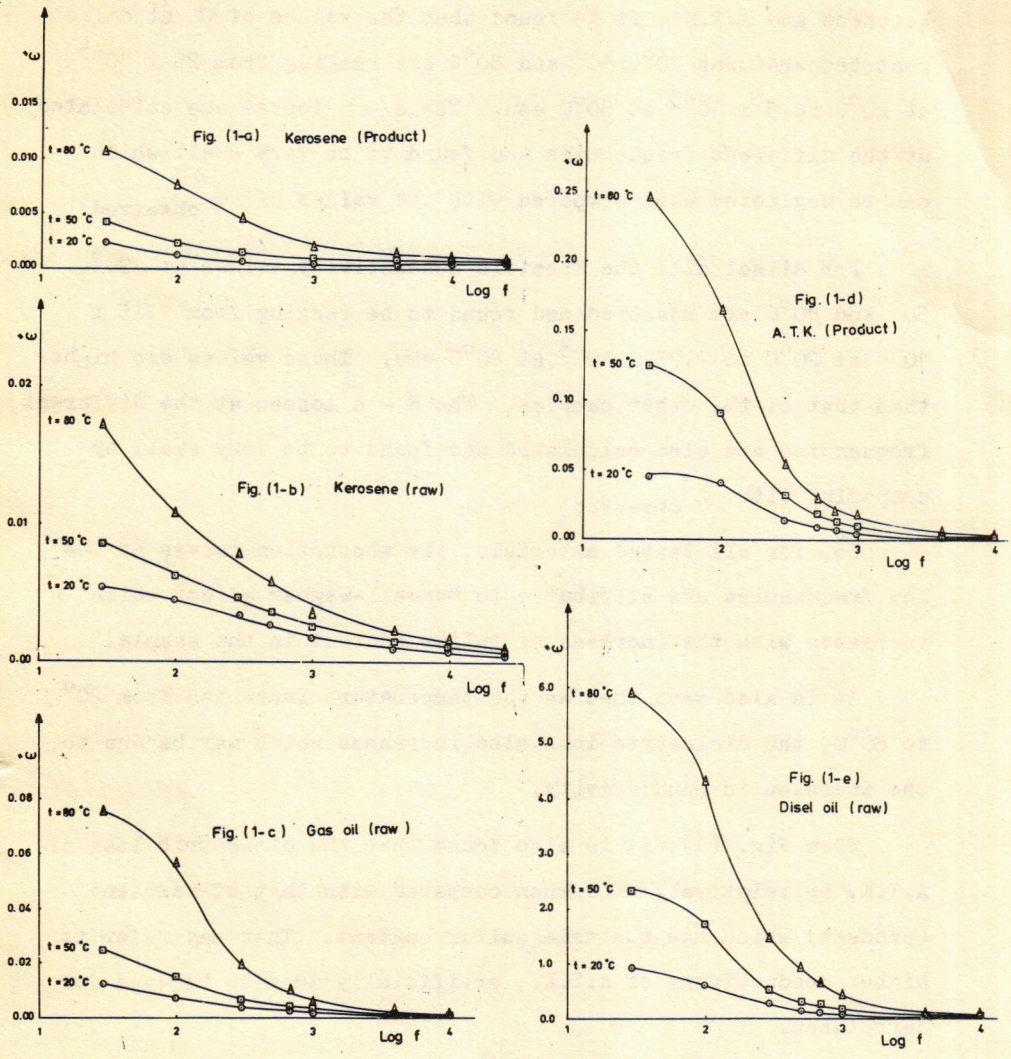

Fig. (1) The dielectric loss versus log F for different oil samples at 20°, 50° and 80°C.

where σ is the specific conductivity in esu, and f is the frequency in Hz. σ is measured by an a - c bridge to avoid polarisation, it is found that there is approximately no change in this conductivity with frequency [7] . In case of the rwo materials, gas oil and kerosene; and also the product materials, kerosene and A.T.K., it is found that the values of σ at different temperatures 20°, 50° and 80°C are ranging from 25 x 10^{-5} at 20°C to 5 x 10^{-5} at 80°C esu. The d - c losses are calculated at the different frequencies and found to be very small which can be neglected when compared with the values of $\epsilon''_{observed}$.

For diesel oil, the specific conductivity values at 20°, 50° and 80°C are measured and found to be ranging from 1.25 x 10^{-3} at 20°C to 2.75 x 10^{-3} at 80°C esu. These values are higher than that of the other samples. The d - c losses at the different frequencies are also calculated and found to be very small by comparing with $\epsilon''_{observed}$.

So, for all tested materials, the absorption curves at the low frequencies are attributed to Maxwell-Wagner effect which increases with the increase of sulfur content in the sample.

It is also seen that as the temperature increases from 20° to 80°C, the dielectric loss also increases which may be due to the increase in conductivity.

From Fig. (1), it is also found that the dielectric loss of A.T.K. is relatively high when compared with that of kerosene (product) which has the same sulfur content. That may refer to higher conductivity of A.T.K., artificially done to be used for aeroplanes.

The dielectric constant ϵ'' of the whole materials are measured at the same temperature range. As shown from the Table below, the dielectric constant for the tested materials except

constant at the measured frequency range [8] . For diesel oil, it is found that at lower frequencies, the dielectric

Table showing the dielectric constant ϵ' at 20°, 50° and 80°C for the oil samples with sulfur content.

Oil Sample	Sulfur content gm%	ϵ' at: 20°C	50°C	80°C
Diesel oil (raw)	1.2800	-	-	-
Gas oil (raw)	1.0000	2.153	2.118	2.078
Kerosene (raw)	0.2310	2.098	2.058	2.020
Kerosene (product)	0.0190	2.074	2.043	2.002
A.T.K. (Product)	0.0197	2.076	2.047	2.002

constant increases with the increase of temperature which is opposite temperature trend. This type of behaviour happens when the transconductance is impeded due to Maxwell-Wagner interfacial polarisation [9] . The variation of the dielectric constant with frequency at different temperatures are shown in Fig. (2). Since the dielectric constant of sulfur is 3.8 [10] which is relatively high with respect to that of oil samples, so, it is found that ϵ' of the oil samples increases with the increase of sulfur content.

When the dielectric constant ϵ' for the whole materials except diesel oil (where ϵ' is not constant over the measured range of frequency) are plotted against sulfur content in the sample as shown in Fig. (3), a linear relation is obtained. The relation helps in estimating the sulfur content in the oil samples which having constant dielectric value over the low frequency

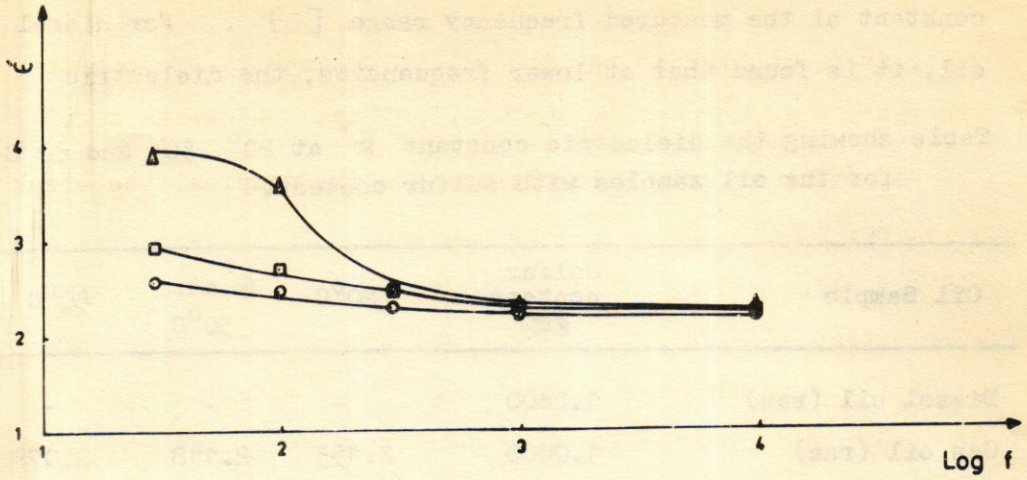

Fig. (2) The dielectric constant versus log F for diesel Oil at different temperatures. Same notations as Fig. (1).

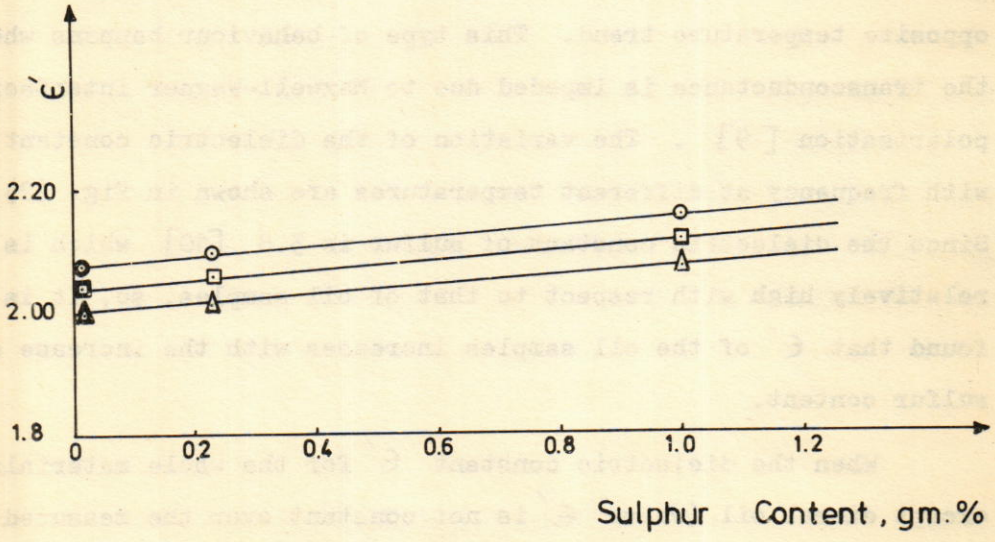

Fig. (3) The dielectric constant versus sulfur content in the oil samples at different temperatures.. Same notations as Fig. (1).

So, it is concluded that the sulfur content in the sample may increase both the dielectric constant and dielectric loss.

By applying several kilovolts on the oil samples, the break down voltage is obtained. At that voltage, the oil material completely losses its insulating properties. It is initiated by some action of electrons or ions and terminates in the formation of highly conductive path through the dielectric [11] . It is also found that the break down voltage decreases with the increase of temperature. Fig. (4) shows the variation of current I with the applied voltage V with the formation of break down voltage at different temperatures for gas oil (raw).

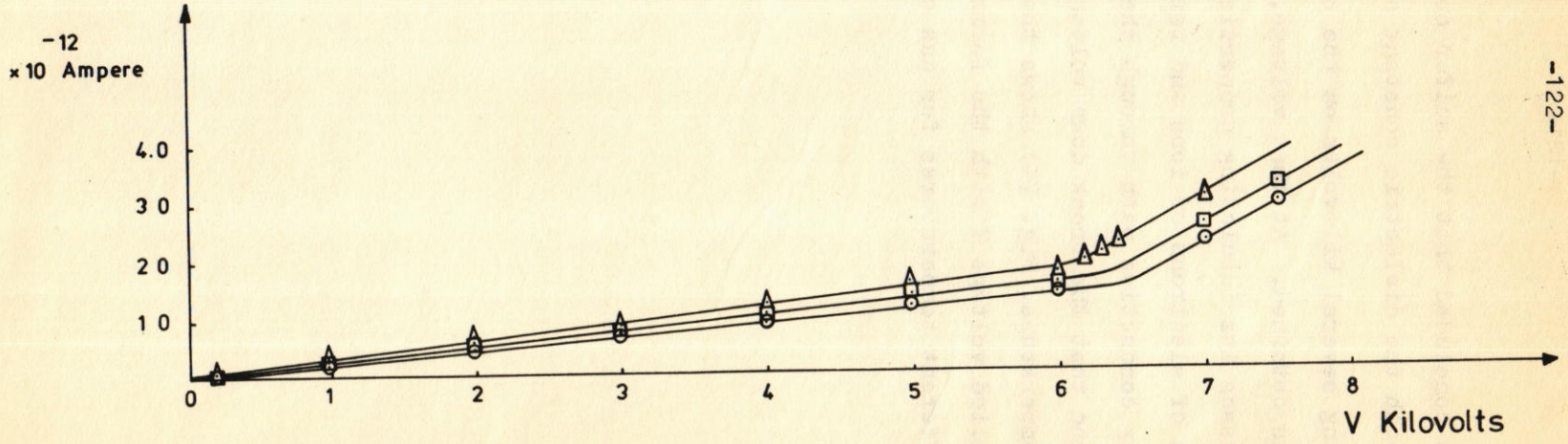

Fig. (4) The current I versus the applied voltage V for gas oil at different temperatures. Same notations as Fig. (1).

References

(1) Dora Refinery, Baghdad-Iraq (1978).

(2) F.F. Hanna and A.M. Ghoneim; Zeit. for Physik. Chemie, 245-308 (1970).

(3) K.W. Wagner; Arch. Elektrochm 2 371 (1941).

(4) B.V. Hamon; Aust. J. Phys. 6 304 (1953).

(5) L.K.H. Van Beek; Archs. Sci. Geneve, Bull Collogue Ampere 229 (1962).

(6) J.B. Hasted and S.H.M. El-Sabeh; Trans. Farad. Soc. 1003 (1952).

(7) S.H.M. El-Sabeh; Physics letters 663 (1966).

(8) P. Debye; Polar Molekeln, Leipzig (1929).

(9) A. Von Hippel; D.B. Knoll and W.B. West Phal; J. Chem. Phys. 54 134 (1971).

(10) B. Tareev; Physics of dielectric materials, Moscow, Mir Publishers. (1975).

(11) A.R.Von Hippel; Dielectric and wave, New York, John Wiley and Sons (1959).

مجلة علوم المستنصرية

المجلد ٤ ، العدد ١ ، حزيران ١٩٧٩

كلية العلوم—الجامعة المستنصرية—بغداد—العراق—

تعليمات للمؤلفين

١. تقدم ثلاث نسخ من البحث مطبوعة على الآلة الكاتبة وعلى ورق ابيض صقيل وتترك مسافة ٢,٥ سم على يسار كل صفحة .

٢. تقدم خلاصة باللغة العربية وأخرى باللغة الانكليزية وتطبع كل منهما على ورقة منفصلة .

٣. يطبع عنوان البحث وكذلك اسم المؤلف (او المؤلفين) وعنوانه على ورقة منفصلة ويكتب اسم المؤلف كاملا كان يكتب (احمد م. علي) .

٤. تقدم الرسوم التوضيحية منفصلة عن مسودة البحث وترسم بالحبر الصيني الاسود على ورق شفاف وترفق ثلاث صور لكل رسم وتكتب عناوين الرسوم على نفس الورقة .

٥. تنظم الجداول باسلوب تجعلها مفهومة دون اللجوء الى النص وذلك باعطاء كل جدول وكل عمود وصفا واضحا .

٦. لايجوز اعطاء المعلومات ذاتها بالرسم وبالجدول في وقت واحد الا اذا اقتضت ضرورة النقاش ذلك .

٧. يشار الى المصدر برقم ضمن قوسين [ ] بعد الجملة مباشرة وتطبع كافة المصادر على ورقة منفصلة .

٨. من المحبذ حيثما كان ممكنا ان يتسلسل البحث ليتضمن المقدمة ، طرق التجربة ، النتائج ، المناقشة .

مجلة علوم المستنصرية

المجلد ٤ العـدد ١ حزيران ١٩٧٩

مطابع ثنيـان بغـداد تلفون : ٦٣١٥٣